Titre: Title:	Modèles déterministes et stochastiques pour la résolution de conflits entre aéronefs
Auteur: Author:	Thibault Lehouillier
Date:	2015
Type:	Mémoire ou thèse / Dissertation or Thesis
Référence: Citation:	Lehouillier, T. (2015). Modèles déterministes et stochastiques pour la résolution de conflits entre aéronefs [Thèse de doctorat, École Polytechnique de Montréal]. PolyPublie. https://publications.polymtl.ca/1947/

URL de PolyPublie: PolyPublie URL:	https://publications.polymtl.ca/1947/
Directeurs de recherche: Advisors:	François Soumis, & Guy Desaulniers
Programme: Program:	Mathématiques de l'ingénieur

UNIVERSITÉ DE MONTRÉAL

MODÈLES DÉTERMINISTES ET STOCHASTIQUES POUR LA RÉSOLUTION DE CONFLITS ENTRE AÉRONEFS

THIBAULT LEHOUILLIER
DÉPARTEMENT DE MATHÉMATIQUES ET DE GÉNIE INDUSTRIEL
ÉCOLE POLYTECHNIQUE DE MONTRÉAL

THÈSE PRÉSENTÉE EN VUE DE L'OBTENTION
DU DIPLÔME DE PHILOSOPHIÆ DOCTOR
(MATHÉMATIQUES DE L'INGÉNIEUR)
DÉCEMBRE 2015

UNIVERSITÉ DE MONTRÉAL

ÉCOLE POLYTECHNIQUE DE MONTRÉAL

Cette thèse intitulée :

MODÈLES DÉTERMINISTES ET STOCHASTIQUES POUR LA RÉSOLUTION DE CONFLITS ENTRE AÉRONEFS

présentée par : LEHOUILLIER Thibault
en vue de l'obtention du diplôme de : Philosophiæ Doctor
a été dûment acceptée par le jury constitué de :

M. HERTZ Alain, Doctorat ès Sc., président
M. SOUMIS François, Ph. D., membre et directeur de recherche
M. DESAULNIERS Guy, Ph. D., membre et codirecteur de recherche
M. LE NY Jérôme, Ph. D., membre
M. MONGEAU Marcel, Ph .D., membre externe

DÉDICACE

À Clothilde et Apolline

REMERCIEMENTS

Premièrement, je tiens à remercier et à exprimer ma plus profonde gratitude à François Soumis. J'ai appris grâce à lui à voir le besoin d'optimisation dans des choses touchant à tous les domaines, que ce soit dans le cadre de ma thèse ou au squash et au tarot. Je garderai d'excellents souvenirs de sa gentillesse et de sa disponibilité tout au long de ma thèse.

Je remercie également Guy Desaulniers pour avoir accepté la co-direction de ma thèse. Sa rigueur dans les relectures, sa disponibilité et sa bonne humeur ont été des aides précieuses au cours de ces quatre années.

Un immense merci à mon co-directeur officieux Jérémy Omer. Sans lui, cette thèse ne se serait sûrement pas terminée. Tout au long de ma thèse, il a su m'aider, s'impliquer plus qu'à 100%, repousser mes limites avec sa rigueur et son perfectionnisme à toute épreuve. Sans cela, je suis sûr que je ne serais pas aussi fier de ce que j'ai produit. Au-delà de son encadrement, je garderai de Jérémy de très bons souvenirs, soit partagés autour d'une bière (ou plus), soit à une table de cartes où ses grognements résonnent encore dans les murs du GERAD !

Un grand merci également à Cyril Allignol et Moncef Ilies Nasri, avec qui j'ai eu beaucoup de plaisir lors de nos travaux ensemble.

J'aimerais remercier les membres de mon jury : Alain Hertz, Jérôme Le Ny et Marcel Mongeau pour avoir accepté de faire partie de mon jury de thèse.

Ensuite, je dois forcément remercier mes camarades étudiants du labo ! J'en ai croisé beaucoup en quatre ans, et en conséquence les souvenirs et les remerciements sont nombreux. Une mention toute particulière pour Antoine, Charles, Jean-Bertrand, Marilène, Mélisende, Régis, Romain, Samuel et Sébastien. J'ai passé grâce à vous d'excellents moments, que ce soit au ou en dehors du GERAD, sans lesquels tout cela aurait sûrement été beaucoup moins agréable. Vous êtes en grande partie responsables de mon envie quotidienne de venir au GERAD. À tous, je vous souhaite de trouver le bonheur et la réussite sur vos chemins respectifs !

Je tiens également à remercier le personnel du GERAD, et plus particulièrement Marie Perreault et Francine Benoît, qui ont toujours été disponibles pour répondre à mes questions, m'aider dans des démarches administratives, ou juste chiâler en bon français !

Un merci particulier à Serge, qui m'a fait découvrir le tarot. Son amour du jeu et sa gentillesse ont fait des pauses midi un plaisir immense pour moi, et je suis sûr que cela me manquera dans le futur.

Enfin, le plus grand merci revient à ma famille : mes parents pour leur soutien, et surtout

mon épouse Clothilde. Tout au long de cette thèse, elle a été la seule à toujours croire en moi, à voir le verre à moitié plein quand je le voyais vide. Elle a su faire preuve de patience, a toujours été derrière moi, et a su m'écouter quand j'en avais besoin. Pour cela, je ne la remercierai sûrement jamais assez. Je remercie enfin Apolline, ma fille, qui même si elle n'en a pas (encore) conscience, a été une source de motivation pour mener à bien cette thèse.

RÉSUMÉ

Cette thèse s'inscrit dans le domaine de la programmation mathématique appliquée au problème de détection et de résolution de conflits entre aéronefs. Un *conflit* est une perte de séparation entre deux ou plusieurs aéronefs qui se retrouvent trop proches selon des normes de sécurité prédéfinies. Étant donnée une configuration initiale d'un ensemble d'aéronefs (position, vitesse, accélération), le problème de détection et de résolution de conflits entre aéronefs consiste à trouver une nouvelle configuration sans conflits futurs et minimisant une fonction de coût choisie par l'utilisateur (critère économique, critère sécuritaire, etc.). Dans le système de gestion du trafic aérien actuel, cette tâche est gérée par un contrôleur aérien visualisant le trafic sur un moniteur. Quand le contrôle anticipe un conflit, il transmet des manœuvres d'évitement aux pilotes des aéronefs concernés. Les pilotes appliquent ces manœuvres avant de rejoindre leur trajectoire prévue par leur plan de vol. Les enjeux de l'optimisation du maintien de séparation entre aéronefs sont multiples. En particulier, le développement de modèles d'aide à la décision pour le contrôle permettrait l'augmentation de la capacité des secteurs aériens. Ainsi, plus d'aéronefs pourraient circuler en même temps, et ce le long de leur trajectoire optimale, tout en diminuant les retards. De plus, au-delà de la complexité du trafic, les imprécisions relatives aux données météorologiques et à l'état des aéronefs, ainsi que les délais de communication, mettent en avant la nécessité de robustesse dans la résolution du problème. Dans cette optique, la communauté de recherche opérationnelle s'est attaquée durant les deux dernières décennies à des variantes du problème de plus en plus complexes permettant de prendre en compte des contraintes opérationnelles difficiles à traiter. Cette thèse s'insère dans cette tendance.

Dans un premier temps, cette thèse présente une étude économique destinée à valider le besoin opérationnel d'outils automatisés d'aide à la décision pour le contrôleur aérien. Plus particulièrement, les interactions entre les décisions tactiques faites lors de l'affectation des créneaux de décollage et les décisions opérationnelles faites lors de la résolution de conflits sont étudiées dans un contexte de trafic augmenté. Pour cela, un simulateur de trafic permettant de travailler avec différents paradigmes d'allocations de créneaux de décollage, de capacité de secteurs, d'augmentation de trafic est utilisé. À partir de données de trafic français datant de 2012, une semaine de trafic standard est générée pour différentes années jusqu'à un horizon allant à 2035. L'étude montre alors que les coûts des retards dus à l'allocation de créneaux de décollage augmentent exponentiellement avec l'augmentation du trafic si la capacité du réseau n'est pas augmentée, tandis que l'augmentation des coûts de résolution de conflits augmente de façon beaucoup plus acceptable avec un réseau de plus grande capacité. Cependant,

l'augmentation de la capacité du réseau entraîne une charge de travail ingérable pour un contrôleur avec les outils actuellement disponibles. L'étude propose ensuite un compromis entre une forte augmentation des coûts de retards et une forte charge de travail, en contrôlant la hausse des coûts des retards en augmentant les capacités des secteurs. La valeur ajoutée de cette étude est que nous sommes désormais capables de quantifier les objectifs de recherche en optimisation du trafic aérien, tout en donnant une légitimité aux travaux déjà existants.

Dans un second temps, cette thèse présente un modèle mathématique de détection et de résolution de conflits dans un cadre déterministe. Le design de la méthode repose sur la volonté d'obtenir un modèle robuste. En d'autres termes, le formalisme mathématique doit demeurer valable, et ce quelles que soient les hypothèses considérées. Pour cela, les aspects relatifs à la modélisation de la dynamique des avions, des manœuvres ainsi que la fonction de coût sont complètement séparés du modèle mathématique de résolution. Formellement, le problème est modélisé comme une recherche de clique de cardinalité maximale et de poids minimum dans un graphe. Les sommets du graphe correspondent à un ensemble de manœuvres possibles pour les aéronefs, et les arêtes lient des manœuvres sans conflit pour des aéronefs différents. Afin de garder un graphe compact, nous modélisons les coûts de façon originale : en effet, ces coûts dépendent des sommets appartenant à la clique et ne sont ainsi plus connus *a priori*. Ce choix de modélisation en fait une nouvelle variante d'un problème de recherche de clique de cardinalité maximale de poids minimum. Nous formulons ensuite le problème comme un programme linéaire à variables mixtes. Deux méthodes de décomposition sont également développées. La première vise à utiliser l'influence du nombre de manœuvres par aéronef sur le temps d'exécution afin de trouver un compromis entre efficacité et temps de résolution, alors que la seconde vise à exploiter les caractéristiques géométriques des instances. Des instances ayant jusqu'à 250 avions répartis sur 20 niveaux sont résolues en moins de 10 secondes de calcul.

La dernière partie de cette thèse traite la prise en compte d'incertitudes lors de la résolution de conflits. Plus particulièrement, nous considérons les incertitudes dues aux erreurs de prévisions météorologiques sur le vent, ainsi que les erreurs de mesure de la vitesse venant de la connaissance incomplète des paramètres physiques des avions. Nous introduisons également un nouveau type d'incertitude : le délai dû aux communications entre le contrôleur et les pilotes. Ces perturbations induisent une erreur longitudinale sur la trajectoire des avions que nous quantifions, afin d'établir une formule analytique de la probabilité de conflit entre chaque paire d'avions. Nous utilisons ensuite cette formule pour modifier la définition des arêtes du graphe présenté dans la seconde partie de la thèse. Nous abordons ensuite le problème de résolution de conflits sous un angle bi-objectif. Pour ce faire, nous considérons un critère économique correspondant à la consommation de carburant pour exécuter les manœuvres,

ainsi qu'un critère de sécurité décrit par l'espérance du nombre de conflits. Nous présentons ensuite une méthode itérative permettant de générer un ensemble de solutions approximant le front de Pareto du problème. Cette approche est innovante car elle nous permet d'avoir une approche bi-objectif du problème de résolution de conflits, ce qui correspond plus à la nature intrinsèque du problème, et elle permet de fournir au contrôleur un ensemble de solutions. Ce dernier point est le plus pertinent car la notion d'optimalité est discutable en résolution de conflits à cause de l'existence de plusieurs "bonnes solutions" proches de la solution optimale, et il peut être intéressant de laisser au contrôleur des options dans sa prise de décision. En moyenne, 6 solutions sont générées en moins de 3 minutes pour des instances ayant jusqu'à 35 avions.

ABSTRACT

This thesis is related to the field of mathematical programming applied to the conflict detection and resolution problem between aircraft. A *conflict* happens when two or more aircraft are too close to each other regarding pre-defined separation distances. Given the initial configuration (position, speed, acceleration) of a set of aircraft, the conflict detection and resolution problem consists in finding a new conflict-free configuration that minimizes a cost function chosen by the user (economical criterion, safety criterion, etc.). In the current air traffic management system, this task is managed by an air traffic controller who monitors traffic on a screen. When he/she anticipates a conflict, he/she communicates avoidance maneuvers to the pilots of the corresponding aircraft. The pilots execute these maneuvers before recovering the trajectory described on their flight plan. The stakes behind the optimization of separation between aircraft are multiple. In particular, the development of automated decision tools for air traffic control would allow the increase in airspace capacity. As a consequence, more aircraft could fly simultaneously while following their optimal trajectory and reducing potential delays. Besides, in addition to traffic complexity, the imprecisions related to weather forecasts, to the aircraft physical parameters and the potential communication delays highlight the need for robustness in the problem resolution. To this end, in the last decades the research community has tackled more complex problems that consider hard-to-solve operational constraints. This thesis follows this trend.

First, this thesis presents an economical study aiming at the validation of an operational need for the development of automated decision tools for the air traffic controller. More specifically, we study the interactions between strategic decisions for take-off slot allocation and the tactical decisions of conflict resolution in a context of increasing traffic. To this end, we use a complete traffic simulator allowing us to consider different paradigms of take-off slot allocation, sector capacities and traffic increase. Using historical French traffic data from 2012, a typical week of traffic is generated to represent traffic for different years until 2035. The study highlights on the one hand that the costs of delays due to the take-off slot allocation increase exponentially with the traffic increase if the network capacity is not increased. On the other hand, the costs of conflict resolution increase in an acceptable fashion in a network of larger capacity but the workload becomes unmanageable for an air traffic controller using the currently available tools. The study then proposes a compromise between a huge increase of delay costs and a heavy workload by controlling the growth of delay costs by increasing sector capacity. This is of great value, since we are now capable of quantifying research objectives for air traffic optimization while legitimizing the research already existing.

Second, this thesis presents a deterministic mathematical model to solve the conflict detection and resolution problem between aircraft. The design of the presented method was driven by robustness. In other words, the proposed mathematical framework must remain valid, whatever the hypotheses considered. To this end, the aspects related to the modeling of aircraft dynamics, maneuvers and the cost function are fully separated from the mathematical resolution process. Formally, the problem is modeled as a search for a clique of maximal cardinality and minimum weight in a graph. The vertices of the graph correspond to possible aircraft maneuvers and edges connect conflict-free maneuvers of different aircraft. To keep the graph compact, we model the vertex costs in an innovative fashion: indeed, these costs depend on the vertices in the clique, and thus cannot be known *a priori*. This choice of modeling corresponds to a new variant of the minimum-weight maximum-cardinality clique problem. We formulate this problem as a mixed integer linear program. We also develop two decomposition methods. The first one aims at taking advantage of the effect of the number of maneuvers per aircraft on the solution time to find a trade-off between solution efficiency and time, while the second one exploits the geometrical characteristics of the set of aircraft. Instances with up to 250 aircraft divided between 20 flight levels are solved within 10 seconds.

The last part of this thesis takes into account uncertainties in the conflict resolution process. More specifically, we consider uncertainties due to errors in weather forecasts, in the aircraft speed measure resulting from the incomplete knowledge of the physical paremeters of the aircraft. We introduce a new type of uncertainty: the delay in the execution of maneuvers due to communications. Those perturbations induce an along-track error on the aircraft trajectory that we can quantify in order to derive an analytical formula of the probability of conflict between every pair of aircraft. We use this formula to modify the definition of edges in the graph presented in the previous section of the thesis. We then tackle the conflict resolution problem as a bi-objective problem. To this end, we consider an economical criterion corresponding to the fuel consumption induced by the execution of maneuvers, along with a safety criterion represented by the expected number of conflicts. We also present an iterative method generating a set of solutions approximating the Pareto front of the problem. This method is innovative, since it uses a bi-objective approach of conflict resolution, which fits more with the inner nature of the problem, while providing the controller with a set of solutions. This last feature is the most relevant because the notion of optimality in conflict resolution is questionable, since there exist several ”good solutions” close to the optimal one, and it could be interesting to give the controller some options in his/her decision making. On average, 6 solutions are generated within 3 minutes for instances with up to 35 aircraft.

TABLE DES MATIÈRES

DÉDICACE iii

REMERCIEMENTS iv

RÉSUMÉ vi

ABSTRACT ix

TABLE DES MATIÈRES xi

LISTE DES TABLEAUX xv

LISTE DES FIGURES xvi

CHAPITRE 1 INTRODUCTION 1

CHAPITRE 2 REVUE DE LA LITTÉRATURE 5
2.1 Détection et résolution de conflits dans un cadre déterministe 5
2.1.1 Détection des conflits 5
2.1.2 Résolution de conflits 6
2.1.3 Tableau de synthèse 12
2.2 Détection et résolution de conflits dans un cadre incertain 13
2.2.1 Les incertitudes en contrôle aérien 13
2.2.2 Modélisation des erreurs 13
2.2.3 Obtention d'une formule analytique de la probabilité de conflit 14
2.2.4 Approches par simulation 15

CHAPITRE 3 ORGANISATION DE LA THÈSE 16

CHAPITRE 4 ARTICLE 1 : MEASURING THE INTERACTIONS BETWEEN AIR TRAFFIC CONTROL AND FLOW MANAGEMENT USING A SIMULATION-BASED FRAMEWORK 18
4.1 Introduction 18
4.1.1 Context and main concepts 18
4.1.2 Contribution statement 20
4.2 Description of the simulation algorithms 21

4.2.1 Traffic increase . . . 21
4.2.2 Ground-Holding procedure . . . 22
4.2.3 Trajectory simulation . . . 24
4.2.4 Conflict resolution . . . 24
4.3 Simulation input . . . 25
4.3.1 Traffic predictions . . . 25
4.3.2 Airspace capacity . . . 26
4.3.3 Description of the reference historical data . . . 26
4.3.4 Delay and maneuver costs . . . 26
4.4 Impact of the ground-holding regulation . . . 27
4.4.1 Impact on the entering flow per hour . . . 28
4.4.2 Impact on the number of conflicts . . . 30
4.4.3 Cost analysis . . . 30
4.4.4 Impact on the number of maneuvers . . . 32
4.5 Finding a compromise between costs and workload . . . 33
4.5.1 Motivation . . . 33
4.5.2 Design of the scenario . . . 33
4.5.3 Cost analysis . . . 35
4.5.4 Workload analysis . . . 35
4.5.5 Summary . . . 37
4.6 Conclusion . . . 38
4.7 Acknowledgement . . . 39

CHAPITRE 5 ARTICLE 2 : TWO DECOMPOSITION ALGORITHMS FOR SOLVING A MINIMUM WEIGHT MAXIMUM CLIQUE MODEL FOR THE AIR CONFLICT RESOLUTION PROBLEM . . . 40
5.1 Introduction . . . 40
5.1.1 Context: challenges of air traffic control . . . 40
5.1.2 Literature review . . . 41
5.1.3 Contribution statement . . . 43
5.2 Problem Formulation . . . 43
5.2.1 Modeling aircraft dynamics . . . 44
5.2.2 Aircraft maneuvers . . . 44
5.2.3 Aircraft separation . . . 49
5.3 Modeling the CR problem as a MWMCC problem . . . 51
5.3.1 Graph theory definitions . . . 51

5.3.2 Graph construction . . . 52
5.3.3 Conflict-free solution: formulation and illustrative example . . . 53
5.3.4 Computing the costs . . . 54
5.4 Methodology . . . 55
5.4.1 MILP formulation . . . 55
5.4.2 Decomposition methods . . . 57
5.5 Results . . . 60
5.5.1 Benchmark description . . . 61
5.5.2 Computational results . . . 63
5.5.3 Detailed results for the SMILO procedure on the benchmark without altitude changes . . . 66
5.5.4 Evaluating the second decomposition method on the multi-level random benchmark . . . 68
5.6 Conclusions . . . 69

CHAPITRE 6 ARTICLE 3 : SOLVING THE AIR CONFLICT RESOLUTION PROBLEM UNDER UNCERTAINTY AS AN ITERATIVE BI-OBJECTIVE MIXED INTEGER LINEAR PROGRAM . . . 71
6.1 Introduction . . . 71
6.1.1 Automating air traffic control . . . 71
6.1.2 The air conflict resolution problem . . . 72
6.1.3 Literature review on the CR problem . . . 72
6.1.4 Critical analysis and contribution statement . . . 74
6.2 Problem Formulation . . . 75
6.2.1 Aircraft dynamics . . . 75
6.2.2 Aircraft maneuvers . . . 76
6.2.3 Aircraft trajectory recovery . . . 76
6.2.4 Maneuver cost . . . 77
6.2.5 Modeling the uncertainties . . . 77
6.2.6 Analytical expressions of the minimum distance and the probability of conflict . . . 79
6.3 Deterministic Model . . . 85
6.3.1 Graph construction . . . 86
6.3.2 MILP formulation . . . 87
6.3.3 Inserting uncertainties into the deterministic model . . . 88
6.4 Bi-Objective Optimization Procedure . . . 88

6.4.1 Optimization Criteria 89
6.5 Results 90
6.5.1 Parameter values and simulations of the uncertainties distributions . . 91
6.5.2 Validating the calculus through simulations 91
6.5.3 Computational results 93
6.5.4 Quantitative analysis of a solution set 96
6.6 Conclusions 98

CHAPITRE 7 DISCUSSION GÉNÉRALE 99
7.1 Synthèse des travaux 99
7.2 Limitations de la solution proposée et améliorations futures 100

CHAPITRE 8 CONCLUSION 102

RÉFÉRENCES 103

LISTE DES TABLEAUX

Tableau 2.1	Synthèse des articles référencés	12
Table 4.1	Summary of traffic forecast for Europe to 2035	25
Table 4.2	Traffic predictions with regulated growth using 2012 as a starting point	26
Table 4.3	Tactical costs (euros, total) of ground-holding delay for different aircraft types.	28
Table 4.4	Increased capacities for scenario S_3	34
Table 5.1	Dimensions of the instances and computational results for the virtual benchmark using only horizontal maneuvers	64
Table 5.2	Dimensions of the instances and computational results on the virtual benchmark including flight level changes	65
Table 5.3	Dimensions of the instances and computational results on the single-level random benchmark including horizontal maneuvers	66
Table 5.4	Dimensions of the instances and computational results on the single-level random benchmark including horizontal maneuvers and flight level changes	66
Table 5.5	Dimensions of the instances and computational results	67
Table 5.6	Dimensions of the instances and computational results for the second decomposition method on the multi-level random benchmark	69
Table 6.1	Comparison of the simulation results and the calculus for the minimum distance and the probability of conflict	92
Table 6.2	Computational results	95

LISTE DES FIGURES

Figure 1.1 Diagramme générique de fonctionnement d'un algorithme de détection et résolution de conflits . . . 2
Figure 4.1 Vertical and horizontal separation. No other aircraft can be inside the cylinder at any time. . . . 20
Figure 4.2 Simulation modules . . . 22
Figure 4.3 CASA procedure for a regulated area . . . 23
Figure 4.4 Entering flow per hour for different traffic volumes in KR sector . . . 29
Figure 4.5 Comparison of the number of conflicts observed with and without ground-holding . . . 30
Figure 4.6 Number of conflicts per hour in KR for different traffic volumes . . . 31
Figure 4.7 Ground-holding and ATC costs for 6/8/2012 . . . 32
Figure 4.8 Maneuvers per hour for +50% traffic volume in KR sector . . . 33
Figure 4.9 Ground-holding costs for increasing capacities . . . 35
Figure 4.10 Ground-holding and ATC costs for the three scenarios on 08/06/2012 . 36
Figure 4.11 $OC(KR)$ for different traffic volumes and ground-holding scenarios . . 36
Figure 4.12 Maneuvers per hour for a +50% traffic volume in KR sector for the three scenarios . . . 37
Figure 5.1 Safety cylinder around an aircraft . . . 41
Figure 5.2 Geometry of the heading change and the flight level change . . . 45
Figure 5.3 Geometry of the trajectory recovery following a heading change . . . 48
Figure 5.4 Geometry of the trajectory recovery following a flight level change . . . 48
Figure 5.5 Illustrative example: instance and solution . . . 54
Figure 5.6 Examples . . . 62
Figure 5.7 Solutions of the examples . . . 63
Figure 5.8 Random instance $\mathcal{U}_{15}$ and its solution . . . 65
Figure 5.9 Influence of the discretization on the optimal value and the CPU time . 68
Figure 6.1 Cross and along-track errors on an aircraft trajectory . . . 73
Figure 6.2 Structure of the maneuver delay . . . 79
Figure 6.3 Ellipse in the coordinate system (O, x_i, x_j) . . . 80
Figure 6.4 Illustration of a maneuver delay for two aircraft performing heading changes . . . 83

Figure 6.5 Comparison of calculus and simulations for two aircraft performing heading changes to avoid at the intersection of their planned trajectories making a 50° angle 93
Figure 6.6 Examples of instances of the benchmark 94
Figure 6.7 Example for the analysis of the generated solutions 96
Figure 6.8 Generated Pareto solutions for instance $\mathcal{R}_8$ 97
Figure 6.9 Two different geometrical solutions for the example 97

CHAPITRE 1 INTRODUCTION

Les systèmes actuels de gestion du trafic aérien consistent pour la plupart en un réseau géographique où les avions sont autorisés à se déplacer le long de routes prédéterminées via un plan de vol décrivant la trajectoire empruntée par l'appareil entre le point d'origine et le point de destination du vol, ainsi que les temps de passage pour certains points de contrôle tout au long de la trajectoire. Sous de tels systèmes, la dynamique du trafic est principalement régie par la structure sous-jacente du réseau. Selon l'Organisation de l'Aviation Civile Internationale, il y a eu au cours de l'année 2012 plus de trente millions de vols commerciaux réguliers, et ce nombre se voit augmenter chaque année. Cette situation conduit inéluctablement vers un état saturé et congestionné du système entier. En conséquence, chaque vol a subi en moyenne 1.15 minutes de retard, selon EUROCONTROL (2012). De plus, les améliorations et technologies apportées en continu aux instruments de navigation ainsi qu'aux outils de communication laissent entrevoir de nouvelles stratégies de gestion du trafic aérien permettant d'éviter ces futurs problèmes.

Récemment, les compagnies aériennes ainsi que la *Federal Aviation Administration* (*FAA*) des États-Unis ont proposé le paradigme du "vol libre" (*Free Flight*) dans RTCA (1995) et Board (1995), dont le principe fondateur repose sur des systèmes de communication, de navigation et de surveillance améliorés, donnant aux compagnies aériennes ainsi qu'à leurs pilotes plus de liberté. Un tel système laisse une plus grande place à l'optimisation, permettant ainsi aux compagnies aériennes d'être de plus en plus compétitives. Par exemple, les pilotes pourraient optimiser leur trajectoire de vol afin de minimiser les coûts encourus, incluant entre autres le coût en carburant qui dépend de la vitesse et de la masse (diminuant au cours du temps) de l'avion, ainsi que de la vitesse des vents, de la densité de l'air et des différentes phases de la trajectoire (montée, descente et croisière). Cependant, le vol libre peut avoir un grand impact sur la sécurité globale du système, et de nombreux conflits peuvent potentiellement avoir lieu. Un conflit en transport aérien est une situation dans laquelle deux ou plusieurs avions se situent à une distance inférieure au seuil minimal requis pour maintenir le système sécuritaire. La détection de conflits consiste en l'identification de situations potentielles de conflits basée sur la prédiction des trajectoires des avions en fonction de leur position géographique, de leur vitesse et cap actuels, ainsi que de leur plan de vol. Une fois qu'un conflit est détecté, il est résolu en modifiant les trajectoires des avions en jeu de façon à ce que l'espacement minimal de sécurité soit de nouveau respecté.

Le diagramme 1.1 décrit le fonctionnement d'un algorithme de détection et résolution de conflits. À partir d'observations faites sur l'espace aérien, des variables d'état dépendant

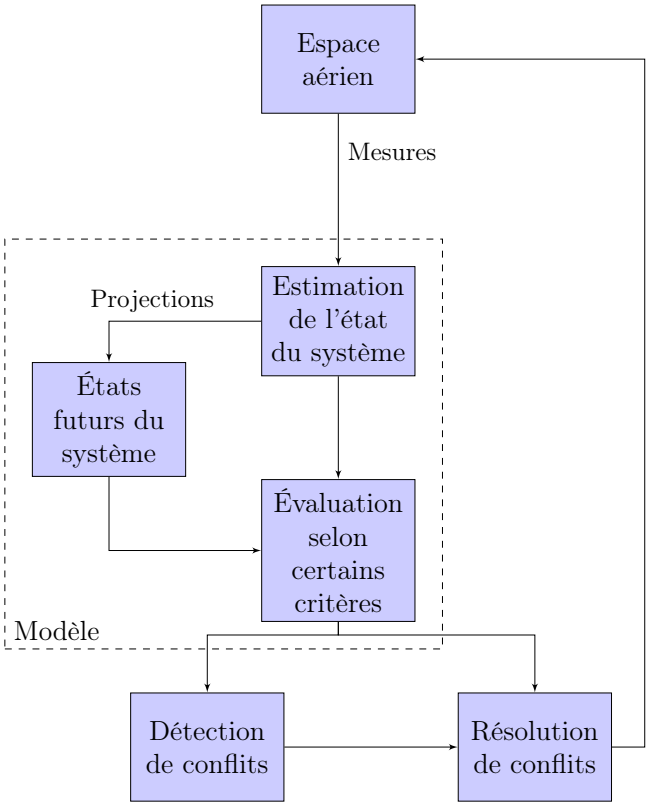

Figure 1.1 – Diagramme générique de fonctionnement d'un algorithme de détection et résolution de conflits

du modèle, par exemple la position, l'altitude, la vitesse ainsi que le cap de chaque avion, sont mesurées. À partir de ces mesures, les états futurs du système via des projections (par extrapolation temporelle d'une trajectoire rectiligne par exemple) sont calculés. Des critères d'évaluation définissant la métrique du problème (comme la distance entre différents appareils, le temps d'approche à un point donné) permettent ensuite de définir l'existence ou non de conflits. Une fois ces conflits détectés, le modèle permettra éventuellement de les résoudre, avant d'effectuer de nouvelles mesures et de réitérer le processus.

Les compagnies aériennes actuelles doivent travailler en collaboration avec des autorités régulant l'espace aérien sur lequel circulent leurs avions. Ces autorités cherchent à utiliser un système de gestion du trafic aérien leur assurant de maintenir une sécurité constante, et permettant aux compagnies d'effectuer leurs opérations à coûts moindres. Un tel outil doit prendre en compte de nombreuses données dont notamment les coûts de consommation en carburant, les conditions météorologiques, l'état de congestion de l'espace aérien, ainsi que des informations relatives aux plans de vol des appareils en circulation. Il doit permettre aux compagnies impliquées de bénéficier d'un outil automatisé prenant en compte les coûts supplémentaires estimés pour chacune d'entre elles et les retards occasionnés pour les passagers

afin de gérer de façon équitable l'espace aérien, ainsi qu'une estimation précise des coûts encourus lors des opérations.

Un tel problème est très complexe en termes de contraintes à respecter (notamment les contraintes de séparation, augmentant énormément avec le nombre d'avions), ainsi qu'en termes de fonction objectif (les coûts de consommation en carburant sont non linéaires et éventuellement non convexes), et il existe actuellement de nombreux modèles mathématiques pour la détection et la résolution de conflits entre aéronefs. Cependant, nous avons identifié plusieurs besoins qui n'ont été que très peu ou pas abordés.

À notre connaissance, il n'existe pas d'étude visant à définir précisément les futurs besoins opérationnels en termes d'optimisation du trafic aérien. Une telle étude permettrait de définir où se situe le besoin en optimisation, et permettrait de donner une légitimité aux travaux déjà existants sur le sujet.

En plus d'avoir un compromis précision / temps de calcul, nous avons également constaté que la robustesse est critique pour obtenir un outil automatisé de résolution de conflits qui soit de qualité. Plus précisément, il est nécessaire de développer un formalisme mathématique qui fonctionne, et ce quelles que soient les hypothèses faites sur les aéronefs, leur dynamique, leur trajectoire, les manœuvres, les normes de séparation ainsi que les fonctions de coût associées. À notre connaissance, il n'y a pas ou très peu de modèles développés dans cette direction, ce qui est regrettable car de tels modèles permettrait de comparer des méthodes différentes en ajustant simplement les paramètres d'entrée.

Enfin, la résolution de conflits entre aéronefs est par nature un problème multi-objectif. En effet, les contrôleurs ne prennent pas qu'un seul aspect de la résolution en compte. Ils doivent trouver le compromis entre l'efficacité, la sécurité, la facilité de mise en place des manœuvres, ainsi que le suivi post-commandes, entre autres. De plus, la notion d'optimalité reste subjective en contrôle aérien dans la mesure où pour un critère donné, il existe beaucoup de "bonnes" solutions, proches de la solution optimale. Si ces solutions venaient à être disponibles au contrôleur, cela pourrait être utile car il/elle pourrait choisir une solution suivant ses préférences. À notre connaissance, il n'existe pas d'étude se concentrant sur ses aspects.

Pour tenter de répondre aux besoins sus-mentionnés, cette thèse se concentrera sur le développement de modèles d'optimisation pour la détection et la résolution de conflits entre aéronefs. Pour ce faire, nous commencerons par effectuer une étude économique visant à quantifier les gains possibles et les futurs objectifs de recherche en contrôle du trafic aérien et à donner une légitimité aux travaux existants. Nous présenterons ensuite un modèle de résolution de conflits dans un cadre déterministe. Ce modèle sera ensuite adapté au cadre incertain, et une méthode bi-objectif itérative générant une approximation du front de Pareto du problème

sera décrite.

Le présent document est structuré comme suit. Le chapitre 2 permet de faire une brève revue de la littérature sur des variantes du problème étudié. Le chapitre 3 introduit le corps de l'ouvrage qui est constitué des chapitres 4, 5 et 6. Le chapitre 4 contient un article soumis à EURO Journal on Transportation and Logistics où une étude économique visant à quantifier les objectifs de recherche en ATC est présentée. Le chapitre 5 est un article soumis à European Journal of Operational Research qui présente une formulation du problème de résolution de conflits entre aéronefs comme une nouvelle variante du problème de recherche de clique maximale de coût minimum dans un graphe. Le chapitre 6 est un article soumis à Transportation Science qui développe une méthode itérative permettant de générer une approximation du front de Pareto du problème de résolution de conflits dans un cadre incertain. Finalement, une discussion générale est présentée au chapitre 7 et des conclusions sont apportées au chapitre 8.

CHAPITRE 2 REVUE DE LA LITTÉRATURE

Ce chapitre présente une revue de la littérature existante dans le domaine concernant notre problème.

Nous commençons par une synthèse des méthodes déterministes. Au cours des vingt dernières années, les systèmes de détection et de résolution de conflits dans un cadre déterministe ont été largement étudiés via des outils très différents, comme par exemple les réseaux de neurones, les champs de force, ou encore les méthodes classiques d'optimisation. Ainsi, afin de rendre compte plus clairement de l'état de l'art actuel, nous allons présenter de façon générale les méthodes existantes de détection de conflits, ainsi qu'une revue détaillée des modèles de résolution de conflits. La littérature étant très dense, nous donnerons également un tableau de synthèse regroupant les principales caractéristiques des modèles évoqués.

La seconde partie de la revue de la littérature s'intéressera à la prise en compte des incertitudes dans la détection et la résolution de conflits. Les travaux existants sont beaucoup plus rares, de par la complexité du problème. Nous passerons en revue l'état de l'art actuel en décrivant les différents techniques utilisées pour étudier le problème.

2.1 Détection et résolution de conflits dans un cadre déterministe

2.1.1 Détection des conflits

La détection de conflits correspond au processus d'identification de conflits entre deux ou plusieurs avions, ou entre un avion et une autre contrainte de l'espace aérien, comme des régions ayant des conditions météorologiques défavorables. Il existe peu de modèles concentrés seulement sur la détection de conflits dans un cadre déterministe. En effet, la plupart des modèles incluent la détection et la résolution de conflits. Nous verrons dans la section 2.2 que dans un cadre incertain, il existe davantage de modèles de détection que de modèles de détection et de résolution.

Chiang *et al.* (1997) appliquent les diagrammes de Delaunay et Voronoi à la détection de conflits, leur permettant de développer un algorithme de complexité $\mathcal{O}(n \log n)$, où n désigne le nombre d'avions présents dans l'espace aérien. Sherali *et al.* (2000) présentent deux modèles : le premier divise l'espace aérien en régions tridimensionnelles non convexes et évalue la congestion de ces secteurs via une procédure itérative traçant le progrès de chaque vol. Ce modèle sert de base pour fournir de l'information en entrée d'un second modèle qui, en fonction des données de congestion, permet d'évaluer les conflits éventuels. En plus de donner les paires d'avions en conflit, le modèle fournit des informations comme le point d'entrée et de

sortie d'un avion dans la zone de sécurité d'un autre avion, ainsi que la durée de l'intrusion. Jardin (2003) utilise une représentation en grille de quatre dimensions (espace-temps) de l'espace aérien, afin de présenter des algorithmes pour la détection stratégique de conflits.

2.1.2 Résolution de conflits

Kuchar et Yang (2000) recensent et classifient les algorithmes de détection et de résolution de conflits selon plusieurs critères, notamment pour la résolution de conflits. Pour notre revue de la littérature, nous retiendrons les critères suivants : méthodes prescrites, méthodes manuelles, modélisations par réseaux de neurones, par champs de force, et enfin les méthodes d'optimisation classiques.

Prescrites

Les méthodes prescrites correspondent aux situations où l'ensemble des manœuvres standards possibles pour éviter des conflits simples est donné, après avoir été déterminé au préalable lors de procédures prédéfinies. Dans Carpenter et Kuchar (1997), les conflits ayant lieu lors de l'approche de pistes d'atterrissage parallèles sont étudiés, et les auteurs estiment que la manœuvre consistant à tourner avec augmentation d'altitude est toujours exécutée. Malgré des avantages comme la possibilité d'exécuter ces manœuvres rapidement, les méthodes prescrites restent peu efficaces car trop peu adaptables à nos problèmes.

Manuelles

Dans ces modèles, l'utilisateur a la possibilité de générer lui-même des scénarios de résolution possibles et d'obtenir un retour sur l'acceptation ou non de sa tentative. De telles méthodes présentent l'avantage d'une plus grande flexibilité car les manœuvres sont générées par un humain, en utilisant des informations pas forcément disponibles pour un automate, comme par exemple les données météorologiques.

Réseaux de neurones

Un modèle de réseaux de neurones est fondé sur des concepts d'estimation statistique, d'optimisation et de théorie de contrôle. Ces méthodes ont souvent été utilisées couplées à des heuristiques, par exemple dans Durand *et al.* (1996) qui utilisent des réseaux de neurones pour modéliser des conflits entre paires d'avions. La méthode s'avère efficace, mais l'extension à des conflits impliquant plus de 2 avions pose beaucoup plus de difficultés.

Plus récemment, Christodoulou et Kontogeorgou (2008) proposent un modèle permettant de prédire les changements de vitesse optimaux pour que deux avions n'entrent pas en collision

dans un environnement en trois dimensions. Dans leur modèle, le réseau de neurones est couplé à de l'optimisation non linéaire.

Enfin, Cetek (1999) présente un modèle qui prend en compte de nombreux paramètres physiques comme la densité de l'air suivant l'altitude, la vitesse du vent, la masse, la vitesse et l'accélération de l'avion, etc. Cependant, les temps de calculs sont trop lourds pour permettre la gestion de conflits à court terme.

Champs de forces

Ce type de modélisation fait une analogie entre chaque avion et une particule chargée dans un champ de forces où les manœuvres de résolution de conflits sont trouvées via la résolution d'équations électrostatiques. Plus précisément, une manœuvre est modélisée via les forces de répulsion entre les avions. Malgré cet aspect semblant simple, ces méthodes doivent être utilisées avec précaution, dans la mesure où elles font certaines hypothèses (par exemple que l'avion peut varier sa vitesse sur un large intervalle pendant la durée d'observation) ne se vérifiant pas en pratique. Ce contrôle supplémentaire nécessaire entraîne ainsi une augmentation de la complexité. Néanmoins, certains travaux établissent des résultats intéressants, comme Duong et Hoffman (1997), Hoekstra *et al.* (1998) et Zeghal et Hoffman (1999).

Optimisation

Les travaux de ce type introduisent, en plus de contraintes, des métriques de coûts à optimiser, par exemple minimiser les retards occasionnés par les manœuvres, ou dans le cadre de notre problème les coûts en carburant. La stratégie du modèle vise alors à déterminer les trajectoires ayant un coût optimal. Les outils mathématiques sous-jacents sont variés : programmation linéaire continue, en nombre entiers, non linéaire, théorie des jeux, algorithmes génétiques, ou encore systèmes intelligents flous (systèmes intégrant et visant à reproduire de l'expertise humaine face à des systèmes complexes).

Une première étude a été faite dans RTCA (1983), où la manœuvre effectuée est choisie comme étant la moins agressive dans un ensemble de manœuvres possibles (montées et descentes). Des fonctions de coûts différentes peuvent être considérées : coûts en temps, carburant, ou encore la charge de travail sont assez simples à modéliser, mais des métriques de coopération ne sont pas envisagées, car plus difficiles à modéliser.

Krozel (1997) traite la résolution de conflits sous le paradigme du vol libre avec des objectifs économiques. L'auteur développe un modèle statistique basé sur le mouvement relatif de deux avions, et considère différents objectifs économiques, comme la consommation de carburant et les coûts en temps pour revenir à la configuration initiale. Il ordonne également les manœuvres

suivant leur coût associé : les changements d'altitude sont considérés alors plus économiques que les changements de vitesse.

Shewchun *et al.* (1997) proposent un modèle utilisant de l'optimisation semi-définie positive. Les auteurs étudient les conflits impliquant deux avions, suivant les prévisions de leur trajectoire, sous une incertitude donnée.

Frazzoli *et al.* (1999) ont développé un modèle en deux dimensions de résolution de conflits impliquant plus de deux avions : les auteurs formulent un problème non convexe et quadratique qu'ils approximent par un programme semi-défini convexe. La solution optimale de ce problème est alors utilisée pour générer aléatoirement des manœuvres de résolution réalisables et localement optimales.

Plusieurs travaux, notamment celui de Galdino *et al.* (2007), ont proposé des approches performantes ne considérant que deux avions, mais pouvant entraîner des collisions "en cascade" pour plus de deux avions.

Hu *et al.* (2002) considèrent des manœuvres comme des fonctions C^1 par morceaux, et recherchent les manœuvres optimales dans un contexte à deux avions en trois dimensions. Pour des cas à plus de deux avions, des manœuvres en triangle sont considérées. Les auteurs utilisent de la programmation conique du second ordre, via des contraintes portant sur la vitesse maximale ainsi que sur les angles de changements de cap. Cependant le modèle se base sur des hypothèses trop restrictives, comme des heures de départ et d'arrivée identiques pour tous les avions. Dans Hu *et al.* (2003), les auteurs se concentrent sur le cas à deux dimensions et développent un algorithme aléatoire d'optimisation convexe.

Christodoulou et Costoulakis (2004) proposent un modèle de programmation non linéaire à variables mixtes pour résoudre le problème en trois dimensions, en autorisant à la fois des changements de cap et de vitesse. Cependant, l'effort de calcul requis est considérable et les auteurs ne précisent pas quels outils de calcul ont été utilisés.

Mao *et al.* (2005) considèrent un modèle où les appareils effectuent des changements de vitesse instantanés entre deux avions en conflit tout en ne déclenchant pas de conflits en cascade pour les avions voisins. Cependant, de telles manœuvres ne sont pas les plus réalistes et l'effort de calcul requis est très conséquent.

Pallottino *et al.* (2002) présentent deux modèles en nombres entiers permettant des manœuvres de résolution de conflits entre avions, basés sur des contraintes de séparation purement géométriques : un premier modèle ne permettant que des changements de vitesse pour les avions, à direction de vol constante, et un autre où le changement de cap est autorisé à vitesse constante. Leurs modèles permettent de résoudre des cas contenant jusqu'à 15 appareils voulant croiser le même point de passage en même temps. Cependant, ce modèle se révèle limité dans la mesure où il ne considère pas les trois dimensions, et que seul un type de

manœuvre est autorisé à la fois. Le défaut de leurs modèles, notamment du modèle de changement de vitesse, réside dans la possibilité d'instances non réalisables, comme le cas de deux avions s'approchant l'un de l'autre en face à face. Concernant le modèle de changement de cap, un retour à la configuration initiale n'est pas envisagé, et il n'est donc pas expliqué comment les avions atteignent leur destination après avoir fait leur manœuvre.

Alonso-Ayuso *et al.* (2010) proposent un modèle amélioré, où ces problèmes peuvent être évités en ajoutant la possibilité pour les appareils de choisir leur altitude de vol, et les cas problématiques sont évités via un prétraitement. Leur modèle permet aux appareils de retrouver leur configuration initiale suite aux manœuvres en introduisant une pénalité dans l'objectif mesurant l'écart entre les configurations finale et initiale de chaque appareil. Leur modèle peut être implémenté pour du temps réel car les temps de calcul sont courts (2.32 secondes pour une instance à 50 avions et 10 altitudes de vol).

Dans Alonso-Ayuso *et al.* (2012), ce modèle est renforcé via une possibilité de changement de vitesse plus continu, géré par une disctrétisation temporelle, et des trajectoires non rectilignes sont prises en compte. Pour résoudre ce problème, les auteurs proposent un algorithme itératif résolvant une relaxation linéaire de leur modèle, contenant des linéarisations des contraintes non linéaires via des polynômes de Taylor.

Dans les travaux récents, Alonso-Ayuso *et al.* (2014) présentent une heuristique de recherche à voisinage variable permettant de résoudre des conflits par changement de cap.

Les contraintes d'espacement énoncées dans Pallottino *et al.* (2002) sont réutilisées dans un article publié par Vela *et al.* (2011). Les auteurs y proposent un modèle de programmation linéaire en nombres entiers qui choisit les déviations et les changements de vitesse pour éviter simultanément tous les conflits en minimisant une approximation du coût en carburant. Tout le travail se fait en 2D (les avions circulent par palier) et les changements de vitesse ou de cap des avions sont instantanés et s'appliquent sur tout le secteur d'observation. Les trajectoires modifiées sont considérées comme rectilignes à vitesse constante et/ou des triangles avec un point à l'entrée du secteur, un à la sortie et le troisième juste hors de la zone critique. L'avantage de la méthode proposée est qu'elle propose des temps de calculs relativement performants (10 secondes pour une instance à 15 avions, et 85 secondes pour une instance à 25 avions). Cependant, aucun retour sur trajectoire n'est prévu dans la résolution.

Dans la lignée directe du précédent article, Vela *et al.* (2009a) développent deux modèles paramétrés prenant en compte la charge de travail des contrôleurs aériens, basés chacun sur une modification du modèle développé dans Vela *et al.* (2011). Le premier utilise β comme seuil maximal d'opérations à traiter, et un terme de pénalité est introduit dans la fonction objectif. Le second modèle n'ajoute pas de contrainte, mais introduit juste dans la fonction objectif la norme $L1$ du vecteur de toutes les manœuvres, pondérée par un paramètre λ. Les

simulations montrent que le second modèle est plus flexible et équilibré que le premier modèle.
Christodoulou et Kodaxakis (2006) proposent un modèle de programmation non linéaire à variables mixtes pour résoudre le problème en trois dimensions, en détectant les conflits et en les résolvant via des changements de vitesse. Ici également, le temps de calcul semble important et les outils utilisés ne sont pas précisés.
Pannequin *et al.* (2007) étudient le problème de conflits entre appareils sous des conditions météorologiques sévères en utilisant un modèle non linéaire de contrôle prédictif.
Dans Durand et Alliot (2009), les auteurs présentent une autre approche utilisant une heuristique de type colonie de fourmis. Chaque fourmi représente une trajectoire d'avion et un algorithme résout le problème en deux dimensions.
Barnier et Allignol (2009) ont développé un modèle de programmation par contraintes considérant des trajectoires à quatre dimensions, i.e., avec une dimension temporelle supplémentaire.
Enfin, Omer (2013) propose dans sa thèse de doctorat des méthodes d'optimisation mathématique permettant de traiter en quelques secondes des conflits compliqués impliquant moins de dix avions. L'auteur développe dans une première partie une méthode d'optimisation en deux temps visant à minimiser la consommation en temps et en carburant des avions. Dans un premier temps, il résout un programme linéaire approximatif à variable mixtes spécifiant ainsi de quel côté de la zone de sécurité les avions vont s'éviter, indiquant ainsi quelles contraintes disjonctives d'espacement vont vraisemblablement être actives. Ceci donne un bon état initial à passer en entrée d'un modèle non-linéaire de résolution de conflits. Omer (2015b) propose un modèle de résolution de conflits utilisant une discrétisation spatiale du problème. Ce modèle est ensuite comparé avec ceux de Omer (2013) dans Omer (2015a).

Autres

Dans cette section, nous donnons une sélection de travaux utilisant des méthodes différentes de celles abordées précédemment.
Tomlin *et al.* (1998a) présentent une méthode de résolution de conflits où à la fois des changements de vitesse et de cap sont autorisés, avec un algorithme utilisant des algèbres de Lie et des équations de type Hamilton-Jacobi-Isaacs.
Bicchi et Pallottino (2000) ont proposé une approche basée sur la théorie des jeux et le contrôle optimal pour traiter la résolution de conflits, sous des hypothèses de trajectoires rectilignes et de vitesse constante.
Bayen *et al.* (2005) ont développé un modèle lagrangien permettant des manœuvres simples comme changer de cap ou augmenter la vitesse, ainsi que des raccourcis dans les trajectoires.
Plus récemment, Alam *et al.* (2009) ont travaillé sur de l'analyse de données de la façon

suivante : les auteurs ont d'abord choisi plusieurs algorithmes (ceux présentés dans Dowek *et al.* (2001) et Erzberger et Paielli (1997)) et, pour chaque conflit, ont comparé les performances de chacun afin de déterminer quel était le plus efficace dans la résolution du conflit. Les manœuvres possibles étaient au préalable définies pour chacun des algorithmes choisis. Leur analyse permet également de déterminer quelles sont les raisons à l'origine de conflits non détectés ou de fausses alertes.

Plus récemment, Peng et Lin (2010) ont étudié deux différents modèles en deux dimensions, où des manœuvres indépendantes sont considérées (changement de cap ou changement de vitesse) et proposent des contraintes géométriques semblables à celles de Pallottino *et al.* (2002).

2.1.3 Tableau de synthèse

Afin de synthétiser la littérature passée en revue, les modèles cités précédemment ainsi que leurs principales caractéristiques sont rassemblés dans le tableau 2.1. Nous distinguons la détection et la résolution des conflits, qui si elles sont traitées, comportent un "O" dans la case correspondante. Les manœuvres autorisées peuvent être verticales (V), horizontales (H) ou changement de vitesse (C). Le nombre d'avions considérés sera noté n si les auteurs considèrent un cas général.

Tableau 2.1 – Synthèse des articles référencés

Article	Détection	Résolution	Manœuvres	Nb d'avions	Dimension
Alonso-Ayuso *et al.* (2012)	O	O	VC	n	3D
Alonso-Ayuso *et al.* (2010)	O	O	VC	n	3D
Alonso-Ayuso *et al.* (2014)	O	O	H	n	3D
Barnier et Allignol (2009)	O	O	HC	n	3D
Bayen *et al.* (2005)	O			n	2D
Bicchi et Pallottino (2000)	O	O	H	n	2D
Carpenter et Kuchar (1997)	O	O	HC	2	2D
Cetek (1999)	O	O	C	2	2D
Christodoulou et Costoulakis (2004)	O	O	HC	n	2D
Christodoulou et Kodaxakis (2006)	O	O	C	n	3D
Christodoulou et Kontogeorgou (2008)	O	O	C	n	3D
Dowek *et al.* (2001)	O	O	HVC	n	3D
Durand *et al.* (2000)		O	H	2	2D
Durand et Alliot (2009)	O	O	H	n	2D
Erzberger et Paielli (1997)	O			2	2D
Erzberger *et al.* (1997a)	O	O	HVC	n	3D
Galdino *et al.* (2007)	O	O	HC	2	2D
Hu *et al.* (2002)		O	HVC	n	3D
Hu *et al.* (2003)	O			n	2D
Jardin (2003)		O	HVC	n	3D
Krozel (1997)	O	O	HVC	n	3D
Mao *et al.* (2005)		O	H	n	2D
Omer (2013)	O	O	HVC	$n < 10$	3D
Omer (2015b)	O	O	HVC	$n < 10$	3D
Pallottino *et al.* (2002)	O	O	HC	n	2D
Pannequin *et al.* (2007)		O	HVC	n	3D
Peng et Lin (2010)	O	O	HC	2	2D
Prandini et Hu (2008)		O	HC	n	2D
Tomlin *et al.* (1998a)		O	H	2,3	2D
Vela *et al.* (2009a)	O	O	H	n	2D
Vela *et al.* (2011)	O	O	HC	n	2D

2.2 Détection et résolution de conflits dans un cadre incertain

2.2.1 Les incertitudes en contrôle aérien

Les études décrites dans la section précédente supposent des hypothèses de prédictions exactes des trajectoires des aéronefs, ainsi que des instructions de résolution de conflits suivies exactement. Cependant en réalité, le trafic évolue de façon incertaine. En effet, les prédictions des trajectoires reposent notamment sur des prévisions météorologiques ou des mesures des paramètres physiques d'avions pouvant être erronées. Par conséquent, la détection de conflits n'est pas toujours exacte, et la résolution de conflits n'est pas forcément effectuée avec précision. Pour assurer la sécurité du réseau, il devient alors primordial de pouvoir prendre en compte ces incertitudes dans le développement de modèles d'optimisation du contrôle aérien.
Dans cette section, nous allons présenter des études se basant sur des prédictions probabilistes des trajectoires des aéronefs. La complexité des calculs dépend alors du type de prédiction et de la modélisation des erreurs. La revue de littérature du domaine est construite de la façon suivante. Nous présentons les différentes méthodes de modélisation des erreurs en section 2.2.2. Les méthodes permettant d'obtenir une formule analytique de la probabilité de conflits sont décrites dans la section 2.2.3. La section 2.2.4 détaille les approches suivant des simulations.

2.2.2 Modélisation des erreurs

Les incertitudes lors de la détection et la résolution de conflits sont prises en compte soit par une observation de leur effet global au niveau du trafic, soit en modélisant mathématiquement les causes de ces incertitudes.

Effet global des incertitudes

Pour des vols stabilisés en altitude, l'effet global des incertitudes est perçu comme une erreur sur les composantes latérale et longitudinale de la trajectoire des aéronefs. L'erreur longitudinale est la distance entre la position prédite et la projection orthogonale de la position réelle sur la trajectoire prédite. L'erreur latérale est la distance entre la position réelle et la trajectoire prédite.
Ballin et Erzberger (1996) quantifient l'erreur longitudinale à partir de données de vols dans la région de Dallas. Les résultats indiquent que l'erreur longitudinale suit une loi normale centrée dans la variance est proportionnelle au temps. Le facteur de proportionnalité a pour valeur typique 0.25NM.min^{-1}. Cette modélisation est suivie par d'autres études comme Bashllari *et al.* (2007) ; Erzberger *et al.* (1997a).
Irvine (2002) modélise également l'effet des incertitudes sur l'erreur latérale par une variable gaussienne. La différence avec l'erreur longitudinale est que cette dernière n'est pas gérée de la

même façon par le *Flight Management System* (FMS) qui ne compense pas pour la rattraper, ce qui fait qu'elle croît plus vite avec le temps.

Modélisation des incertitudes

Une majorité des études modélisant les perturbations plutôt que leurs effets se sont concentrées sur la modélisation du vent. En effet, le vent est une structure complexe à modéliser : il se décompose en une composante nominale (les prédictions) et une composante aléatoire (l'écart relatif aux prédictions), et il possède une corrélation spatio-temporelle qu'il faut prendre en compte. En effet, sans corrélation, les erreurs de prédiction deviennent indépendantes par avion (voir Vela *et al.* (2009c) pour un exemple). Ceci n'est pas réaliste car des aéronefs proches vont subir des vents corrélés, ce qui peut impacter la détection et la résolution de conflits.

Les travaux utilisant des structures de corrélation du vent se basent sur les études statistiques de Cole *et al.* (1998) et Schwartz *et al.* (2000) modélisant analytiquement la covariance du vent horizontal. Pour ce faire, les auteurs ont comparé des mesures réelles de vent avec un modèle météorologique prédictif. Parmi les articles utilisant ces résultats, Glover et Lygeros (2004) décrivent l'effet du vent pendant un virage ainsi que l'adaptation nécessaire du FMS pour effectuer le virage avec un rayon de courbure constant. Lygeros et Prandini (2002) développent également un modèle d'action du FMS suivant l'effet du vent.

Un autre type d'erreurs ayant été traité dans la littérature sont les erreurs de mesure de la vitesse des aéronefs. Chaloulos et Lygeros (2007) décrivent l'erreur longitudinale résultant de ces erreurs, qu'ils modélisent comme des variables aléatoires gaussiennes centrées, indépendantes entre aéronefs.

2.2.3 Obtention d'une formule analytique de la probabilité de conflit

L'avantage des méthodes obtenant une formule analytique de la probabilité de conflit est qu'elles permettent une intégration plus aisée dans des modèles d'optimisation. Cependant, les hypothèses faites afin d'obtenir les formules peuvent parfois être restrictives.

Irvine (2002) se base sur une interprétation géométrique de la configuration des avions afin de trouver une formule analytique des erreurs latérale et longitudinale dues à l'effet global des incertitudes. Il cumule ensuite ces erreurs à l'instant initial pour faire évoluer les aéronefs dans un cadre déterministe. Irvine (2003) intègre l'expression trouvée de la probabilité de conflit dans un modèle de résolution de conflits à deux aéronefs.

Alliot et Durand (2011) étudient l'effet d'un champ de vent constant sur les aéronefs, afin de quantifier le nombre maximal de conflits supplémentaires à détecter. Pour cela, les auteurs

calculent un intervalle dans lequel les aéronefs doivent se situer à l'instant initial afin de ne pas être en conflit.

Prandini *et al.* (2000) proposent un modèle probabiliste de résolution de conflits utilisant un algorithme de descente de gradient. Cet algorithme utilise une formule approchée de la probabilité de conflits entre aéronefs. Les trajectoires sont déterminées à chaque pas de temps : le nouveau cap à suivre est calculé selon une combinaison du gradient de la probabilité de conflit et de la destination des aéronefs.

Vela *et al.* (2009c) présentent un modèle d'optimisation stochastique à deux niveaux avec recours. Dans un premier temps, des manœuvres en vitesse sont envoyées, et des manœuvres de recours sont envoyées dans un second temps si la réalisation des incertitudes fait que la séparation n'est pas maintenue avec les manœuvres communiquées en premier. Omer (2013) propose également un modèle d'optimisation stochastique avec recours, où il étend un des modèles déterministes présentés plus tôt dans sa thèse au cadre stochastique.

2.2.4 Approches par simulation

L'avantage de ces méthodes est qu'elles permettent de prendre en compte des modèles complexes d'incertitudes. Cependant les temps de calculs demeurent très grands.

Dans Sherali *et al.* (2003), une formulation considérant deux représentations probabilistes des trajectoires des vols, prenant en compte les erreurs dues aux systèmes de navigation, ou encore au vent, est présentée. Ce module est couplé à celui de Sherali *et al.* (2000) avant de développer les contraintes de résolution de conflits. La modélisation de l'équité entre les différentes compagnies aériennes impliquées est complexifiée : la formulation prend en compte les coûts relatifs d'une compagnie par rapport aux coûts totaux, et formule des contraintes sur la dispersion de l'efficacité relative des compagnies par rapport à une efficacité globale pondérée. Dans Sherali *et al.* (2006), le détail des fonctions de coût est donné, ainsi que des procédures pour attribuer des valeurs aux différents paramètres du problème et une batterie de tests et différentes analyses de sensibilité.

Lymperopoulos et Lygeros (2010) utilisent des simulations de Monte-Carlo afin d'obtenir un modèle prédictif de trajectoires des aéronefs. Visintini *et al.* (2006) se sont basés sur les travaux de Lymperopoulos et Lygeros (2010) pour optimiser les trajectoires d'aéronefs suivant le processus de Monte-Carlo. Enfin, Prandini et Hu (2008) formulent un schéma d'approximation stochastique permettant d'estimer la probabilité qu'un appareil traverse une zone interdite de l'espace aérien sous un horizon fini, en utilisant des chaînes de Markov.

Erzberger et Paielli (1997) se basent sur l'estimation de la probabilité qu'un conflit se produise, en fonction des trajectoires prévues et l'incertitude autour de ces prédictions. Des simulations de Monte Carlo sont ensuite faites sur des exemples numériques.

CHAPITRE 3 ORGANISATION DE LA THÈSE

Cette thèse a pour objectif de développer des méthodes mathématiques d'optimisation du problème de détection et de résolution de conflits entre aéronefs. Dans le chapitre 2, nous avons présenté les travaux les plus pertinents pour le résoudre le problème, à la fois dans un contexte déterministe et dans un contexte incertain. Cependant, au meilleur de nos connaissances, il n'existe que très peu d'études se basant sur du trafic augmenté permettant d'anticiper de futures difficultés et de quantifier des objectifs de recherche en optimisation du trafic aérien. De plus, la plupart des modèles présentés ne fonctionnent que sous des hypothèses précises, et la modification de ces hypothèses peut complètement invalider le formalisme mathématique sous-jacent.

En premier lieu, nous quantifions des objectifs de recherche pour le développement d'outils automatisés d'aide à la décision pour le contrôle aérien. Plus précisément, nous étudions les interactions entre les coûts des retards venant de l'allocation de créneaux de décollage et ceux des manœuvres de résolution de conflits, et ce dans un contexte de trafic augmenté. Deux résultats principaux sont mis en avant. Premièrement, la capacité du réseau est critique quand le trafic augmente : en effet, si celle-ci n'est pas modifiée, les coûts des retards dus à l'allocation de créneaux de décollage augmentent exponentiellement. Deuxièmement, l'augmentation de la capacité du réseau n'est pas envisageable d'un point de vue de la charge de travail du contrôleur si les outils disponibles n'évoluent pas. Afin d'obtenir un compromis entre des coûts de retard élevés et une charge de travail trop importante, nous présentons un scénario où la hausse des coûts est contrôlée par une augmentation de capacité. Les nouvelles valeurs des capacités de secteurs représentent un objectif à atteindre pour la recherche dans le domaine du développement d'outils automatisés d'aide à la décision pour le contrôle aérien. Nous présentons les résultats obtenus dans le chapitre 4.

En deuxième lieu, nous présentons un modèle déterministe pour le problème de détection et de résolution de conflits entre aéronefs. Les aspects liés à la dynamique des avions, à leurs manœuvres ainsi que la fonction de coût sont complètement séparés du processus de résolution. En conséquence, le formalisme mathématique présenté reste valide, et ce quelles que soient les hypothèses faites sur les avions, les manœuvres et les coûts. Nous modélisons le problème comme une recherche de clique de cardinalité maximale et de coût minimum dans un graphe. Les sommets du graphe correspondent à des manœuvres des aéronefs, et les arêtes connectent des manœuvres sans conflit d'aéronefs distincts. Ce modèle est en fait une nouvelle variante du problème de recherche de clique de coût minimum, dans le sens où les coûts des sommets dépendent des autres sommets de la clique. Nous formulons cette nouvelle

variante comme un programme linéaire à variables mixtes. Nous présentons également deux méthodes de décomposition pour le problème. La première vise à étudier l'impact du nombre de manœuvres par aéronef sur le temps de résolution, et permet de trouver un compromis entre l'effort calculatoire et l'efficacité de la solution. La seconde vise à exploiter la structure géométrique de l'ensemble d'aéronefs considérés. Le chapitre 5 présente les résultats obtenus avec le modèle et les méthodes de décomposition. Des instances ayant jusqu'à 65 avions sur un seul niveau sont résolues en moins de deux minutes par le modèle classique, et les méthodes de décomposition permettent de résoudre des instances ayant jusqu'à 250 avions répartis sur 20 niveaux de vol en moins de 10 secondes.

En troisième lieu, nous étendons le modèle du chapitre 5 au cadre incertain. Plus particulièrement, nous considérons les erreurs sur la prévision de la trajectoire des aéronefs venant de l'imprécision des prévisions météorologiques et des mesures de vitesse dues à une connaissance incomplète des paramètres physiques des aéronefs. Nous introduisons également l'incertitude liée à l'instant de déclenchement des manœuvres venant des communications entre les contrôleurs aériens et les pilotes. Nous quantifions ces erreurs et donnons une expression analytique de la probabilité de conflit entre chaque paire d'aéronefs. Cette formule est utilisée pour modifier la définition d'arêtes dans le graphe présenté au chapitre 5. Nous étudions ensuite le problème avec un angle bi-objectif, en considérant un critère économique (coûts des manœuvres) et un critère sécuritaire (espérance du nombre de conflits), afin de développer une méthode itérative permettant de générer un ensemble de solutions approximant le front de Pareto du problème. Le chapitre 6 présente les principaux résultats obtenus par cette méthode. En moyenne, 6 solutions sont générées en moins de 3 minutes pour des instances ayant jusqu'à 35 avions.

Finalement, une discussion générale est apportée dans le chapitre 7 et une conclusion est présentée au chapitre 8.

CHAPITRE 4 ARTICLE 1 : MEASURING THE INTERACTIONS BETWEEN AIR TRAFFIC CONTROL AND FLOW MANAGEMENT USING A SIMULATION-BASED FRAMEWORK

Auteurs : Thibault LEHOUILLIER, Jérémy OMER, Cyril ALLIGNOL, François SOUMIS.
Soumis à : EURO Journal on Transportation and Logistics.

Abstract

Air traffic in Europe is predicted to increase considerably over the next decades. In this context, we present a study of the interactions between the costs due to ground-holding regulations and the costs due to en-route air traffic control. We describe a traffic simulator that considers the regulation delays, aircraft trajectories, and air conflict resolution. Through intensive simulations based on traffic forecasts extrapolated from French traffic data for 2012, we compute the regulation delays and avoidance maneuvers according to two scenarios: the current regulations and no regulations. The resulting cost analysis highlights the exponential growth in regulation costs that can be expected if the procedures and the airspace capacity do not change. Compared to the delay costs, the costs of the air traffic control are negligible with or without regulation. The analysis reveals the heavy controller workloads when there are no regulations, suggesting the need for regulations that are appropriate for large traffic volumes and an improved ATC system. These observations motivate the design of a third scenario that computes the sector capacities to find a compromise between the increase in the delay costs due to ground-holding regulations and the increase in the controller workload. The results reveal the sensitivity of the delay costs to the sector capacity; this information will be useful for further research into ATM sector capacity and ATC automated tool design.

4.1 Introduction

4.1.1 Context and main concepts

Delays in air traffic can arise from many sources, including the regulations required to avoid congestion on the network. In Europe in 2012, the average delay due to regulations reached 1.15 minutes per flight, as stated in EUROCONTROL (2012). According to the latest long-term forecast issued by EUROCONTROL (2013), traffic volumes are predicted to increase by 20% to 80% between 2012 and 2035, resulting in much higher congestion around and between airports and increased regulation delays. Joint European projects that are currently underway aim to remodel air traffic management (ATM) in Europe to adapt it to future traffic flow

characteristics. Many of these projects are included in the SESAR (Single European Sky ATM Research) program, whose master plan is detailed in SESAR Joint Undertaking (2012). Currently, the European ATM system is composed of several layers with different time horizons, aiming to safely and efficiently handle the flow of aircraft. A few months in advance, the airspace management filter is triggered. It defines the structure of the route network and the navigation procedures. The airspace is divided into control sectors, which are three-dimensional regions that are each the responsibility of a pair of controllers.

To maintain the workload of the controllers at an acceptable level, each control sector has a *capacity*, defined as the maximum number of aircraft entering the sector in one hour (typically, between 20 and 40 aircraft per hour for a control sector in Europe). Airspace capacity estimation methods have already been developed. A study estimating the airspace capacity in Europe as a combination of different types of air traffic movement in different sectors has been performed by Majumdar *et al.* (2002). More recently, a simulation-based approach has been designed by Steiner and Krozel (2009). They used ensemble-based weather forecasts to generate probability distributions of airspace capacities. Their model has been extended by Clarke *et al.* (2013), who developed a more general model including an air traffic control (ATC) module and capturing traffic-related uncertainties. However, they did not analyze the costs incurred or the impact on the network.

From a few days to a few hours in advance, air traffic flow management (ATFM) regulates the traffic to enforce the sector capacities. This task is assigned to the Central Flow Management Unit (CFMU), whose work relies on traffic predictions based on pilots' flight plans. During peak periods, the CFMU issues ground-holding regulations for flights over congested areas of the airspace by automatically assigning take-off slots via the computer assisted slot allocation (CASA) algorithm, which works in a greedy *first-planned, first-served* fashion. The ground-holding problem (GHP) was defined by Vranas *et al.* (1994b) and has been widely studied since. The techniques in the articles include stochastic models (see for instance Murkherjee and Hansen (2007)) and shortest path problems (see Vranas *et al.* (1994a)). Since congestion in the United States is primarily related to important hubs whereas in Europe both airspace and airport capacities can cause congestion issues, most studies focus on European traffic. For instance, the difficulties and potential improvement points of European ATFM have been studied by Lulli and Odoni (2007).

ATC aims to manage air traffic on a short-term horizon. The main tasks of the controllers are to monitor the traffic and to keep the aircraft separated by at least 5 NM horizontally or 1000 ft vertically, as depicted in Figure 4.1. To resolve conflict situations, i.e., to avoid predicted losses of separation between two or more aircraft, the controllers issue maneuvers to the pilots. These maneuvers involve changes in the speed, heading, or flight level, and they

induce costs due to fuel consumption and delays.

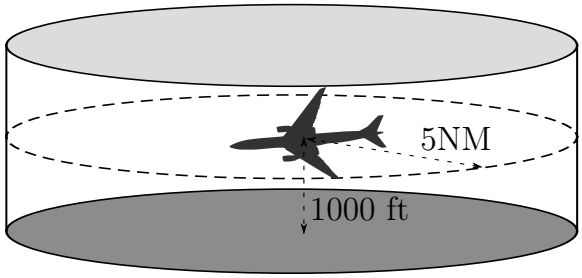

Figure 4.1 – Vertical and horizontal separation. No other aircraft can be inside the cylinder at any time.

In their study of traffic complexity, Kopardekar *et al.* (2008) states that if the traffic becomes twice as dense, no controller will be able to monitor and issue maneuvers without an automated tool, which indicates the need for optimization in this domain. Automated ATC has been thoroughly studied, and numerous algorithms have been developed. The literature on aircraft conflict detection and resolution is vast; the techniques applied include mixed integer linear programming (see Omer (2013); Vela *et al.* (2011)), nonlinear programming (see Raghunathan *et al.* (2004); Alonso-Ayuso *et al.* (2012)), metaheuristics (Durand *et al.* (1996); Alonso-Ayuso *et al.* (2014) for example), semidefinite programming, like Frazzoli *et al.* (1999), and force field models (see Hoekstra *et al.* (1998)). Martin-Campo (2010) provides a comprehensive survey. Research has been conducted to test conflict resolution in a context of growing traffic. For instance, Farley and Erzberger (2007) base their computational tests on future traffic.
In a second step, we aim at studying how quantified objectives could be set for a continuous improvement of ATM. Our main assumption in this study is that the delay costs due to ground holding regulations should not grow faster than linearly with the increase of traffic.

4.1.2 Contribution statement

Our literature review highlights that significant progress has been achieved at all levels of decision of ATM. To push the research further, more bridges between those levels have to be built. In other words, a better understanding of the interactions between the different decision levels would help the improvement of the ATM system as a whole. More specifically, a study focusing on these interactions in a context of extrapolated traffic would be of great value to the field, since it would be fundamental for a better understanding of future situations and their inherent difficulties. To find possible solutions to these upcoming challenges, the knowledge of the aforementioned interactions could highlight key features needed from future optimization tools, and could drive the research towards the main subjects of improvement.

Despite the diversity of the literature, we have found few work aiming at filling these gaps. Our motivation is two-fold. We first want to identify the main bottlenecks in terms of costs and security in ATFM and ATC. For this, our approach is to apply a progressive increase in the traffic volume using the reference values of EUROCONTROL (2010, 2013), and analyze the evolution of the ATFM and ATC costs, and that of the controllers' workload. For ATFM, we focus on the ground-holding and the delay costs, whereas for ATC we study the avoidance maneuver costs and the controller workload. In a second step, we aim at studying how quantified objectives could be set for a continuous improvement of ATM. Our main assumption in this study is that the delay costs due to ground holding regulations should not grow faster than linearly with the increase of traffic. For this, we design a scenario controlling the growth in ground-holding costs with an increase in sector capacities. The capacity values computed allow us to determine objectives for research on ATM improvement.

The paper is be organized as follows. Section 4.2 describes the mechanics of the automated tools we used in our simulations. Section 4.3 describes the traffic data used, along with the ground-holding cost model and the controller's workload measures. In Section 4.4, we study the interactions between ATC and ATFM by simulating traffic with and without ground holding regulations. Section 4.5 provides a possible answer to observations made in Section 4.4, with a design of a scenario representing a trade-off between high ground-holding costs and heavy workloads.

4.2 Description of the simulation algorithms

The study of the interactions between ATFM and ATC requires several automated procedures: a trajectory simulator, a ground-holding algorithm, and a conflict solver. Figure 4.2 provides an overview, with references to the sections in which we discuss each component.

4.2.1 Traffic increase

To increase the traffic to reflect the available forecasts, we use a procedure parametrized by a multiplying factor. Given an increase factor f (e.g., $f = 0.4$ for a 40% increase) and an initial set T of n flights, $n_+ = f \times n$ new flights are created. To create a new flight, we randomly choose a flight in T and create a copy with a small random modification to its departure time. The random shift typically lies in $[-15, -1] \cup [+1, +15]$ minutes to avoid the exact duplication of the flight. Excluding the interval $(-1, 1)$ ensures aircraft separation, since an offset of one minute for aircraft taking off at 150 kts ensures the separation.

The main advantage of this method is that it maintains a similar distribution of the departure times over a day of traffic. Indeed, the random shift tends to broaden and flatten the peaks of the distribution, hence giving a conservative lower bound on the actual distribution. A

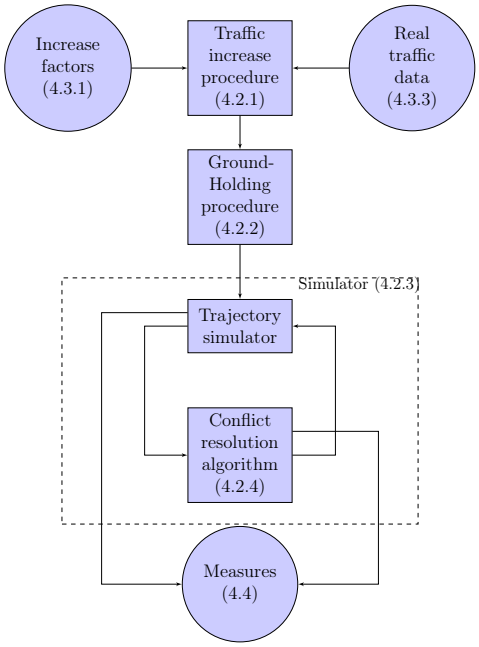

Figure 4.2 – Simulation modules

more realistic forecast would be based on a market study carried out on a global scale, but such information is not yet available.

A drawback of duplicating flights in this fashion is the creation of conflicts with pursuing aircraft. Depending on the random shift, the process may lead to flights that follow each other very closely. To overcome this, we apply a regulation at each airspace entry point to enforce the necessary separation between the flights. Typically, we impose at least two minutes between two flights entering the airspace at the same entry point.

4.2.2 Ground-Holding procedure

The regulations imposed by the CFMU affect the flights crossing regulated areas. These areas are determined on a daily basis by experts, depending mainly on the expected traffic. In a given regulated area, the departure slots are allocated with a ground-holding procedure following a *first planned, first served* scheme, meaning that the order in which aircraft enter the area is not modified.

Figure 4.3 gives a flowchart of the ground-holding algorithm described in Eurocontrol (2011) for a given regulated area. For each such area, CASA maintains a *slot allocation list*, which is a series of consecutive slots of equal length covering the regulation period. For instance, a two-hour period with a capacity of 30 results in an allocation list with 60 two-minute slots. A flight crossing this area has a priority linked to its estimated time over (ETO) the point where it enters the area: the earlier the ETO, the higher the priority. It is important to notice

the cascade effect of this mechanism. Reallocating slots to flights can have consequences for other flights that must also be reallocated, hence increasing the number of delays in the network. One limitation of this algorithm is the independent regulation of each area. If a given flight is regulated in two or more areas, its departure slot must satisfy the most restrictive regulation, which may violate constraints in the other areas. In other words, the ground holding effectively assigned to a flight will be the maximum over the ground-holding delays computed for each regulated area the flight will cross.

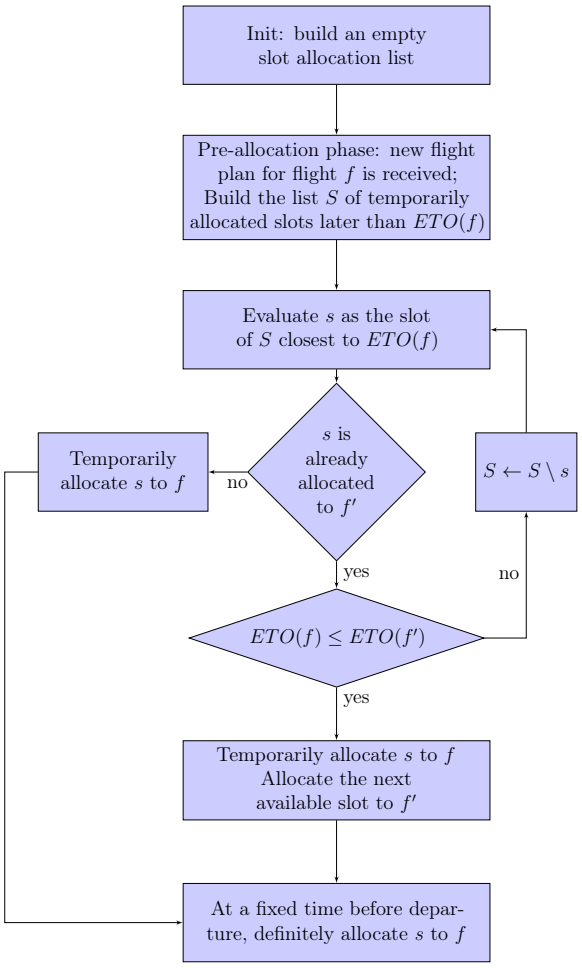

Figure 4.3 – CASA procedure for a regulated area

We implement the CASA algorithm in our simulation engine. For this we use the 2012 French control sectors with their nominal capacities. In pratice, the shape and the capacities of the control sectors can be modified dynamically to adapt to, e.g., bad weather conditions. Although this limitation could have an impact on the results, it does not jeopardize the whole process. Indeed, as stated in Section 4.1 the objective of this paper is to obtain an insight into a future need for optimization. As a consequence, we will be basing our interpretations

on the trends indicated on the results, instead of the accuracy of the figures themselves.

4.2.3 Trajectory simulation

The flight simulations are performed by the Complete Air Traffic Simulator (CATS) described by Alliot *et al.* (1997). CATS is an en-route air traffic simulation engine based on a time-discretized execution model, i.e., the position and velocity vectors of every aircraft are computed at times separated by a period τ set by the user. The aircraft specifications and performance, such as the horizontal and vertical speeds and the fuel consumption, are extracted from the Base of Aircraft Data (BADA) summary tables based on the total energy model described in EUROCONTROL (1998). The simulation engine processes data corresponding to real flight plans and gives detailed outputs including traffic statistics, sector occupation at any time, and a thorough examination of the conflicts: geometry, duration, and conflict-resolution statistics.

4.2.4 Conflict resolution

Our goal is not to study the performance of a particular algorithm or to prove that it is suitable for practical implementation. The conflict resolution module is used only to estimate the costs incurred by the maneuvers that are necessary to maintain the aircraft separation. It is impossible to precisely correlate the costs of the maneuvers designed by an automated conflict solver with those selected by a controller, but the order of magnitude is the same.
The conflict resolution algorithm designed by Durand *et al.* (1996) is used in the simulations because it is already embedded in CATS. Moreover, the performed tests highlight that the maneuvers computed by the model in Durand *et al.* (1996) are more conservative than the ones generated by the native solver in CATS. In the first step, conflicts are detected over a 20-minute horizon, and they are aggregated into independent *clusters*. For instance, if aircraft A conflicts with aircraft B and aircraft B conflicts with aircraft C, then aircraft A, B, and C are aggregated into the same cluster. Each cluster is then deconflicted independently, using a genetic algorithm.
The genetic algorithm is based on the concepts described by Goldberg (1989). The principle is to manipulate a *population* where each *individual* is a candidate solution to the problem. The population is composed of n possible trajectories, one per aircraft. For a given aircraft, the possible trajectories correspond to the discretized set of permissible maneuvers: 7 heading-change values between -30° and 30°, 5 speed changes between -6% and $+3\%$, and, incidentally, altitude maneuvers corresponding to climb interruptions and descent anticipations.
The population is initialized with randomly generated maneuvers for each aircraft. At each step, the quantity to optimize, called the fitness, is computed for each individual, and the

best individuals are selected according to their fitness. These individuals are used as inputs to the cross-over and mutation operators that aim to generate new individuals in the current population.

4.3 Simulation input

4.3.1 Traffic predictions

Medium- and long-term traffic forecasts are regularly issued by EUROCONTROL. Based on a thorough study of current traffic trends and statistics and recent air-industry-related events, the latest mid-term forecast EUROCONTROL (2010) provides predictions for 2013 to 2019, while the long-term forecast EUROCONTROL (2013) extends the analysis to 2035 . Since the predictions depend on the evolution of the global economic situation, several scenarios are considered, and annual growth rates are estimated for each. Table 4.1 summarizes EUROCONTROL (2013).

Table 4.1 – Summary of traffic forecast for Europe to 2035

	Annual growth			
Scenario	Global Growth	Regulated Growth	Happy Localism	Fragmented World
2012–2019	3.4%	2.3%	2.3%	0.9%
2019–2020	3.7%	2.2%	1.5%	0.6%
2021–2025	2.5%	1.9%	1.5%	0.8%
2026–2030	2.2%	1.5%	1.2%	0.4%
2031–2035	1.9%	1.2%	1.1%	0.7%

The scenarios listed in Table 4.1 correspond to different assumptions about the future. Global Growth and Fragmented World depict two extremes situations in which the economic and political circumstances allow flourishing exchanges or cause a recession. In our computational tests, the increased traffic reflects the in-between Regulated Growth scenario, which is more likely. This scenario represents average economic growth along with regulations to address environmental and sustainability issues. Moreover, with this scenario it is assumed that the projected traffic growth will respect future airport departure and arrival capacities. A sufficient range of traffic-increase rates is then achieved by focusing on six specific years between 2014 and 2035. These years and the corresponding traffic rates are given in Table 4.2.

Table 4.2 – Traffic predictions with regulated growth using 2012 as a starting point

Year	2014	2017	2020	2025	2030	2035
Increase	+5%	+12%	+20%	+32%	+42%	+50%

4.3.2 Airspace capacity

CASA needs the capacity of each regulated area. We run the simulations with the following three scenarios:

— S_1 - the capacities remain constant;

— S_2 - the capacities are deleted: there is no ground-holding;

— S_3 - the capacities satisfy a condition corresponding to a controlled growth in the delay costs due to ground-holding.

The scenarios S_1 and S_2 correspond to two extreme situations: in S_1 nothing new is designed to handle greater traffic, and in S_2 the traffic flows freely without any constraint. Our study of S_1 will give a better understanding of the need to modify the current procedures. Focusing on S_2 will enable us to quantify the effect of a worst-case scenario from the ATC point of view. Indeed, S_2 should lead to the worst possible situation in terms of conflicts and the controller workload. Since the design of S_3 is motivated by the results given in Section 4.4, we describe this scenario in Section 4.5.

4.3.3 Description of the reference historical data

The study focuses on French traffic, because we were able to get traffic data and information on the sector capacities and geometry. Moreover, the French airspace is dense because it is a crossroads of various European hubs. We use data for the 2012 traffic over France in our tests. Simulations focus on June, 8^{th}, 2012, since it was a typical busy day.

4.3.4 Delay and maneuver costs

EUROCONTROL (2012) estimates that in 2012, ATFM delays in Europe cost €0.85 billion. For a given flight, the costs depend on a variety of factors, such as the operational conditions, the phase of flight where the delay occurs, the type and size of the aircraft, and the load factor. As a consequence, we need a large quantity of data for a thorough study of the cost model.

Our study focuses on two types of costs. First, we consider delays induced by maneuvers issued by the ATC. These costs depend on the maneuver model and on the air conflict solver used, since its performance will impact the commands issued. We observe again that if the traffic becomes twice as dense, no controller will be able to monitor and issue maneuvers

without an automated tool, as stated by Kopardekar *et al.* (2008). Thus, a conflict solver is a valid tool for addressing the ATC costs. The planned maneuvers lead to extra fuel consumption. We use the model described in the BADA user manual EUROCONTROL (2011) to compute the consumption, which depends mostly on the type, speed, and altitude of the aircraft. It is computed for three maneuvers: speed, heading, and altitude changes. Second, delay costs are introduced when the ground-holding leads to allocated slots that differ from the airlines' preferred slots. Modeling these costs properly is a complex task; the passenger, crew, and maintenance costs must be taken into account. It is also important to study the consequences of a delay on the whole network: one delay will lead to further delays in the rotation that includes the delayed flight.

In the literature, passenger costs are usually divided into "hard" costs representing compensation costs such as the cost of rebooking passengers, and "soft" costs such as the cost of passengers switching to another airline because of recurring delays. Joint work on this topic between the University of Westminster and EUROCONTROL resulted in a series of articles published between 2004 and 2011. The cost per minute per passenger of ground and airborne delays due to ATFM is derived in Cook *et al.* (2004). In Cook and Tanner (2009), the authors estimate the airline delay costs as a function of the delay magnitude. This function is combined with fuel consumption and future emission charges to derive a cost-benefit trade-off during the ground and airborne phases. In Cook and Tanner (2011a), the authors focus on the costs related to delay propagation in the network. Those delays can be either rotational (i.e., related to flights within the rotation) or nonrotational. Using values extracted from Beatty *et al.* (1999), the authors derive cost values that depend on the rotation structure, the aircraft involved, and the magnitude of the delay. The results from the earlier articles are collected in Cook and Tanner (2011b), which gives reference values for the delay costs incurred at both the strategic and tactical levels. The report presents cost values for all the phases of a flight: at-gate, taxi, cruise extension, and arrival. The values are assigned under different scenarios (low, base, and high), for twelve different aircraft types. Sample costs are given in Table 4.3 for the at-gate base scenario.

We use the costs that were computed under the base-case hypotheses in Cook and Tanner (2011b). We also assume that companies ask for their preferred take-off slots. Thus, the slots allocated by CASA provide a valid estimate of the ground-holding-related delays.

4.4 Impact of the ground-holding regulation

In this section, we focus on the potential impact ground-holding regulations have from an economical and operational point of view. More specifically, we study the evolution of delay costs due to ground-holding regulations, along with the costs of ATC maneuvers. We also

Table 4.3 – Tactical costs (euros, total) of ground-holding delay for different aircraft types.

	Delay (min)			
Aircraft type	15	60	120	240
B733	360	5780	29730	53720
B752	520	8780	45610	81610
B763	880	14510	84200	149510
B744	1230	20760	120940	213950
A320	410	6800	35280	63530
A321	470	8150	42460	76140

quantify the effects on controllers' workload. The air traffic controllers' workload primarily consists of four tasks: monitoring the sector, coordinating the traffic with adjacent sectors, communicating with pilots, and maintaining separation. These tasks are demanding, and it is crucial to determine the impact of increased traffic on the controller workload. We define several performance indicators for the scenarios described in Section 4.3.2:

— the entering flow per hour for a sector, which is correlated with the monitoring and coordination;

— the number of conflicts, which is related to the complexity of maintaining separation;

— the number of conflict-resolution maneuvers, which affects both the monitoring and communications.

We chose this set of measures because they are easy to compute and give a good indicator of the cognitive charge of the controller and the safety risks that could arise in the airspace.

4.4.1 Impact on the entering flow per hour

The airspace surrounding Reims is particularly challenging in terms of traffic complexity: the control sectors are quite small, and they include routes that connect important European hubs such as London, Milan, Zurich, and Frankfurt. We focus on the KR sector, which is a busy sector in the Reims control zone. The motivation behind this choice is to study a zone as challenging as possible, to identify possible bottlenecks in ATC or ATFM. Figure 4.4 displays the flow entering KR per hour for different volumes of traffic, i.e., the current traffic and the traffic increased by 32%, 42%, and 50%. For each traffic volume, statistics are extracted for scenarios S_1 and S_2; in S_1 the ground-holding scheme is based on the nominal sector capacities of 2012, and in S_2 there is no ground-holding regulation.

Figure 4.4 clearly indicates that the flow depends on the presence or absence of ground-holding regulation. Without it, the entering flow distribution tends to aggregate into a peak over the period from 10 a.m. to 12 a.m., leading to a large overcapacity. A threshold on the controller

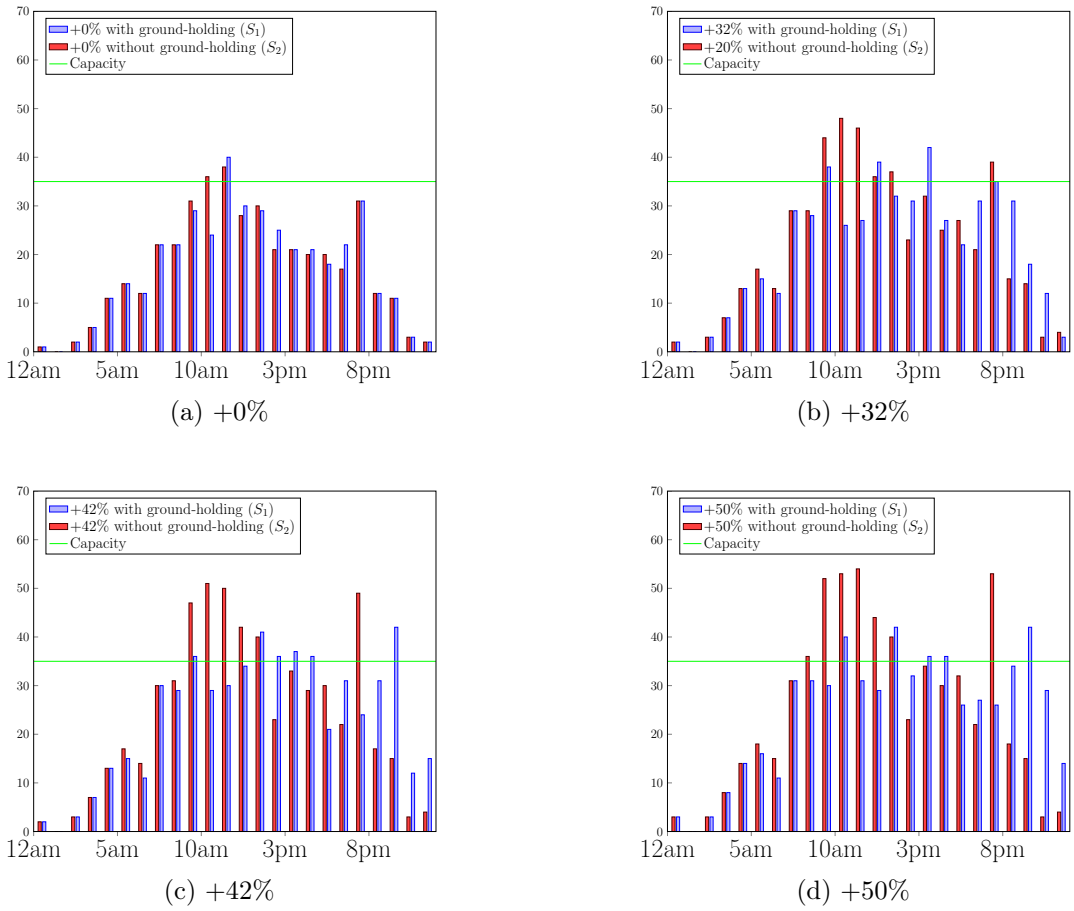

(a) +0% (b) +32%

(c) +42% (d) +50%

Figure 4.4 – Entering flow per hour for different traffic volumes in KR sector

workload may thus be distinguished. Indeed, for traffic volumes greater than +32%, the entering flow per hour may exceed the capacity by more than 12 flights without ground-holding. This would require a tremendous monitoring effort. This suggests that increased traffic needs to be handled with modified regulations or with automated tools that decrease the controller workload. On the other hand, if ground-holding is present, it controls the entering flow to prevent overcapacity. However, the capacity is still exceeded in several cases; this is because of the difficulties the CASA algorithm encounters when a flight is regulated in several sectors. A saturated capacity plateau can be seen, and increasing the traffic volume enlarges the plateau. Moreover, it is important to recall that CASA regulates the traffic by postponing flights. A drawback of this approach can be seen in the last blue column in Figure 4.4d: many flights are delayed between 9 p.m. and 10 p.m., leading to an entering flow of 40 flights, which is 5 flights over the declared capacity of 35 flights per hour.

4.4.2 Impact on the number of conflicts

In addition to the effects on the flow distribution, ground-holding has an impact on the conflicts. Figure 4.5 displays, for each traffic volume previously described, the total number of conflicts per day, along with the number of conflicts per day for different sectors, with and without ground-holding. The sectors represent different types of flow density: two dense sectors, three average sectors, and two sparse sectors.

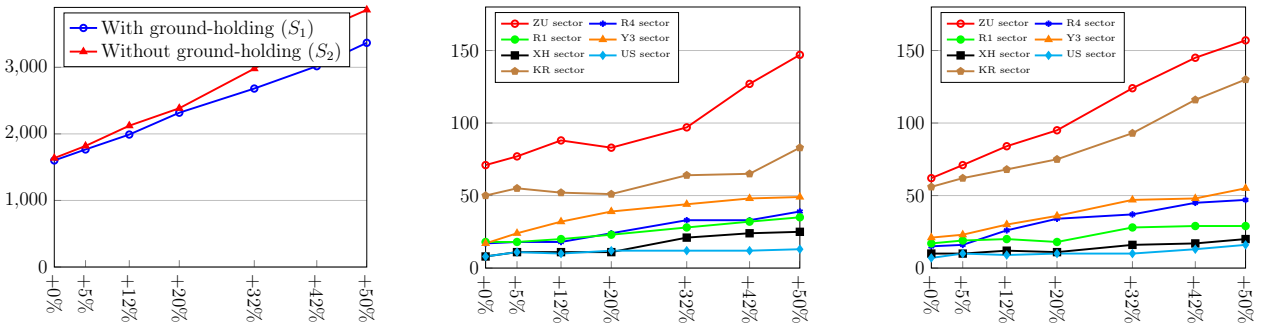

(a) Total (b) With ground-holding (S_1) (c) Without ground-holding (S_2)

Figure 4.5 – Comparison of the number of conflicts observed with and without ground-holding

Surprisingly, Figure 4.5a shows that the removal of the ground-holding does not imply a greater number of conflicts until a traffic volume of +20%. Beyond this approximate threshold, the number of conflicts without ground-holding increases faster than when ground-holding is maintained, leading to a 15% difference for a +50% traffic volume. This observation at the global scale can be paired with an observation at the sector level. The evolution of the number of conflicts with increasing traffic depends on the type of sector, as highlighted by Figures 4.5b and 4.5c. Results suggest that the ground-holding has an impact only on sectors where capacities are already saturated. One of the regulation's main benefits can be highlighted: to prevent overcapacity in different sectors, the ground-holding scheme smoothes the flow, spreading the number of conflicts over the day, as shown in Figure 4.6. This also reduces the workload of the controllers, especially in monitoring and communications. Indeed, as depicted by Figure 4.6d the number of conflicts per hour explodes when no ground-holding regulation is performed, with up to 27 conflicts within an hour.

4.4.3 Cost analysis

Ground-holding and conflict-resolution induce delays whose costs are important aggregate indicators of the overall traffic complexity. These costs are computed as described in Section 4.3.4 and are displayed in Figures 4.7a and 4.7b for scenarios S_1 and S_2. Clearly, there is

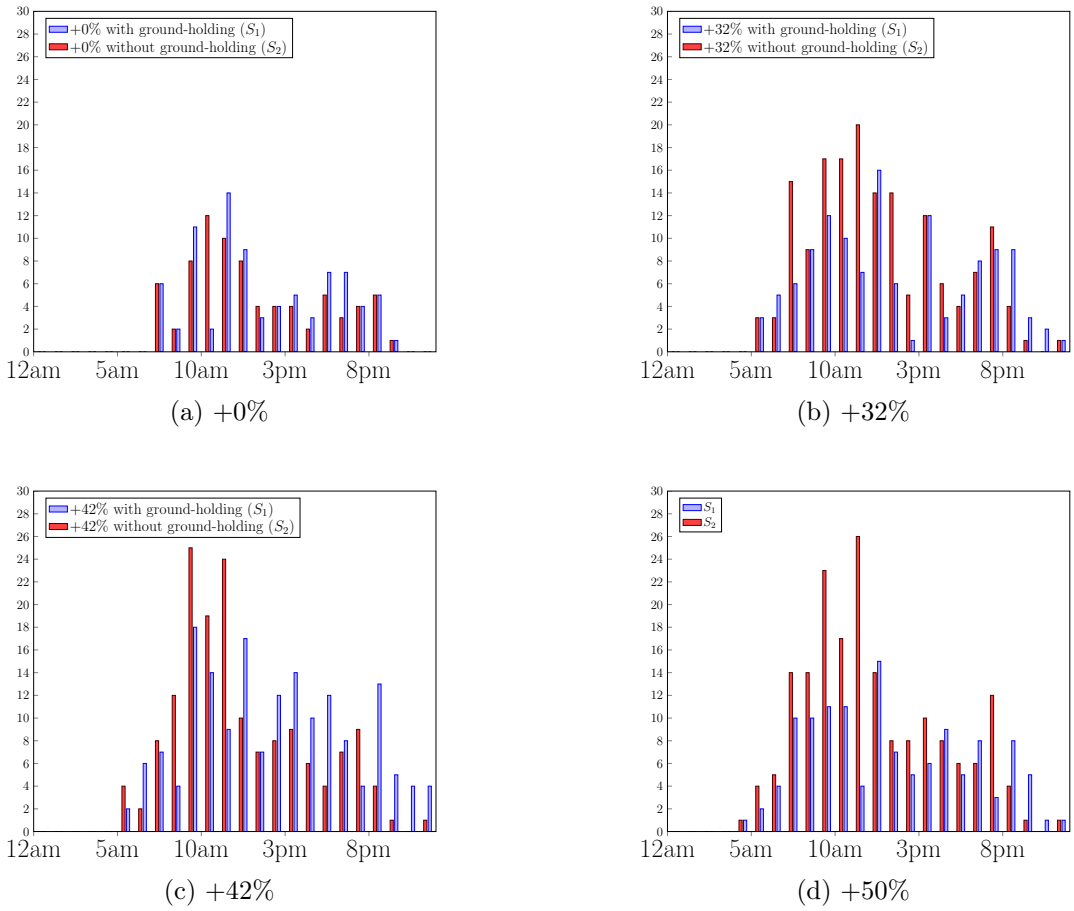

(a) +0% (b) +32%

(c) +42% (d) +50%

Figure 4.6 – Number of conflicts per hour in KR for different traffic volumes

no regulation cost in S_2.

Figure 4.7a suggests that the global costs resulting from ground-holding vary exponentially with the traffic volume. This is a logical trend considering that the intensification of the traffic mainly affects the congested areas during peak periods. Moreover, the plateau effect highlighted in Figure 4.4 shows that the peak periods tend to be flattened and widened, which leads to larger and more expensive delays. This indicates that significant savings could be made by improving the regulation procedure, and it also emphasizes that this improvement is necessary to handle larger traffic volumes.

The expected disadvantage of suppressing ground-holding is that it would result in extra conflict-resolution costs. Without ground-holding, a larger traffic flow must be handled, which increases the number of conflicts and the resolution maneuvers issued in response. Figure 4.7b shows the deconfliction costs for scenarios S_1 and S_2. These global costs are the sum of the costs of the different types of maneuvers described in Section 4.3.4. Of these maneuvers,

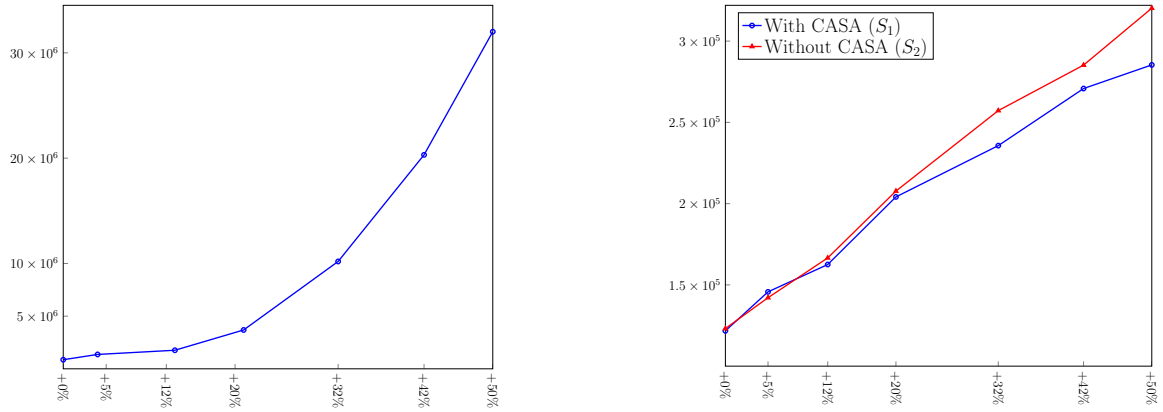

(a) Ground-holding costs (€): 6/8/2012

(b) Deconfliction costs (€): 6/8/2012

Figure 4.7 – Ground-holding and ATC costs for 6/8/2012

speed changes, which are seldom performed and relatively cheap, represent around 1% of the total cost. The remaining costs are equally divided between heading changes and altitude changes, which are more numerous and more expensive. The total costs are similar until the +32% traffic volume, where the conflict-resolution costs increase faster in S_2 than in S_1. This results in 15% larger costs in S_2 for a traffic volume of +50%. Although this is an important increase, the conflict-resolution costs are much smaller than the ground-holding costs: around €250 000 for conflict resolution versus €32 000 000 for ground-holding costs. Thus, the extra costs necessary to handle the traffic are negligible compared to the potential savings made by removing the ground-holding policies.

4.4.4 Impact on the number of maneuvers

Section 4.4.3 shows that removing the ground-holding regulations induces small additional costs for ATC compared to the potential savings, but the impact on the number of maneuvers is major. Indeed, as shown in Figure 4.8, the number of maneuvers issued per hour in dense areas becomes much higher than the current value: up to 27 maneuvers are performed within one hour for a traffic volume of +50%, which represents approximately one command every 2.5 minutes. This corresponds to a considerable workload in addition to the monitoring workload, making the controllers' task even more intensive. Moreover, it represents 27 opportunities where a dramatic incident could occur if mistakes were to be made during the execution of maneuvers.

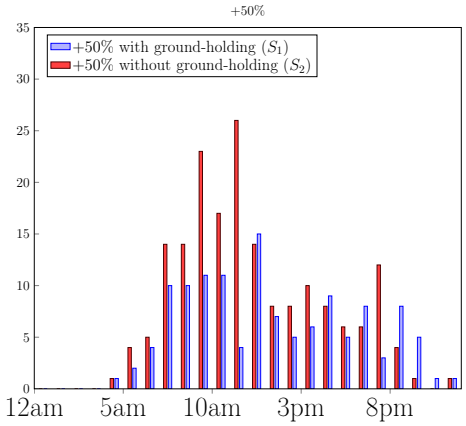

Figure 4.8 – Maneuvers per hour for +50% traffic volume in KR sector

4.5 Finding a compromise between costs and workload

4.5.1 Motivation

The previous section presented a traffic and cost analysis for scenarios S_1 and S_2, which correspond to two extreme situations. The results show that retaining the current sector capacities induces an exponential growth in the ground-holding costs. However, suppressing ground-holding leads to a large increase in the controller workload that is unrealistic with today's tools.

In this section, we make the reasonable assumption that air transportation companies could not handle a growth in the costs of delays due to ground-holding that is linear with the traffic volume. It therefore seems worth investigating a scenario that yields such a growth while keeping the controllers' workload manageable. Such a scenario would set sector capacity values controlling the growth in ground-holding costs. This would be of great value to the field, since it would quantify objectives for the continuous improvement of the ATM system.

4.5.2 Design of the scenario

Figure 4.7a indicates that the ground-holding costs grow exponentially with the traffic volume. The function linking these quantities can be described by a sequence of positive slopes denoted $(s_i)_{i=1,\dots,6}$, with each slope indicating the magnitude of the increase in the delay costs between two consecutive traffic volumes. In other words, a steep slope emphasizes that retaining the current capacities between two traffic volumes leads to a large increase in the regulation costs. Scenario S_3 represents a trade-off situation where the growth in the ground-holding costs is controlled with an increase in the sector capacity. Figure 4.7a is used to determine the average slope s^* for the next five years; this represents an indicator for short-term trends in the cost

increase. This value is used as a ceiling growth rate for the future traffic, hence yielding a bounded increase in the ground-holding costs. To enforce this constraint, we determine the new capacity values for each traffic increase iteratively via Algorithm 4.1. Basically, the algorithm increases the sector capacities until the rate of the cost increase drops below s^*.

Algorithm 4.1. Determining sector capacities for traffic volume increased by $\alpha\%$

1: $\mathcal{C}$: set of current sector capacities
2: D: cost of delays due to the ground-holding for the current traffic
3: $\mathcal{C}_\alpha$: set of sector capacities for a traffic volume increased by $\alpha\%$
4: R_α: cost of delays due to the ground-holding for a traffic volume increased by $\alpha\%$
5: $\mathcal{C}_\alpha \leftarrow \mathcal{C}$
6: **while** $\frac{R_\alpha - D}{\alpha} > s^*$ **do**
7: **for** $c \in \mathcal{C}_\alpha$ **do**
8: $c \leftarrow c + \frac{1}{100}c$

Applying Algorithm 4.1 leads to the capacity-increase percentages listed in Table 4.4. The sector capacities are obtained by rounding down to the nearest integer. These new capacity values represent an interesting indicator for future objectives in terms of continuous improvement of ATC with a fixed growth rate in ATFM costs.

Table 4.4 – Increased capacities for scenario S_3

Traffic volume	Capacity increase
+5%	+4%
+12%	+5%
+20%	+8%
+32%	+16%
+42%	+24%
+50%	+32%

Since the new sector capacities are determined iteratively, it is interesting to plot the ground-holding costs computed at each step of the algorithm; see Figure 4.9.
Figure 4.9 shows that the ground-holding costs are an approximately stepwise decreasing function of the increase in capacity. The increased capacities yielding similar ground-holding costs can be gathered into clusters. Two capacity sets with a difference of 1% are separated by a gap, indicating a large difference in the ground-holding costs. For instance, for a +20% traffic volume, €700000 could be saved daily by increasing the sector capacities by 7% instead of 6%. This difference can be explained by observing the distribution of the magnitude of the delays assigned by the ground-holding regulation. Some capacity values, especially for dense

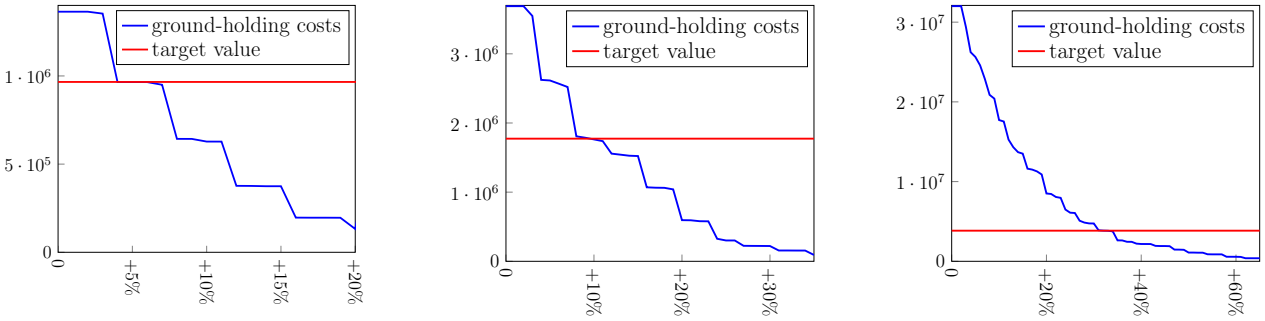

(a) Traffic volume +5%

(b) Traffic volume +20%

(c) Traffic volume +50%

Figure 4.9 – Ground-holding costs for increasing capacities

sectors, can trigger a bottleneck effect on the traffic flow, inducing long and costly delays. This observation is supported by the expanding plateau effect seen in Figure 4.4, where the flights are more and more delayed during peak periods. It is therefore possible to identify threshold capacity values that are critical with respect to the issued delays. Moreover, the shape of the curves indicates that one can expect stepwise improvements in the ground-holding costs.

4.5.3 Cost analysis

Figure 4.10 shows the ground-holding and conflict-resolution costs for the three scenarios. The results for the ground-holding costs suggest an almost linear growth for S_3, as imposed by the constraints of Algorithm 4.1, hence indicating considerable potential savings. The results provide evidence that S_3 represents a compromise situation for ATC. It appears that S_3 is closer to S_2 than to S_1 for high traffic volumes. This is because the constraint on the controlled ground-holding costs imposed in the design of S_3 is strict. More precisely, since the maximum increase rate allowed in the ground-holding costs in S_3 is small compared to the natural rate, the constraint is closer to S_2 than S_1 for high traffic volumes.

4.5.4 Workload analysis

To evaluate how S_3 compares to S_1 and S_2 in terms of the workload, we introduce the metric $OC(.)$ defined as

$$OC(s) = \sum_{h=1}^{24} \max\{0; f_s(h) - c_s\}^2 \tag{4.1}$$

where c_s is a reference capacity value for sector s, and $f_s(h)$ is the entering flow of aircraft for sector s in a given hour h. The measure $OC(s)$ represents aggregated information on the

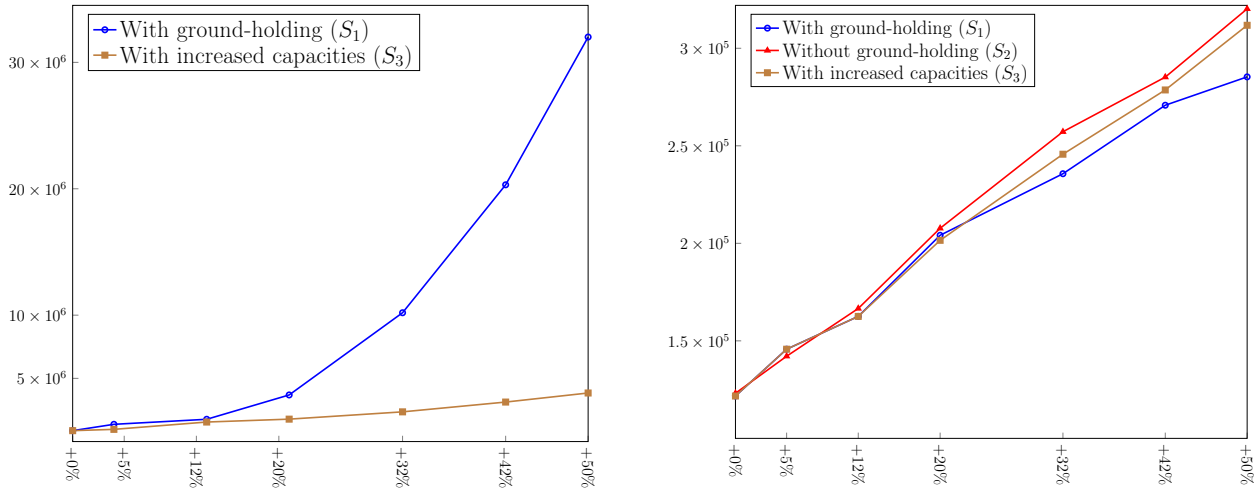

(a) Ground-holding

(b) ATC

Figure 4.10 – Ground-holding and ATC costs for the three scenarios on 08/06/2012

overcapacity for sector s for a given regulation scenario. The greater the value of $OC(s)$, the more effort required from the controller. Moreover, $OC(s)$ tends to penalize situations with high peaks over a short period of time more than situations with lower peaks that last longer. This is consistent for a measure of the controller workload, because a short, high peak is much harder to handle than a lower, broad peak. Figure 4.11 depicts $OC(KR)$ for the traffic simulated under the scenarios S_1, S_2 and S_3 with nominal sector capacities. More specifically:

— the blue curve with circles shows $OC(KR)$ for S_1;

— the red curve with squares shows $OC(KR)$ for S_2;

— the green curve with triangles shows $OC(KR)$ for S_3.

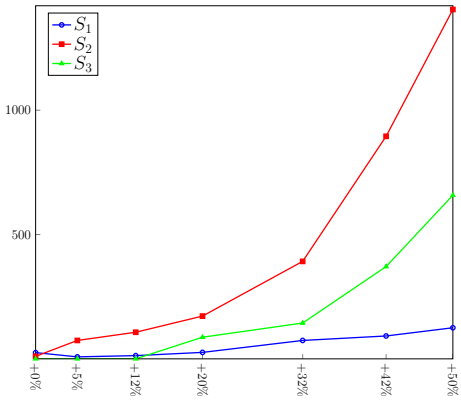

Figure 4.11 – $OC(KR)$ for different traffic volumes and ground-holding scenarios

Figure 4.11 shows that $OC(KR)$ grows exponentially for S_2 whereas it increases slowly for S_1. This observation corroborates our observations in Section 4.4.1: localized high peaks appear in the entering flow distribution for S_2, whereas broader but smaller overcapacity plateaus emerge for S_1. S_3 appears to be a compromise scenario for OC. The curve tends to grow exponentially, but with a much gentler slope than that of S_2, indicating that the traffic simulated with S_3 would require less monitoring and management by the controllers.
The differences between the three scenarios in terms of number of conflict avoidance maneuvers are shown in Figure 4.12. The maximum number of maneuvers computed by the solver in sector KR is reduced from 27 to 20 during the busiest hour, leading to a less challenging situation. The number of maneuvers can be greater for S_3 than for S_2 for several hours after the high peak of S_2. This can be explained by the ground-holding that is applied for S_3: the flights are delayed after the busy peak period, which leads to a greater flow entering the sector and more numerous conflict situations. However, this does not represent an unmanageable task for the controller. Indeed, the high peaks for the conflict-resolution maneuvers are the main challenge for the controllers. Therefore, S_3 represents a situation with a relatively high workload but where the peaks are more manageable than in S_2.

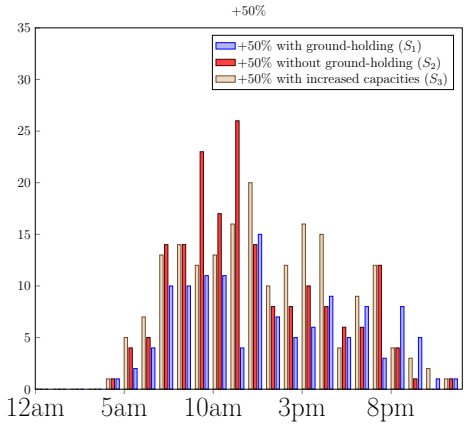

Figure 4.12 – Maneuvers per hour for a +50% traffic volume in KR sector for the three scenarios

4.5.5 Summary

The cost analysis provides insights into possible future ATM network-design objectives: the capacities should find a trade-off between the costs and the workload. The sensitivity of the ground-holding costs to the sector capacity suggests that the ground-holding should be more robust to capacity variations in terms of the costs incurred.

4.6 Conclusion

We have analyzed the interactions between two layers of the ATM, namely the ATFM and the ATC. More specifically, we evaluated the impacts of the current ground-holding regulation scheme on the delay costs, sector loads, and conflict-resolution costs. We used a traffic simulator with modules to compute the regulation delays, to simulate the trajectories, and to resolve the conflicts. We chose French traffic data for a particularly busy day in 2012 as the input for the simulator, and we developed a traffic increase procedure to generate meaningful predictions to 2035.

The analysis of the impact of a traffic increase on ATFM and ATC leads to two major results. First, it shows that the costs due to ground-holding delays are several orders of magntiude larger than those due to conflict resolution maneuvers. Moreover, the ATFM costs should grow exponentially with traffic volume if the capacity of control sectors remain unchanged. Second, it is apparent that ground-holding regulations are necessary from a safety point of view. Without this regulation, the largest number of conflicts to handle in one hour could be multiplied by two. One important consequence of these results is that the improvement of ATC is necessary for the efficiency of the overal ATM system. The air transportation industry will not be able to support an exponential growth in ground-holding delay costs, so there is an absolute need to increase the capacities of the densest control sectors.

The second part of our study aims at setting quantified objectives for these improvements. We thus make the reasonable assumption that ATFM costs should grow at most linearly with traffic volume. A simulation-based iterative procedure then allows us to determine the increase in capacity that will provide such growth in ATFM costs. With these increased capacities, the maximum number of conflicts that a controller has to handle in one hour stays more reasonable than without ground-holding regulation. Nevertheless, the resulting overcapacity with respect to the current capacities suggests that the required increase in workload will be achieved only through a major shift in ATC procedures. This is a fundamental motivation for the development of automated tools for ATC including, for instance, automated conflict solvers that would provide an efficient operation and decision aid to controllers.

Finally, we have developed a simulation-based framework that could be used for evaluating any automated tool of air conflict resolution or ground-holding delay assignment. This framework will enable to study the performance of such tools independently or jointly under various scenarios.

Future work could develop more sophisticated traffic-increase procedures, based on more detailed local forecasts extracted from EUROCONTROL (2013). This would lead to a geographically heterogenous increase in the traffic, which is more realistic. It would also be interesting to compare several conflict solvers, and in particular their performace on

direct routes. Different regulation procedures that include realistic predictions for the sector capacities should also be considered, keeping in mind that the interaction of regulation procedures and conflict-resolution algorithms should be optimized. Future work could also explore traffic scenarios that include the ability of companies to adapt their schedule according to the regulations applied; this would give more meaningful simulation results. Indeed, whatever the future ATM framework, companies will adapt their schedule to avoid unnecessary delays.

4.7 Acknowledgement

The research conducted for this paper is part of the project OPR-601 funded by the CRIAQ. The authors are indebted to the different stakeholders involved in the project.

CHAPITRE 5 ARTICLE 2 : TWO DECOMPOSITION ALGORITHMS FOR SOLVING A MINIMUM WEIGHT MAXIMUM CLIQUE MODEL FOR THE AIR CONFLICT RESOLUTION PROBLEM

Auteurs : Thibault LEHOUILLIER, Jérémy OMER, François SOUMIS, Guy DESAULNIERS.
Soumis à : European Journal of Operations Research.

Abstract

In this article, we tackle the conflict resolution problem using a new variant of the minimum weight maximum clique model. The problem consists in identifying maneuvers that maintain the required separation distance between all pairs of a set of aircraft while minimizing fuel costs. To this end, we design a graph whose vertices correspond to a finite set of maneuvers and whose edges connect conflict-free maneuvers. A maximum clique of minimal weight yields a conflict-free situation involving all aircraft and minimizing the costs induced. The innovation of the model relies on the cost structure: the cost of the vertices cannot be determined a priori, since they depend on the vertices in the clique. To tackle this feature, we formulate the problem as a mixed integer linear program. Since the modeling of aircraft dynamics and the computation of trajectories is separated from the solution process, the model is flexible. As a consequence, the mathematical framework presented in this article remains valid, whatever the hypotheses considered. In particular, in this paper aircraft can perform dynamic velocity, heading and flight level changes. To solve instances involving a large number of aircraft spread on several flight levels, we introduce two decomposition algorithms: the first one is a sequential mixed integer linear optimization procedure that iteratively refines the discretization of the maneuvers to yield a trade-off between solution time and cost. The second is a large neighborhood search heuristic that uses the first one as a subroutine. The best solutions for the available set of maneuvers are obtained in less than 5 seconds for instances with up to 250 aircraft randomly allocated to 20 flight levels.

5.1 Introduction

5.1.1 Context: challenges of air traffic control

In the last few years air traffic management (ATM) has attracted more and more attention, in particular with research on advanced decision algorithms. Such automated tools are recognized as key-components of future ATM systems like the Single European Sky ATM Research (SESAR) project in Europe (see SESAR Joint Undertaking (2012)) and the Next

Gen program in the United States (see Joint Planning and Development Office (2008) for details). Optimization algorithms for air traffic control (ATC) are particularly relevant in the current context of growing traffic, where the airspace capacity and safety become issues. Indeed, the latest long-term forecast published by EUROCONTROL (2013) states that the traffic demand will increase by 20% to 80% between 2012 and 2035. Besides, a simulation-based study performed by Lehouillier *et al.* (2014) shows that for a 50% increase in traffic, the controllers in charge of busy sectors would have to solve on average 27 conflicts per hour. This workload exceeds the human capacity and decision tools are necessary to help the controllers.

5.1.2 Literature review

One complex and central problem encountered in ATC is the air conflict resolution (CR) problem. A conflict occurs when two aircraft are too close to each other regarding predefined horizontal and vertical separation distances of respectively 5NM and 1000ft, as illustrated in Figure 5.1. To resolve a conflict, the controllers issue maneuvers that can be either speed, heading or altitude changes. Given the current position, speed, acceleration and the predicted trajectory of a set of aircraft, the CR problem consists in identifying the conflict-free maneuvers that minimize a given cost function.

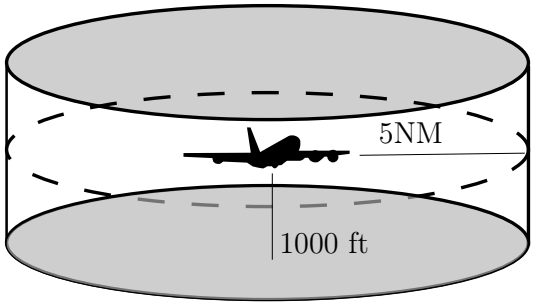

Figure 5.1 – Safety cylinder around an aircraft

The CR problem is one of the most widely studied problems in ATM. We provide a synthetic analysis of the studies that were most influential to our work, but a more complete coverage of the existing literature may be found in the review performed in Martin-Campo (2010). Because aircraft trajectories are time-continuous, the most natural approach is to model the problem with optimal control (see for instance Zhou *et al.* (1996)). Analytical solutions can be found only for the simplest cases, but coupled with nonlinear programming techniques, the models can be solved numerically. For instance, Raghunathan *et al.* (2004) use a time discretization of the problem to derive solutions for instances with more than two aircraft. One difficulty is that the nonlinear program (NLP) is nonconvex, so the global optimum

cannot be found in a reasonable amount of time and the solution is very sensitive to the starting point.

To find feasible solutions in a few seconds, several heuristics have been developed. Durand *et al.* (1996) present a genetic algorithm and Qi (2012) develop an ant colony algorithm, where maneuvers are chosen within a finite discrete set of heading changes performed at constant speed. Alonso-Ayuso *et al.* (2014) adapt a variable neighborhood search algorithm considering only heading changes. Other fast methods include conflict resolution using maneuvers extracted from a prescribed set (see Vivona *et al.* (2006)), particle swarm optimization (see Gao *et al.* (2012) for heading changes), or neural networks (see Durand *et al.* (2000); Christodoulou and Kodaxakis(2006) for speed changes). Such methods present the asset of bringing fast solutions, but the convergence is not guaranteed.

Mixed integer linear and nonlinear programming are powerful theoretical frameworks for the study of CR. With the realistic restriction that the aircraft perform at most one maneuver at the initial time, Pallottino *et al.* (2002) exploit the geometry of the separation constraints to develop two mixed integer linear programs (MILPs) that allow either a speed change with constant heading or a heading change with constant speed. In the same context, Vela *et al.* (2011) develop a MILP that considers both speed and heading changes, and Christodoulou and Costoulakis (2004) describe a nonlinear model for three-dimensional conflict resolution. Another MILP has been described by Alonso-Ayuso *et al.* (2011) to allow both velocity and altitude changes. In Alonso-Ayuso *et al.* (2012), Alonso-Ayuso *et al.* also extend the model of Pallottino *et al.* (2002) by introducing continuous instead of instantaneous speed changes. Schouwenaars (2006) or, more recently, Omer (2013) perform a time-based discretization of the optimal control formulation. Vela *et al.* (2009b) and Omer (2015b) also develop MILPs with a space discretization that focus on the main points of interest of the conflict resolution.

Graph theory has also been used in ATM, but mostly for air traffic flow management (ATFM) (see Bertsimas and Patterson (1998; 2000) for examples). In ATC, conflicts between aircraft are generally modeled by a graph whose vertices represent the different aircraft and whose edges link pairs of conflicting aircraft. Vela (2011) and Sherali *et al.* (2002) use conflict graphs in their models. Resmerita *et al.* (2003) study *a priori* conflict resolution by developing a multi-agent system where each aircraft has to choose a path in a resource graph whose vertices represent zones of the airspace and where chosen paths have to be conflict-free. Barnier and Brisset (2004) assign different flight levels to aircraft with intersecting routes by looking for maximum cliques in a graph defining an assignment of all aircraft to a set of given flight levels.

5.1.3 Contribution statement

In this paper, we present a formulation of the CR problem as a variant of the minimum-weight and maximum cardinality clique (MWMCC) problem. We design a graph whose vertices represent possible aircraft maneuvers and where edges link conflict-free maneuvers of different aircraft. The innovation of this model relies on the cost structure. Indeed, the costs of the vertices are not known *a priori* since they depend on which maneuvers are in the clique. This model is flexible because it separates the resolution process from the modeling of the aircraft dynamics and their maneuvers. As a consequence, the mathematical framework used in the optimization method remains valid whatever the considered hypotheses on the aircraft dynamics and maneuvers, the computation of separation distances and the cost evaluation method. This feature highlights robustness, which is really important in ATC because we want to solve a large span of conflicts. For a fast solution of large instances, the explosion of the number of vertices needs to be addressed, since it is critical in terms of computational effort. To this end, we develop two decomposition algorithms. The first one is a sequential mixed integer linear optimization (SMILO) procedure that iteratively refines the discretization of the set of maneuvers without changing the number of vertices in the graph. This yields a trade-off between solution time and the cost of the optimal solution. This procedure is then used as a subroutine within a spatial decomposition that takes advantage of the geometric structure of the instances. The spatial decomposition is a large neighborhood search metaheuristic exploiting the weak interdependency between subsets of aircraft.
Finally, we test our model on an extended benchmark that includes structured instances with up to 20 aircraft, and random instances involving up to 60 aircraft on a single flight level and 250 aircraft on several flight levels. From a practical point of view, the results show that automated conflict resolution could be performed for large and dense areas of the airspace within a few seconds.

5.2 Problem Formulation

In this section, we detail the modeling of the aircraft dynamics and maneuvers, the computation of separation distances and the cost evaluation method. The choices or assumptions made in this section represent a possible modeling of the problem. Nevertheless, since they are fully independent of the resolution method, considering other alternatives would not impact the validity of the overall method presented in this article.

5.2.1 Modeling aircraft dynamics

As in the majority of the literature, we use a three-dimensional point-mass model for aircraft dynamics:

$$\frac{dp_x}{dt} = V\cos\gamma\cos\chi \tag{5.1}$$
$$\frac{dp_y}{dt} = V\cos\gamma\sin\chi \tag{5.2}$$
$$\frac{dp_z}{dt} = V\sin\gamma \tag{5.3}$$
$$\frac{d\gamma}{dt} = \frac{g_0}{V}(n\cos\phi - \cos\gamma) \tag{5.4}$$
$$\frac{d\chi}{dt} = \frac{g_0}{V}\frac{n\sin\phi}{\cos\gamma} \tag{5.5}$$
$$\frac{dV}{dt} = \frac{F_T - F_D}{m} - g_0\sin\gamma \tag{5.6}$$

The position of the aircraft is given by the coordinates (p_x, p_y, p_z) of its center of gravity in a local coordinate system, (p_x,p_y) being its coordinates in a horizontal plane and p_z its altitude. The aircraft flies at speed V and the angles χ, ϕ and γ correspond respectively to its heading, roll and pitch. Variables F_T and F_D denote the norm of the thrust and drag forces respectively, m is the aircraft mass, n is the load factor and g_0 corresponds to the gravitational acceleration.

We assume that aircraft follow their trajectory with a stepwise-constant acceleration. Maneuvers are executed with constant acceleration and yaw rate, and the speed vector remains constant between two consecutive maneuvers. This assumption is realistic because it respects the time-continuity of speed, and it corresponds to a setting where maneuvers are performed smoothly. If other speed changes were to be considered, it would not jeopardize the resolution process, since it will solely impact the computation of the separation distances and maneuvers costs.

In the remainder of the article, $\mathcal{F} = [\![1; N]\!]$ denotes the set of the considered aircraft.

5.2.2 Aircraft maneuvers

Types of maneuvers

The maneuvers considered can be of the following types:

— variable *NIL* refers to the *null* maneuver, i.e., when no maneuver is performed;

— variable H_θ is a heading change by an angle $\theta \in [-\frac{\pi}{6}; \frac{\pi}{6}]$ [1];

1. positive angles correspond to counter-clockwise rotations

— variable S_δ is a relative speed change of $\delta\%$. We use relative speed changes because they have already been chosen in large-scale projects such as the ERASMUS project described in Brochard (2009);
— variable $V_{\delta h}$ is a change of δh flight levels.

Figure 5.2 describes the geometry of the heading change and the flight level change. Heading changes are performed in a turning point fashion as depicted on Figure 5.2a. Flight level changes are followed by a return toward the initial flight level, as on Figure 5.2b.

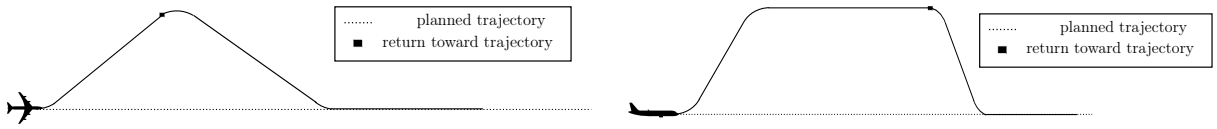

(a) Projection of a heading change on the horizontal plane (b) Projection of a flight level change on a vertical plane

Figure 5.2 – Geometry of the heading change and the flight level change

We define $\mathcal{M} = \cup_{f=1}^{n} \mathcal{M}_f$ as the set of all possible maneuvers, $\mathcal{M}_f$ being the set of maneuvers for aircraft $f \in \mathcal{F}$.

Dynamics of the maneuvers

Since the analysis carried out by Omer (2013) concludes that considering instantaneous maneuvers can lead to a significant error in the separation distance, we follow the model with constant acceleration described in Paielli (2003). Paielli (2003) state that the typical acceleration during a speed adjustment for commercial transport aircraft is in the order of 0.4kn/s or 0.02 g. This value is set to respect the comfort of passengers. Heading changes are approximated by a steady turn of constant rate and radius, given by the following equations:

$$\omega = \frac{d\chi}{dt} = \frac{g_0 \tan\phi}{V} \tag{5.7}$$

$$r = \frac{V^2}{g_0 \tan\phi} \tag{5.8}$$

We also consider the altitude maneuvers to be dynamic. The changes of flight level are performed with a vertical speed which is a function of thrust, drag, and true airspeed. Details on the computation of the vertical speed can be found in the BADA user manual (EUROCONTROL (2011)).

Trajectory recovery

In this article, we consider that aircraft follow a 4D contractual trajectory, which represents a compromise between the user's preferences and the capacity constraints of the network. The trajectories of the aircraft then have to meet time and space requirements over a sequence of 4D points. Noncompliance with this contract induces penalty fees to companies. As a consequence, it is important to make sure that, after resolving every conflict, every aircraft recovers its initial 4D trajectory. Ensuring a strict velocity control can be very costly and almost impossible in practice. Time recovery is therefore not required, but it is favored by giving a penalty on the time shift between the trajectory without conflict and the 4D trajectory after the loss of separation is avoided. The method for computing the penalty costs follows the one by Omer (2013): the penalty shift is estimated as the total cost induced by a time recovery of the 4D trajectory, at a speed depending on the sign of the shift.

Maneuvers costs

In this subsection we give some details about the computation of the cost of a maneuver. The purpose is to highlight that, even though computations can be complex, it does not interfere whatsoever with the resolution method that is described in Section 5.4. Additionally, if more complex cost models were to be considered, it would be possible without changing anything in the solution method.
For a jet commercial aircraft f with constant altitude, the fuel consumption by time and distance unit is given by (5.9) and (5.10):

$$C_{t,f}\left(t, V_f(t)\right) = c_{1,f}\left(1 + \frac{V_f(t)}{c_{2,f}}\right) F_{T,f}(t) \tag{5.9}$$

$$C_{d,f}\left(t, V_f(t)\right) = \frac{C_{t,f}\left(t, V_f(t)\right)}{V_f(t)} \tag{5.10}$$

where variables $c_{1,f}$ and $c_{2,f}$ are numerical constants depending on the type of aircraft f.
Depending on the type of the maneuver, a different approach is followed.

Speed change Consider a change of speed $V_f' = V_f^n(1+\delta)$ during a time t, where variable V_f^n is the nominal speed of aircraft f. Let C_{speed} denote the cost of the maneuver. Variable C_{speed} is the sum of:

1. the cost of the additional fuel burnt during the maneuver, C_s^f;
2. the penalty for not respecting the 4D contract, C_s^{4D}.

$$C_{\text{speed}} = C_s^f + C_s^{4D} \tag{5.11}$$

To compute C_s^f, it is useful to distinguish the cost incurred during the the transition from V_f^n to V_f', C_s^t, and that incurred on the portion of trajectory flown with the new speed, C_s^n:

$$C_s^f = C_s^t + C_s^n \tag{5.12}$$

Let $t_{\delta,V}$ denote the time required to go from V_f^n to V_f'. We compute C_s^t as the following expression

$$C_s^t = \int_0^{t_{\delta,V}} C_{t,f}\left(t, V_f(t)\right) dt - t_{\delta,V} C_{t,f}\left(t, V_f^n\right) \tag{5.13}$$

The cost C_s^n is given by

$$C_s^n = (t - t_{\delta,V})\left(C_{t,f}(t, V_f') - C_{t,f}(t, V_f^n)\right) \tag{5.14}$$

The penalty C_s^{4D} is deduced from the delay d_s^{4D} created by the maneuver, which is computed as follows.

$$d_s^{4D} = \int_0^{t_{\delta,V}} V_f(t)dt + (t - t_{\delta,V})V_f' - tV_f^n \tag{5.15}$$

Depending on the sign of d_s^{4D}, a different recovery speed is used to catch up with the 4D trajectory, inducing the cost C_s^{4D}.

Heading change Let C_{heading} denote the cost of a heading change by an angle θ during a period t. The quantity C_{heading} is decomposed as the sum of:

1. the cost on the additional distance induced by the maneuver, C_h^d;
2. the penalty for not respecting the 4D contract, C_h^{4D}.

$$C_{\text{heading}} = C_h^d + C_h^{4D} \tag{5.16}$$

To recover the spatial trajectory, the aircraft performs a turn with an angle -2θ as detailed on Figure 5.3.
The aircraft flies an extra distance d given by

$$d = \sum_{i=1}^{5} l_i - l_i^p \tag{5.17}$$

where the expressions of the variables l_i and l_i^p are given on Figure 5.3. The cost of the extra fuel burnt on d is then computed as follows:

$$C_d^h = C_{d,f}(t, V_f)d \tag{5.18}$$

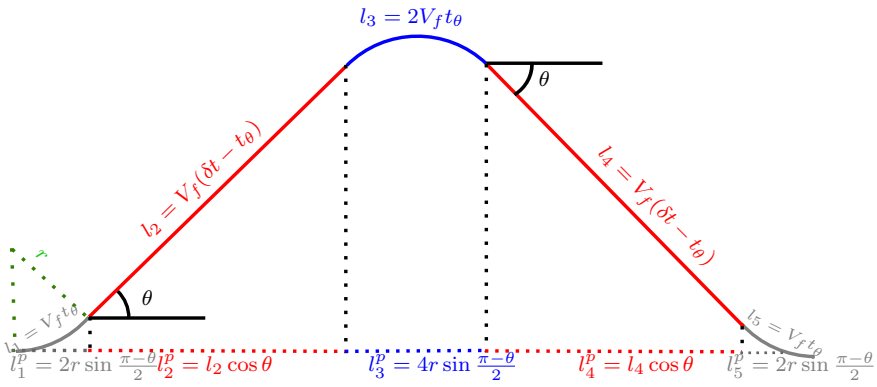

Figure 5.3 – Geometry of the trajectory recovery following a heading change

The penalty C_h^{4D} is then deduced from the delay d_h^{4D} due to the extra distance, d, flown during the heading change:

$$d_h^{4D} = \frac{d}{V_f^n} \tag{5.19}$$

where d is the extra distance flown during the maneuver. Depending on the sign of d_h^{4D}, a different recovery speed is used to catch up with the 4D trajectory, inducing the cost C_h^{4D}.

Flight level change Consider a change of δh flight levels during a period t. To illustrate the geometry of the maneuver, Figure 5.4 details the example where an aicraft climbs one level.

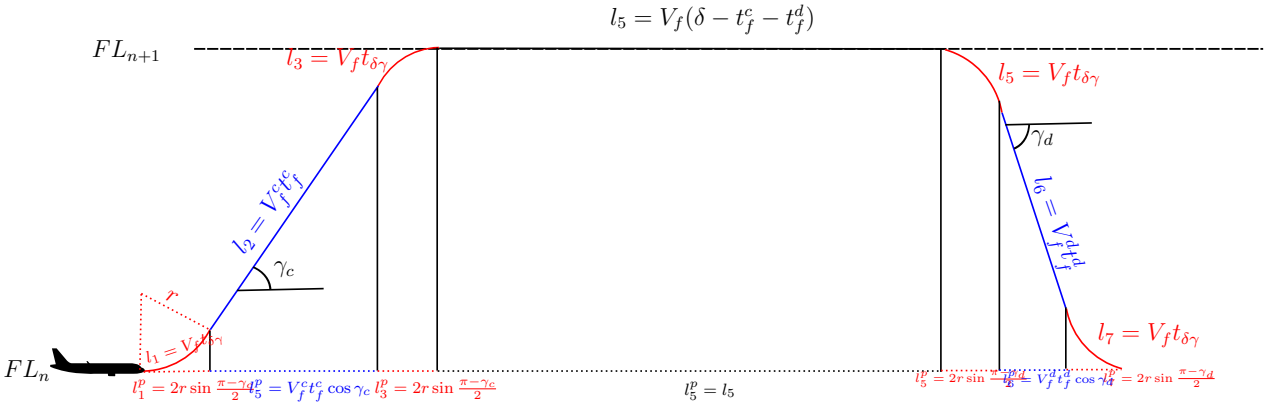

Figure 5.4 – Geometry of the trajectory recovery following a flight level change

Let C_{FL} denote the cost of this maneuver. Variable C_{FL} is the sum of the following quantities:

1. the extra cost during the ascent and descent, denoted C_{FL}^a and C_{FL}^d, respectively;

2. the difference between the cost on the initial flight level and that on the new flight level, denoted $C_{\mathrm{FL}}^{\delta h}$;
3. the cost on the additional distance flown d denoted C_{FL}^{d};
4. the 4D contract penalty C_{FL}^{4D}.

$$C_{\mathrm{FL}} = C_{\mathrm{FL}}^{a} + C_{\mathrm{FL}}^{d} + C_{\mathrm{FL}}^{\delta h} + C_{\mathrm{FL}}^{d} + C_{\mathrm{FL}}^{p} \tag{5.20}$$

C_{FL}^{a} and C_{FL}^{d} are derived by

$$C_{\mathrm{FL}}^{a} = t_a \left(C_{a,t}(f, V_f^a) - C_{t,f}(t, V_f^n) \right) \tag{5.21}$$

$$C_{\mathrm{FL}}^{d} = t_d \left(C_{d,t}(f, V_f^d) - C_{t,f}(t, V_f^n) \right) \tag{5.22}$$

$$\tag{5.23}$$

where t_a , t_d are the durations of ascent and descent, $C_{a,t}$ and $C_{d,t}$ are the fuel costs during the climb and the descent, and V_f^a and V_f^d represent the climb and descent speeds, respectively. The fuel consumption and the ascent and descent speeds are taken from the BADA tables corresponding to the aircraft types.
Equation (5.24) derives the difference of fuel consumption between the two levels.

$$C_{\mathrm{FL}}^{\delta h} = (\delta t - t_a - t_d)(C_{FL_{n+\delta h}} - C_{FL_n}) \tag{5.24}$$

where $C_{FL_{n+\delta h}}$ and C_{FL_n} denote the fuel consumption per time unit on the new and initial flight level, respectively. The fuel burnt on the additional distance flown d is derived with (5.25).

$$C_{\mathrm{FL}}^{d} = C_{d,f}(t, V_f)d \tag{5.25}$$

where the distance d is computed by (5.26):

$$d = \sum_{i=1}^{7} l_i - l_i^p \tag{5.26}$$

where the expressions of the variables l_i and l_i^p are given on Figure 5.4.
The computation of the 4D contract penalty, C_{FL}^{4D}, is then similar to that performed for the heading maneuvers.

5.2.3 Aircraft separation

To determine whether two aircraft are separated we use the following notation:

— $\mathcal{T}$: time horizon for the conflict resolution;

— $\boldsymbol{p}_i(t) \in \mathbb{R}^3$: position vector of aircraft i at time t. Variables $p_{i,x}(t)$ $p_{i,y}(t)$ and $p_{i,z}(t)$ denote respectively the abscissa, ordinate and altitude components of the position vector;

— $\boldsymbol{s}_i(t) \in \mathbb{R}^3$: speed vector of aircraft i at time t. Variables $s_{i,x}(t)$ $s_{i,y}(t)$ and $s_{i,z}(t)$ denote respectively the abscissa, ordinate and altitude components of the speed vector;

— $\boldsymbol{a}_i(t) \in \mathbb{R}^3$: acceleration vector of aircraft i at time t. Variables $a_{i,x}(t)$ $a_{i,y}(t)$ and $a_{i,z}(t)$ denote respectively the abscissa, ordinate and altitude components of the acceleration vector.

Let i and j be two aircraft applying maneuvers m_i and m_j, respectively. Aircraft i and j are said to be separated at time t if and only if at least one of constraints (5.27) and (5.28) holds.

$$d_{ij}^h(t)^2 = (p_{i,x}(t) - p_{j,x}(t))^2 + (p_{i,y}(t) - p_{j,y}(t))^2 \geq D_{\text{h,min}}^2 \tag{5.27}$$

$$d_{ij}^v(t)^2 = (p_{i,z}(t) - p_{j,z}(t))^2 \geq D_{\text{v,min}}^2 \tag{5.28}$$

At any time $t \in \mathcal{T}$, either none, one or both aircraft are maneuvering. The set $\mathcal{T}$ can thus be divided into intervals where both i and j have a constant acceleration. For each interval, we compute the time at which the aircraft are the closest to verify if the separation constraints hold. Let $\mathcal{T}_k$ be one of these intervals. Consider i and let $t_0 \in \mathcal{T}$ be the starting time of maneuver m_i. If we assume that maneuver m_i is applied with a constant acceleration, we obtain the position and the speed vector of i at time $t_0 + t$ with t such that $t - t_0 \leq |\mathcal{T}_k|$:

$$\boldsymbol{p}_i(t_0 + t) = \boldsymbol{p}_i(t_0) + (t - t_0)\boldsymbol{s}_i(t_0) + \frac{(t - t_0)^2}{2}\boldsymbol{a}_i(t_0) \tag{5.29}$$

$$\boldsymbol{s}_i(t_0 + t) = \boldsymbol{s}_i(t_0) + (t - t_0)\boldsymbol{a}_i(t_0) \tag{5.30}$$

Let $\boldsymbol{p}_{ij}^h$ (respectively $\boldsymbol{s}_{ij}^h$, $\boldsymbol{a}_{ij}^h$) denote the horizontal position (respectively the speed and the acceleration) of aircraft j relatively to aircraft i. We define

$$\begin{aligned} d_{ij}^h(t + \tau) &= ||\boldsymbol{p}_{ij}^h(t + \tau)|| \\ &= ||\boldsymbol{p}_{ij}^h(t) + \tau\boldsymbol{s}_{ij}^h(t) + \frac{\tau^2}{2}\boldsymbol{a}_{ij}^h(t)|| \end{aligned} \tag{5.31}$$

where $\tau \geq 0$.

Let $\tau_{ij} \in \underset{\tau \geq 0}{\operatorname{argmin}}\, d_{ij}^h(t + \tau)^2$, and $t_{ij}^h \in \underset{t \in \mathcal{T}}{\operatorname{argmin}}\, d_{ij}^h(t)^2$.

We have:

$$t_{ij}^h = \begin{cases} 0 & \text{if } \tau_{ij} = 0 \\ |\mathcal{T}_k| & \text{if } \tau_{ij} \geq |\mathcal{T}_k| \\ \tau_{ij} & \text{otherwise} \end{cases}$$

where $|\mathcal{T}_k|$ is the length of interval $\mathcal{T}_k$. Aircraft i and j are horizontally separated during interval $\mathcal{T}$ if and only if

$$d_{ij}^h(t_{ij}^h)^2 \geq D_{\text{h,min}}^2 \tag{5.32}$$

By a similar reasoning, aircraft i and j are vertically separated during interval $\mathcal{T}$ if and only if

$$d_{ij}^v(t_{ij}^v)^2 \geq D_{\text{v,min}}^2 \tag{5.33}$$

Let $\mathcal{I}_{i,j}^h$ and $\mathcal{I}_{i,j}^v$ denote the intervals during which i and j are not separated horizontally and vertically, respectively. i and j are separated if and only if

$$\mathcal{I}_{i,j}^h \cap \mathcal{I}_{i,j}^v = \emptyset \tag{5.34}$$

5.3 Modeling the CR problem as a MWMCC problem

In this section, we describe how the CR problem can be modeled as a MWMCC problem. This model is based on a preliminary study that we presented in Lehouillier *et al.* (2015b).

5.3.1 Graph theory definitions

Let $\mathcal{G} = (\mathcal{V}, \mathcal{E})$ be an undirected, simple graph with a vertex set $\mathcal{V}$ and an edge set $\mathcal{E} \subseteq \mathcal{V} \times \mathcal{V}$. A *clique* in graph $\mathcal{G}$ is a vertex set $\mathcal{C}$ with the property that each pair of vertices in $\mathcal{C}$ is linked by an edge:

$$\mathcal{C} \subseteq \mathcal{V} \text{ is a clique} \Leftrightarrow \forall (u,v) \in \mathcal{C} \times \mathcal{C}, u \neq v, (u,v) \in \mathcal{E} \tag{5.35}$$

A *maximum* clique in $\mathcal{G}$ is a clique that is not a subset of any other clique in $\mathcal{G}$. The cardinality of a maximum clique of $\mathcal{G}$ is called *clique number* and is denoted by $w(\mathcal{G})$. Let $c : \mathcal{V} \to \mathbb{R}$ be a vertex-weight function associated with $\mathcal{G}$. A maximum clique of *minimum* weight in $\mathcal{G}$ is a maximum clique $\mathcal{C}$ that minimizes $\sum_{v \in \mathcal{C}} c(v)$.

A *stable set* $\mathcal{S} \subseteq \mathcal{V}$ is a subset of vertices no two of which are adjacent in $\mathcal{G}$. A *bipartite* graph is a graph whose vertices can be partitioned into two distinct stable sets $\mathcal{V}_1$ and $\mathcal{V}_2$. Each edge of the graph then connects one vertex of $\mathcal{V}_1$ to a vertex of $\mathcal{V}_2$. This concept is extended to $k-$*partite* graphs, where the vertex set is partitioned into k distinct stable sets.

The *density* of a graph $\mathcal{G} = (\mathcal{V}, \mathcal{E})$ is defined as the ratio of the number of edges $|\mathcal{E}|$ over the number of edges in a complete graph with $|\mathcal{V}|$ vertices:

$$d_{\mathcal{G}} = \frac{|\mathcal{E}|}{\frac{|\mathcal{V}|(|\mathcal{V}|-1)}{2}} \tag{5.36}$$

5.3.2 Graph construction

In this subsection, we introduce the *conflict graph* $\mathcal{G} = (\mathcal{V}, \mathcal{E})$ used to model the CR problem.

Defining the vertices

The set of vertices is defined as $\mathcal{V} = [\![1; |\mathcal{M}|]\!]$. We note $\mathcal{V}_f$ the set of vertices corresponding to aircraft f. In emergency scenarios where the feasibility of the problem can be an issue, it is possible to introduce n vertices corresponding to costly emergency maneuvers. Such maneuvers have already been studied, and can for instance correspond to maneuvers implemented by Administration (2011), or to the maneuvers described by Schouwenaars (2006). However, since feasibility has not been an issue in our tests, we did not add these vertices in our implementation.

Defining the edges

Let $(i, j) \in \mathcal{V} \times \mathcal{V}$ be a pair of vertices representing maneuvers $(m_i, m_j) \in \mathcal{M} \times \mathcal{M}$ of aircraft $(i, j) \in \mathcal{F} \times \mathcal{F}$. For $i \neq j$, we write $m_i \square m_j$ when no conflict occurs if aircraft f_i follows maneuver m_i while aircraft f_j performs maneuver m_j. The set of edges $\mathcal{E}$ corresponds to the pairs of maneuvers performed by two different aircraft without creating conflicts:

$$\mathcal{E} = \{(i, j) \in \mathcal{V} \times \mathcal{V}, i \neq j : m_i \square m_j\} \tag{5.37}$$

Relative density

We can define a measure of density taking advantage of the structure of the conflict graph. Indeed, it is important to note that there is no edge between two different maneuvers of a given aircraft, which yields Observation 5.3.1.

Observation 5.3.1. *For all $f \in \mathcal{F}, \mathcal{V}_f$ is a stable set, i.e there is no edge linking two distinct vertices of $\mathcal{V}_f$. Hence, the graph $\mathcal{G}$ is $|\mathcal{F}|$-partite.*

We define the *relative density* of $\mathcal{G}$ in Equation (5.38), which is the adaptation of the density of a graph to the conflict graph using Observation 5.3.1. This quantity is more meaningful, since it compares the number of edges of a conflict graph to the maximum number of edges a conflict graph could have.

$$d^*_{\mathcal{G}} = \frac{|\mathcal{E}|}{\frac{|\mathcal{V}|(|\mathcal{V}|-1)}{2} - \sum_{f \in \mathcal{F}} \frac{|\mathcal{M}_f|(|\mathcal{M}_f|-1)}{2}} \tag{5.38}$$

5.3.3 Conflict-free solution: formulation and illustrative example

As mentioned in Section 6.1, given the current position, speed, acceleration and the planned trajectories of a set of aircraft, solving the CR problem consists in finding a conflict-free set of maneuvers that minimizes the total cost. Observation 5.3.2 links the cliques in $\mathcal{G}$ to the CR problem:

Observation 5.3.2. *Let $\mathcal{C}$ be a clique in graph $\mathcal{G}$. Then $\mathcal{C}$ represents a set of conflict-free maneuvers for a subset of $\mathcal{F}$ of cardinality $|\mathcal{C}|$.*

Observation 5.3.2 indicates that finding a set of conflict-free maneuvers for $\mathcal{F}$ is equivalent to finding a clique of $\mathcal{G}$ of cardinality $|\mathcal{F}|$. We derive the following proposition:

Proposition 5.3.3. *If a conflict-free solution exists, then $\omega(\mathcal{G}) = |\mathcal{F}|$. Otherwise, $\omega(\mathcal{G})$ is the maximum number of flights involved in a conflict-free situation.*

For the sake of clarity, an illustrative example with three aircraft and the corresponding solution are presented in Figure 5.5. If each aircraft follows its planned trajectory as indicated in Figure 5.5a, conflicts will happen between the blue aircraft and the two others. For this example, we assume that, in addition to the null maneuver, only two heading changes ($\pm 30°$) are allowed. We build the CR graph shown in Figure 5.5b. The graph is multipartite, each stable set representing the set of the possible maneuvers for one aircraft. Solving the CR problem is then equivalent to searching for a minimum-weight clique of three vertices, i.e., a triangle. Figures 5.5c and 5.5d denote the corresponding solution and the triangle of minimum weight respectively.

We define the problem $\mathrm{CR}_{\mathcal{M}}$ as the restriction of the CR problem to the set of maneuvers $\mathcal{M}$. Using both Observations 5.3.2 and 5.3.3, we can state anew the $\mathrm{CR}_{\mathcal{M}}$ problem as follows: searching for a conflict-free solution of minimum cost is equivalent to solving the $\mathrm{CR}_{\mathcal{M}}$ problem consisting of finding a clique of maximum cardinality and minimal cost in graph $\mathcal{G}$.

As stated in Subsection 5.2.2, the cost of a maneuver depends on the time during which it is executed. A first idea to model this would be to discretize this execution time and to create the vertices accordingly. Computing the cost of the vertices would be straightforward, using the method described in Subsection 5.2.2. The drawback of this method is the explosion of the number of vertices, which will drastically increase the runtime of any solution algorithm. To address this issue, we decided to maintain the graph small by considering one vertex per maneuver. By making this choice, the cost of the vertices cannot be determined *a priori* anymore, since it depends on the maneuvers executed by the other aircraft. In other words, the cost of each vertex depends on the vertices in the clique. This problem is a new variant of the maximum clique of minimum weight problem, where even though the weights considered are on the vertices, these weights depend on the vertices in the clique.

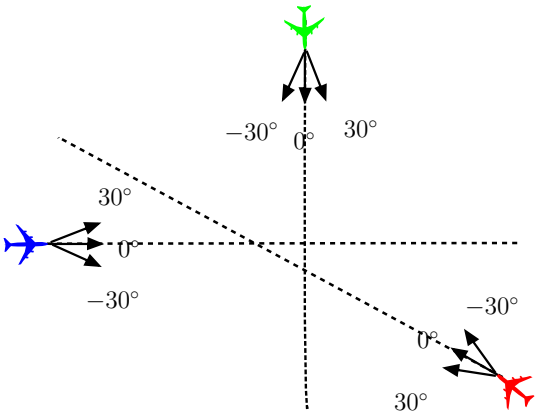

(a) Illustrative example with three aircraft

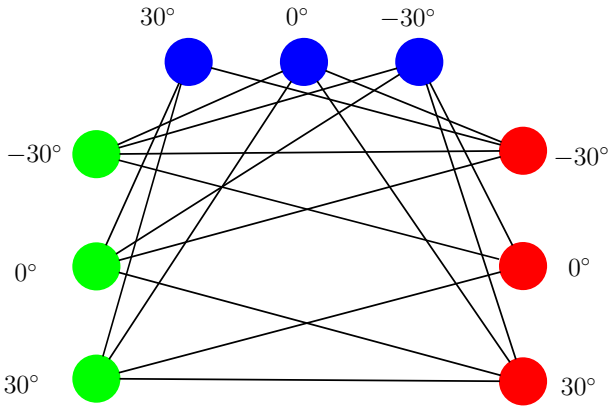

(b) Conflict graph $\mathcal{G}$ associated with the illustrative example

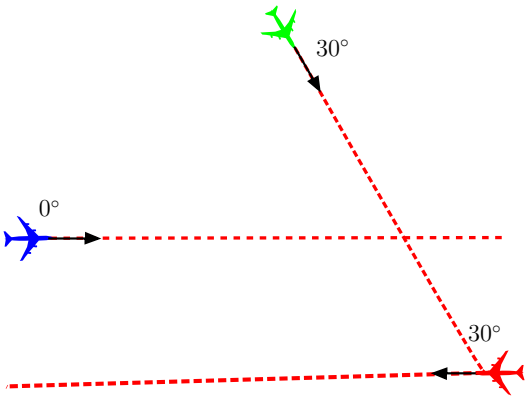

(c) Solution of the problem

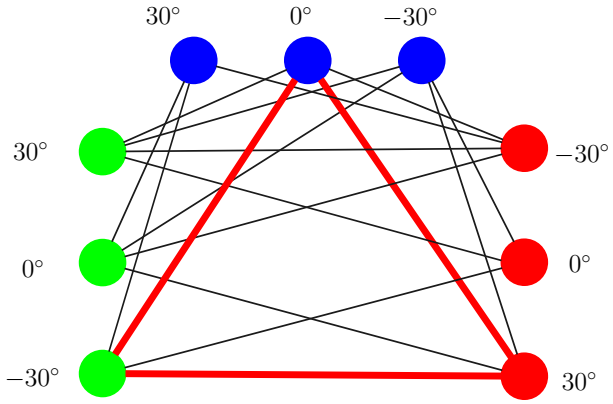

(d) Corresponding clique in the conflict graph $\mathcal{G}$

Figure 5.5 – Illustrative example: instance and solution

5.3.4 Computing the costs

For a more synthetic presentation, and without loss of generality, no distinction is made between a vertex and the corresponding maneuver in this subsection. As explained in the previous subsection, the cost of a maneuver depends on its execution, which itself varies with the maneuvers performed by the other aircraft. As a consequence, we need to define the cost of the edges before the cost of the vertices.

Cost of the edges

For a more synthetic presentation, an edge $e = (i, j)$ will be considered as a pair of maneuvers. We compute the cost of an edge $e = (i, j)$ as a pair constituted of the cost of maneuvers i and j, denoted $C_i^{(i,j)}$ and $C_j^{(i,j)}$. These costs correspond to an execution time t_i^j which is

the minimum time during which i and j have to be executed before a safe return can be performed by at least one of the aircraft.

Cost of the vertices

Let us consider a maneuver i. To determine the cost of i, denoted c_i, we need to compute the time t_i during which it is actually applied. If i is not in the optimal solution, then $t_i = 0$. Otherwise, t_i is given by

$$t_i = \max_{j \in \mathcal{V} \cap \mathcal{C}} t_i^j \tag{5.39}$$

Equation (5.39) states that maneuver i has to be applied long enough in order to be conflict-free with every other chosen maneuvers. Indeed, if aircraft i and j are conflict-free when they execute their maneuvers during a duration t, then they will remain conflict-free if they perform their maneuvers during $T > t$.
We can determine c_i:

$$c_i = \begin{cases} \max\limits_{j \in \mathcal{V} \cap \mathcal{C}} C_i^{(i,j)} & \text{if } i \in \mathcal{C} \\ 0 & \text{otherwise} \end{cases}$$

5.4 Methodology

5.4.1 MILP formulation

Motivations

Finding a maximum clique in an arbitrary graph is a well-known optimization problem that is among the $\mathcal{NP}$-hard problems enumerated in Karp (1972). Due to its high complexity, the problem has been thoroughly studied and several methods, both exact and heuristic, have been developed. For a comprehensive coverage of the theoretical results, complexity study and existing methods overview, one can refer to Bomze *et al.* (1999) and Wu and Hao (2015). In the cited methods, the weight of the vertices are known beforehand and are data of the problem. However, in our model the costs of the vertices are not determined *a priori*, since they depend on which vertices are in the clique. As a consequence, the dedicated algorithms of existing graph theory libraries cannot be used in this study. To address this issue, we formulate our problem as a MILP that can be solved with any generic MILP solver.

Formulation

The decision variables of the model all relate to the vertices of the graph. They correspond to the choice of the vertices in the clique and the cost of each vertex:

— $x_i = \begin{cases} 1 & \text{if vertex } i \text{ is part of the maximum clique} \\ 0 & \text{otherwise} \end{cases}$

— $c_i \in \mathbb{R}_+$ is the cost of vertex i.

The clique search can then be modeled as the following MILP, denoted MIP:

$$\text{minimize} \sum_{i \in \mathcal{V}} c_i \tag{5.40}$$

$$\text{subject to } x_i + x_j \leq 1, \forall (i,j) \notin \mathcal{E} \tag{5.41}$$

$$\sum_{i \in \mathcal{V}} x_i = N \tag{5.42}$$

$$c_i \geq C_i^{(i,j)}(x_i + x_j - 1), \forall (i,j) \in \mathcal{E} \tag{5.43}$$

$$x_i \in \{0;1\}, \forall i \in \mathcal{V} \tag{5.44}$$

$$c_i \in \mathbb{R}_+, \forall i \in \mathcal{V} \tag{5.45}$$

The objective function (5.40) minimizes the cost of the maneuvers. Constraints (5.41) are clique constraints stating that two nonadjacent vertices must not be part of the clique. In terms of conflict resolution, it means that two maneuvers in conflict must not be part of the solution. Constraint (5.42) exploits Proposition 5.3.3 defining the cardinality of the maximum clique. Constraints (5.43) are used to compute the cost of the vertices: if a vertex is in the maximum clique, then its cost must be greater than the cost on every edge connecting it to other vertices in the clique. Otherwise, no particular constraint is imposed on the vertex cost. Constraints (5.44)–(5.45) are binarity and positivity constraints, respectively.

Strengthening the linear relaxation

Strengthening the linear relaxation of an MILP can yield improvements for the resolution. Indeed, it allows the explored branch-and-bound nodes to have a better lower bound. We tighten the linear relaxation by including the following constraints in our model:

$$\sum_{j \in \mathcal{V}_f} x_j = 1, \forall f \in \mathcal{F} \tag{5.46}$$

Constraints (5.46) simply illustrate that each aircraft must be assigned a maneuver. These constraints were not included in the original formulation, since the constraints (5.41), (5.42) and (5.44) make them redundant. Indeed, each set of nodes $\mathcal{M}_f$ is a stable set, meaning that only one maneuver can be assigned to each aircraft in a clique. Since (5.42) requires that the number of vertices in the clique is equal to the number of aircraft, (5.46) is always satisfied in a solution of (5.41)–(5.45). However these constraints improve the linear relaxation of the

MILP, because they prevent it from considering a solution where the fractional maneuvers are all assigned to the same aircraft.

5.4.2 Decomposition methods

The motivations for the design of decomposition methods are two-fold. First, as the MWMCC problem is known to be $\mathcal{NP}$-hard, an increase in solution time with the size of the instances can be expected. Moreover, the size of the sets of maneuvers can also impact the required computational effort. Second, in practice the instances have important inherent geometric characteristics. Indeed, aircraft evolving on different flight levels are weakly interdependent, meaning that they will almost never interfere with each other. However, these geometric considerations do not appear explicitly in our model.
To address these observations, we design two decomposition methods. The analysis of the answers to the observations provided by the methods will be discussed in Section 5.5.

SMILO procedure

In this subsection, we present a SMILO procedure for the CR problem. This procedure iteratively solves several MILPs on graphs having the same number of vertices, but where the discretization values are updated in a fashion similar to a trust region method. The motivations behind the design of this procedure is to obtain a trade-off between the solution time and cost, and to study the impact of the chosen discretization. Algorithm 5.1 describes the mechanics of the SMILO procedure.
The parameters describe a conflict graph with the following features:

- $\mathcal{F}$: the set of aircraft;
- $v^f_{\min}, v^f_{\max}$: minimum and maximum speed deviation allowed for aircraft f;
- $\chi^f_{\min}$, $\chi^f_{\max}$: minimum and maximum heading deviation allowed for aircraft f;
- $\delta^f_v, \delta^f_\chi$: speed and heading discretization steps of the maneuvers of aircraft f;
- n^f_s, n^f_χ: number of speed and heading nodes for aircraft f. The values are computed using the values of $v^f_{\min}, v^f_{\max}, \chi^f_{\min}, \chi^f_{\max}, \delta^f_v$ and δ^f_χ.

The procedure starts by storing the number of vertices representing speed and heading maneuvers for each aircraft. It sequentially solves MIP until no improvement is achieved while updating the set of nodes $\mathcal{M}$ between two consecutive resolutions. The update of the vertices $\mathcal{M}$ depends on whether or not the current instance of the graph is feasible. If it is feasible, the update varies with the maneuver assigned to f in the current solution:

- if f perfoms no maneuver, $\mathcal{M}_f$ is erased, except for the NIL node. New sets of speed and heading maneuvers are added to $\mathcal{F}$ in order to obtain intervals centered around 0;
- if f performs a heading change of magnitude m, all the speed nodes are deleted from

Algorithm 5.1. SMILO procedure for the CR problem

procedure SMILO($\mathcal{F}, v^1_{\min}, \ldots, v^N_{\min}, v^1_{\max}, \ldots, v^N_{\max}, \ldots, \chi^1_{\min}, \chi^N_{\min}, \chi^1_{\max}, \ldots, \chi^N_{\max}, \delta^1_v, \ldots, \delta^N_v, \delta^1_\chi, \ldots, \delta^N_\chi$)
  for $f \in \mathcal{F}$ **do**
    $n^f_v \leftarrow \frac{v^f_{\max} - v^f_{\min}}{\delta^f_v}$
    $n^f_\chi \leftarrow \frac{\chi^f_{\max} - \chi^f_{\min}}{\delta^f_\chi}$
  $z_c \leftarrow +\infty$
  while $|z - z_c| > 0.01$ **do**
    $z \leftarrow z_c$
    $z \leftarrow Solve\_MIP(\mathcal{F}, v^1_{\min}, \ldots, v^N_{\min}, v^1_{\max}, \ldots, v^N_{\max}, \ldots, \chi^1_{\min}, \ldots, \chi^N_{\min}, \chi^1_{\max}, \ldots, \chi^N_{\max}, \delta^1_v, \ldots, \delta^N_v, \delta^1_\chi, \ldots, \delta^N_\chi)$
    if $z < +\infty$ **then**
      for $f \in \mathcal{F}$ **do**
        Let m be the maneuver of aircraft f in the last solution found
        if m is the null maneuver **then**
          Erase all the heading and speed nodes of aircraft f
          $\chi^f_{\max} \leftarrow \lfloor \frac{n^f_\chi}{2} \rfloor$
          $\chi^f_{\min} \leftarrow -\chi^f_{\max}$
          $\delta^f_\chi \leftarrow 1$
          Build heading nodes with the values of $\chi^f_{\max}, \chi^f_{\min}$ and δ^f_χ
          $v^f_{\max} \leftarrow \lfloor \frac{n^f_v}{2} \rfloor$
          $v^f_{\min} \leftarrow -v^f_{\max}$
          $\delta^f_v \leftarrow 1$
          Build speed nodes with the values of $v^f_{\max}, v^f_{\min}$ and δ^f_v
        else
          if m is a heading maneuver **then**
            Erase all speed nodes of aircraft f
            $\chi^f_{\max} \leftarrow \max\{m, 0\}$
            $\chi^f_{\min} \leftarrow \min\{m, 0\}$
            $\delta^f_\chi \leftarrow \lfloor \frac{|m|}{n^f_\chi} \rfloor$
            Build heading nodes with the values of $\chi^f_{\max}, \chi^f_{\min}$ and δ^f_χ
          else
            Erase all heading nodes of aircraft f
            $v^f_{\max} \leftarrow \max\{m, 0\}$
            $v^f_{\min} \leftarrow \min\{m, 0\}$
            $\delta^f_v \leftarrow \lfloor \frac{|m|}{n^f_v} \rfloor$
            Build speed nodes with the values of $v^f_{\max}, v^f_{\min}$ and δ^f_v
    else
      for $f \in \mathcal{F}$ **do**
        $v^f_{\max} \leftarrow 2v^f_{\max}$, $\chi^f_{\max} \leftarrow 2\chi^f_{\max}$, $v^f_{\min} \leftarrow 2v^f_{\min}$, $\chi^f_{\min} \leftarrow 2\chi^f_{\min}$, $\delta^f_v \leftarrow 2\delta^f_v$, $\delta^f_\chi \leftarrow 2\delta^f_\chi$
    $z_c \leftarrow Solve\_MIP(\mathcal{F}, v^1_{\min}, \ldots, v^N_{\min}, v^1_{\max}, \ldots, v^N_{\max}, \ldots, \chi^1_{\min}, \ldots, \chi^N_{\min}, \chi^1_{\max}, \ldots, \chi^N_{\max}, \delta^1_v, \ldots, \delta^N_v, \delta^1_\chi, \ldots, \delta^N_\chi)$

$\mathcal{M}_f$ and the heading interval is replaced with another interval having 0 and m as extremums. The discretization step is chosen in order to keep n_χ^f heading nodes;

— if f performs a speed change of magnitude m, all the heading nodes are deleted from $\mathcal{M}_f$ and the speed interval is replaced with another interval having 0 and m as extremums, depending on the sign of m. The discretization step is chosen in order to keep n_v^f speed nodes.

In the situation where the current instance is not feasible, all the parameters describing the maneuvers $\mathcal{F}$ are doubled, in order to allow for larger maneuvers while maintaining a constant number of vertices in the graph.

Second decomposition method

The decomposition method is inspired from the POPMUSIC algorithm developed by Taillard et Voss (2002). This meta-heuristic is applied to various combinatorial optimization problems that can be partially optimized. It was designed to address the limitations of local search methods applied to problems of large size. It provides a method for generating neighborhoods that are a better fit for these problems. These neighborhoods need not being enumerated, since they can be implicitly explored with an optimization procedure. Algorithm 5.2 details the mechanics of the method.

Algorithm 5.2. Large Neighborhood Search (LNS) Algorithm

```
1: procedure LNS(r)
2:     Input: Solution S composed of parts s_1, ..., s_p
3:     O ← ∅
4:     while O ≠ {s_1, ..., s_p} do
5:         Select s_i ∉ O
6:         Create a subproblem R_i composed of the r parts {s_{i_1}, ..., s_{i_r}} most related to s_i
7:         Optimize R_i
8:         if R_i has been improved then
9:             Update S
10:            O ← ∅
11:        else
12:            O ← O ∪ {s_i}
```

To apply Algorithm 5.2, the user needs to define four key elements:

1. the definition of the parts of a solution;
2. the selection procedure in O;

3. the definition of relatedness between solution parts;
4. the sub-problem optimizer.

The algorithm works on a solution divided into p parts. While some parts still need to be selected, the algorithm selects a part p_0 to be optimized. To this end, a subproblem is created with the r parts of the solution that are the most related to p_0 . If the subproblem yields an improvement of p_0 , then all parts can be selected again. Otherwise, p_0 cannot be chosen again.

In a nutshell, the algorithm iteratively tries to improve the current solution by performing several neighborhood searches to improve every part of the solution. The neighborhood of a part of the solution is defined according to a relatedness criterion defined by the user.
We apply Algorithm 5.2 to large instances with aircraft randomly generated on different flight levels. We design the above-mentioned points as follows:

1. A solution part per flight level;
2. the selection procedure in O is the lowest flight level in O;
3. the relatedness between solution parts is defined as the vertical distance between their corresponding flight level;
4. the sub-problem optimizer is Algorithm 5.1.

Algorithm 5.3 gives the details of the overall procedure. The set of aircraft is sorted by flight level. A first loop is performed, where for each flight level, Algorithm 5.1 is used to optimize the problem for the corresponding aircraft, but allowing only horizontal maneuvers. In the second part of the algorithm (corresponding to the *for* loop), for each flight level, Algorithm 5.1 is used to optimize the problem for the corresponding aircraft. The difference is that they can change of flight level, but the constraints take into account the maneuvers of the set of aircraft on the adjacent levels. In other words, we authorize all types of maneuvers on the flight level, but we fix the maneuvers of the aircraft on adjacent levels to those that appear in the last solution found. Algorithm 5.3 stops when no improvement is achieved.
For this study, we apply Algorithm 5.3 to instances with aircraft randomly spread on several flight levels. However, Algorithm 5.3 could be applied to other types of instances. The only thing to adapt is the relatedness between subsets of aircraft, which would divide the set of aircraft into different clusters.

5.5 Results

In this section, the proposed model is validated with a benchmark of structured instances known in the literature as complex to solve, both two-dimensional and three-dimensional. The data that was used to compute the maneuvers and their costs were all extracted from

Algorithm 5.3. Spatial decomposition method

procedure SPATIAL_ DECOMPOSITION($\mathcal{F}$)
    Input: $\mathcal{F}$: set of aircraft randomly generated on p flight levels
    for $i = 1, \ldots, p$ **do**
        Solve conflicts for flight level i without altitude maneuvers
        $s_i \leftarrow$ result of the resolution for flight level i
Call LNS(2)
    Input: Solution S composed of parts $s_1, \ldots, s_p$
    R_1: solve conflicts for Flight Level (FL) 1 allowing altitude maneuvers, given the maneuvers of s_2
    R_p: solve conflicts for FL p allowing altitude maneuvers, given the maneuvers of s_{p-1}
    for $i = 2, \ldots, p-1$ **do**
        R_i: solve conflicts for FL i allowing altitude maneuvers, given the maneuvers of s_{i-1} and s_{i+1}

the BADA table that refers to the Airbus A-320. All tests were performed on a computer equipped with the following hardware: Intel Core i7-3770 processor, 3.4 GHz, 8-GB RAM. The algorithms were implemented in C++ and relies on CPLEX 12.5.1.0 CPL (2014) with default options to solve every instance.

The tables presented in this section gather information about the problems dimensions and computational results. The headings are given as follows:

— *Case*: case configuration;
— $|\mathcal{F}|$: number of aircraft;
— $|\mathcal{V}|$: number of vertices;
— $|\mathcal{E}|$: number of edges;
— d^*: relative graph density;
— n: number of variables;
— m: number of constraints;
— z_{ip}: optimal value of the problem (in kilograms of fuel);
— n_{nodes}: number of branch-and-bound nodes;
— t_{lp}: time (in seconds) to solve the continuous relaxation of the MILP;
— t_{ip}: time (in seconds) to obtain the z_{ip} value.

5.5.1 Benchmark description

Structured instances

This benchmark gathers three types of instances. The first ones are roundabout instances $\mathcal{R}_n$, where n aircraft are distributed on the circumference of a 100NM radius and fly towards

the center at the same speed and altitude. The second set gathers crossing flow instances $\mathcal{F}_{n,\theta,d}$, where two trails of n aircraft separated by d nautical miles intersect each other with an angle θ. The last type of instances are grids $\mathcal{G}_{n,d}$ constituted of two flow instances $\mathcal{F}_{n,\frac{\pi}{2},d}$, one instance being translated 15NM North-East from the other. One example of each type of instance is given on Figure 5.6.

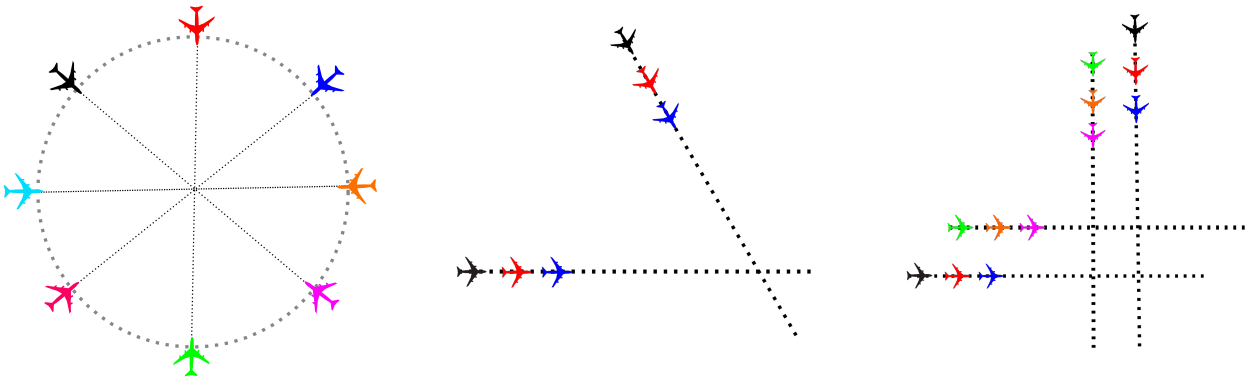

(a) Roundabout (b) Crossing Flow (c) Grid

Figure 5.6 – Examples

Single-level random benchmark

This benchmark consists of random instances, where aircraft are uniformely distributed within a square sector with side length 50NM. To avoid generating infeasible instances, we perform a preprocessing before solving the problem: for each pair of aircraft that will loose separation within the first 30 seconds of observation, we randomly delete one of the two aircraft. For a desired number of aircraft, we generate 15% more aircraft to anticipate the effect of the preprocessing. If more aircraft than desired remain after the preprocessing, extra aircraft are randomly removed until the desired number is reached.

Multi-level benchmark

We design this benchmark to study instances closer to the operational context. We generate a larger number of aircraft than for the single-level benchmark (from 50 to 200 aircraft with increments of 25 aircraft). The generation of aircraft is performed following the same procedure as for the single-level case. The aircraft are later randomly assigned to the different flight levels, following a uniform distribution. We denote $\mathcal{M}_{n,m}$ the instance where n aircraft are assigned to m different flight levels.

5.5.2 Computational results

Structured instances

Solutions for the instances described in Figure 5.6 are displayed on Figure 5.7. Figure 5.7a depicts the optimal solution for the instance $\mathcal{R}_8$ where all aircraft perform a right turn of 5° and avoid each other in a roundabout fashion before returning to their initial trajectory. Instance $\mathcal{F}_{5,\frac{\pi}{4},10}$ is solved in a symmetric fashion: each trail of aircraft perform the same set of heading changes. Instance $\mathcal{G}_{3,10}$ is also solved symmetrically, where the horizontal trails follow the same set of maneuvers, as well as the vertical trails.

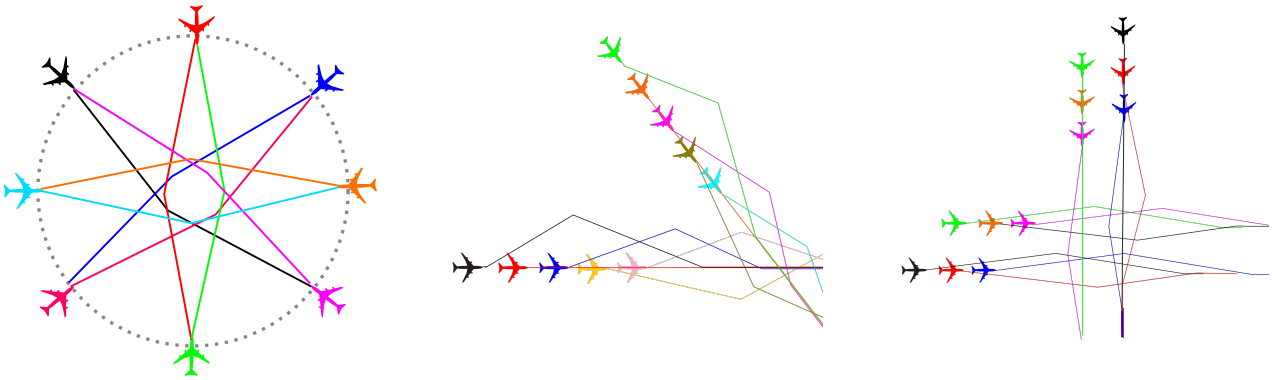

(a) Roundabout (b) Crossing Flow (c) Grid

Figure 5.7 – Solutions of the examples

The first set of simulations considers only horizontal maneuvers, with relative speed changes of $\pm 2\%$, $\pm 4\%$ and $\pm 6\%$ and heading changes of $\pm 5°, \pm 10°, \pm 15°$. Table 5.1 gathers the main information about the dimensions of the instances, along with the computational results of the original model. Results of the SMILO procedure on these instances are gathered in Subsection 5.5.3. Algorithm 5.3 was not applied to this benchmark because the symmetry inherent to the instances make the design of a relatedness procedure not necessarily relevant. The original model yields the optimal solution in real-time. Indeed, problems known to be complex with up to 20 aircraft are solved to optimality in less than 15 seconds. This result is very satisfying since the density of the graph is high.

In the second simulation set, we introduce altitude maneuvers: aircraft are allowed to move to an adjacent flight level. Table 5.2 reports the main results. Solution times tend to slightly increase. This is explained by the introduction of a new set of high degree vertices. Indeed, every change of flight level is conflict-free with all the horizontal maneuvers. Nevertheless, the solution can still be computed in a short time. These results are promising since the tested instances involve a traffic denser than real-life situations.

Table 5.1 – Dimensions of the instances and computational results for the virtual benchmark using only horizontal maneuvers

		Graph $\mathcal{G}$				MILP		Resolution			
Instance type	Case	$\lvert\mathcal{F}\rvert$	$\lvert\mathcal{V}\rvert$	$\lvert\mathcal{E}\rvert$	d	m	n	z_{ip}	$nodes$	t_{lp}	t_{ip}
Roundabout	$\mathcal{R}_4$	4	52	612	0.6	104	1333	2.66	27	0.02	0.07
	$\mathcal{R}_8$	8	104	2744	0.58	208	5705	5.34	75	0.02	0.51
	$\mathcal{R}_{12}$	12	156	6300	0.56	312	12925	19.99	84	0.02	2.95
	$\mathcal{R}_{16}$	16	208	11396	0.56	416	23225	42.73	39	0.02	6.99
	$\mathcal{R}_{20}$	20	260	17756	0.55	520	36053	86.59	71	0.02	11.63
Flows	$\mathcal{F}_{1,60,10}$	2	26	102	0.6	52	259	1.32	0	0.02	0.05
	$\mathcal{F}_{2,60,10}$	4	52	736	0.73	104	1581	2.66	0	0.02	0.06
	$\mathcal{F}_{3,60,10}$	6	78	1980	0.78	156	4123	4	0	0.02	0.18
	$\mathcal{F}_{4,60,10}$	8	104	3846	0.81	208	7909	5.34	57	0.02	0.57
	$\mathcal{F}_{5,60,10}$	10	130	6349	0.83	260	12969	6.68	0	0.02	0.9
	$\mathcal{F}_{6,60,10}$	12	156	9483	0.85	312	19291	9.96	70	0.02	1.96
	$\mathcal{F}_{7,60,10}$	14	182	13252	0.86	364	26883	13.3	0	0.02	1.44
	$\mathcal{F}_{8,60,10}$	16	208	17659	0.87	416	35751	18.66	0	0.02	1.7
	$\mathcal{F}_{9,60,10}$	18	234	19057	0.88	468	42579	30.18	10	0.02	1.79
	$\mathcal{F}_{10,60,10}$	20	260	22563	0.87	520	47264	41.61	0	0.02	1.85
Grids	$\mathcal{G}_{2,1,10}$	4	52	787	0.78	104	1683	1.32	35	0.02	0.18
	$\mathcal{G}_{2,2,10}$	8	104	3780	0.8	208	7777	3.33	0	0.02	0.28
	$\mathcal{G}_{2,3,10}$	12	156	9072	0.81	312	18469	6.01	29	0.02	1.98
	$\mathcal{G}_{2,4,10}$	16	208	16854	0.83	416	34141	11.23	55	0.02	5.87
	$\mathcal{G}_{2,5,10}$	20	260	27207	0.85	520	54955	16.06	138	0.02	13.59

Single-level random benchmark

Figure 5.8a displays a randomly chosen instance $\mathcal{U}_{15}$ along with the corresponding solution on Figure 5.8b. Initial speed vectors are represented by dotted vectors, whereas requested maneuvers are given by solid vectors. The two aircraft circled in red changed their flight level. The computational results are reported in Table 5.3. Figures displayed are averages over 100 simulations.

Table 5.4 displays the computational results for the single-level random benchmark with the addition flight level changes: aircraft can climb to the next level or descend to the one underneath.

The computational time remains short, but for some generated instances it tends to increase. To investigate this issue, we ran other simulations while changing the number of possible maneuvers. Results highlighted a high sensitivity of the computational time of the model regarding the number of vertices for a given instance. This observation is at the core of the design of the SMILO procedure presented in Subsection 5.4.2.

Table 5.2 – Dimensions of the instances and computational results on the virtual benchmark including flight level changes

		Graph $\mathcal{G}$				MILP		Resolution			
Instance type	Case	$\lvert\mathcal{F}\rvert$	$\lvert\mathcal{V}\rvert$	$\lvert\mathcal{E}\rvert$	d	m	n	z_{ip}	$nodes$	t_{lp}	t_{ip}
Roundabout	$\mathcal{R}_4$	4	60	936	0.69	120	1997	2.66	0	0.02	0.08
	$\mathcal{R}_8$	8	120	4256	0.68	240	8761	5.34	67	0.02	0.7
	$\mathcal{R}_{12}$	12	180	9864	0.66	360	20101	19.99	108	0.02	4.27
	$\mathcal{R}_{16}$	16	240	17876	0.66	480	36249	42.73	96	0.02	16.63
	$\mathcal{R}_{20}$	20	300	28016	0.66	600	56653	86.59	277	0.02	37.1
Flows	$\mathcal{F}_{1,60,10}$	2	30	156	0.69	60	375	1.32	0	0.02	0.02
	$\mathcal{F}_{2,60,10}$	4	60	1068	0.79	120	2261	2.66	54	0.02	0.22
	$\mathcal{F}_{3,60,10}$	6	90	2814	0.83	180	5815	4	0	0.02	0.23
	$\mathcal{F}_{4,60,10}$	8	120	5406	0.86	240	11061	5.34	75	0.02	0.98
	$\mathcal{F}_{5,60,10}$	10	150	8859	0.87	300	18029	6.68	0	0.02	1.19
	$\mathcal{F}_{6,60,10}$	12	180	13167	0.89	360	26707	8.97	74	0.02	2.4
	$\mathcal{F}_{7,60,10}$	14	210	18334	0.9	420	37103	11.15	123	0.02	3.6
	$\mathcal{F}_{8,60,10}$	16	240	24363	0.9	480	49223	14.39	103	0.02	7.2
	$\mathcal{F}_{9,60,10}$	18	270	31261	0.91	540	63081	24.16	79	0.02	9.13
	$\mathcal{F}_{10,60,10}$	20	300	39036	0.91	600	78693	30.04	92	0.02	11.51
Grids	$\mathcal{G}_{2,1,10}$	4	60	1115	0.83	120	2355	1.32	53	0.02	0.1
	$\mathcal{G}_{2,2,10}$	8	120	5332	0.85	240	10913	3.33	0	0.02	0.42
	$\mathcal{G}_{2,3,10}$	12	180	12744	0.86	360	25861	6.01	0	0.02	2.01
	$\mathcal{G}_{2,4,10}$	16	240	23542	0.87	480	47581	9.78	185	0.02	10.05
	$\mathcal{G}_{2,5,10}$	20	300	37807	0.87	600	76235	13.24	180	0.02	19.91

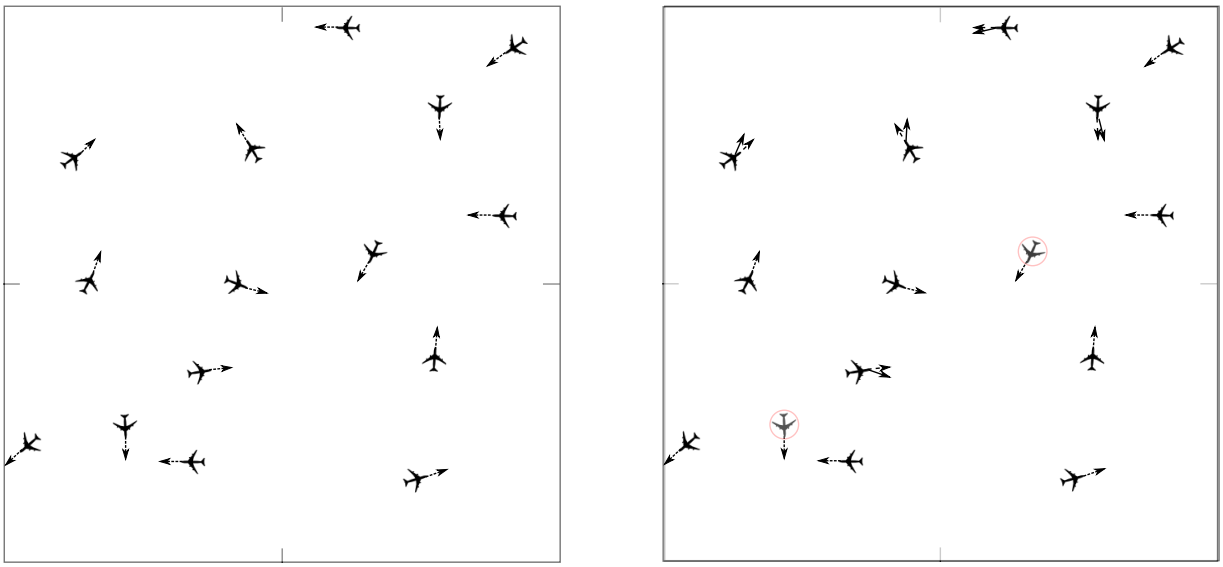

(a) Random instance (b) Solution

Figure 5.8 – Random instance $\mathcal{U}_{15}$ and its solution

Table 5.3 – Dimensions of the instances and computational results on the single-level random benchmark including horizontal maneuvers

		Graph $\mathcal{G}$				MILP		Resolution			
Instance type	Case	$\lvert\mathcal{F}\rvert$	$\lvert\mathcal{V}\rvert$	$\lvert\mathcal{E}\rvert$	d	m	n	z_{ip}	$nodes$	t_{lp}	t_{ip}
Random	$\mathcal{U}_5$	5	55	726	1	110	1567	0.05	0	0.02	0
	$\mathcal{U}_{10}$	10	110	4830	0.99	220	9890	0.23	0	0.02	0
	$\mathcal{U}_{15}$	15	165	9865	0.99	330	20075	0.86	0	0.02	7.56
	$\mathcal{U}_{20}$	20	220	14365	0.99	440	29190	1.54	8	0.02	11.1
	$\mathcal{U}_{25}$	25	275	19182	0.98	550	38939	2.15	19	0.02	12.1
	$\mathcal{U}_{30}$	30	330	28750	0.99	660	58190	2.21	45	0.02	14.32
	$\mathcal{U}_{35}$	35	385	31406	0.99	770	63617	2.41	75	0.02	16.25
	$\mathcal{U}_{40}$	40	440	52766	0.99	880	106452	3.21	119	0.02	19.63
	$\mathcal{U}_{45}$	45	495	62051	0.99	990	125137	3.26	179	0.02	20.02
	$\mathcal{U}_{50}$	50	550	57215	1	1100	115580	3.87	225	0.02	20.06
	$\mathcal{U}_{55}$	55	605	69090	0.99	1210	139445	4.83	346	0.02	22.21
	$\mathcal{U}_{60}$	60	660	75338	0.98	1320	152056	6.32	561	0.02	29.35

Table 5.4 – Dimensions of the instances and computational results on the single-level random benchmark including horizontal maneuvers and flight level changes

		Graph $\mathcal{G}$				MILP		Resolution			
Instance type	Case	$\lvert\mathcal{F}\rvert$	$\lvert\mathcal{V}\rvert$	$\lvert\mathcal{E}\rvert$	d	m	n	z_{ip}	$nodes$	t_{lp}	t_{ip}
Random	$\mathcal{U}_5$	5	75	1209	1	150	2573	0.01	0	0.02	0.01
	$\mathcal{U}_{10}$	10	150	4839	1	300	9988	0.01	0	0.02	7.07
	$\mathcal{U}_{15}$	15	225	8939	0.98	450	18343	0.32	0	0.02	15.25
	$\mathcal{U}_{20}$	20	300	16732	0.99	600	34084	0.97	0	0.02	18.55
	$\mathcal{U}_{25}$	25	375	22345	0.98	750	45465	1.29	38	0.02	20.55
	$\mathcal{U}_{30}$	30	450	32248	0.99	900	65426	1.37	31	0.02	21.46
	$\mathcal{U}_{35}$	35	525	42027	0.99	1050	85139	1.76	0	0.02	25.22
	$\mathcal{U}_{40}$	40	600	50386	0.99	1200	102012	2.04	0	0.02	29.15
	$\mathcal{U}_{45}$	45	675	60764	0.99	1350	122923	3.18	41	0.02	34.02
	$\mathcal{U}_{50}$	50	750	69035	0.99	1500	139620	3.12	0	0.02	37.47
	$\mathcal{U}_{55}$	55	825	84344	0.99	1650	170393	4.55	89	0.02	40.16
	$\mathcal{U}_{60}$	60	900	75126	0.99	1800	152112	6.24	26	0.02	55.25

5.5.3 Detailed results for the SMILO procedure on the benchmark without altitude changes

This simulation set was designed to address two points of investigation. The first one is to identify the impact of the number of maneuvers on the objective function and the computational time. The second one was to evaluate the performances of the SMILO procedure, and to classify it in terms of trade-off between the optimal value and the computational time. These simulations were ran with four different parameter sets:

— a large discretization, with relative speed changes of $\pm 6\%$ and heading changes of $\pm 15°$

, yielding an objective function value z^l_{ip} within time t^l_{ip};

— a medium discretization, with relative speed changes of $\pm 2\%$, $\pm 4\%$ and $\pm 6\%$ and heading changes of $\pm 5°, \pm 10°, \pm 15°$, yielding an objective function value z^m_{ip} within time t^m_{ip};

— a narrow discretization, with 12 relative speed changes between -6% and 6% with a step of 1% and heading changes between $-15°$ and $15°$ with a step of $1°$. These parameters yield an objective function value z^n_{ip} within time t^n_{ip};

— the SMILO procedure applied with four speed changes and four heading changes, yielding an objective function value z_{SMILO} within time t_{SMILO}.

Table 5.5 – Dimensions of the instances and computational results

Instance type	Case	Large discretization		Medium discretization		Narrow disctretization		Iterative procedure		
		z^l_{ip}	t^l_{ip}	z^m_{ip}	t^m_{ip}	z^n_{ip}	t^n_{ip}	z_{SMILO}	t_{SMILO}	CPLEX Calls
Roundabout	$\mathcal{R}_2$	2.58	0.01	0.65	0.02	0.21	0.27	0.21	0.02	2
	$\mathcal{R}_6$	13.29	0.01	4	0.14	2.56	5.62	2.73	0.17	3
	$\mathcal{R}_{10}$	26.67	0.31	16.64	1.17	9.62	244.39	10.84	1.33	3
	$\mathcal{R}_{14}$	37.38	1.73	35.38	2.65	27.11	1382.58	29.19	2.74	4
	$\mathcal{R}_{18}$	119.34	6.21	77.91	5.11	53.11	1845.45	67.38	6.14	3
Flows	$\mathcal{F}_{1,\frac{\pi}{4},10}$	2.58	0.01	1.32	0.02	0.84	2.58	1.06	0.03	2
	$\mathcal{F}_{3,\frac{\pi}{4},10}$	7.93	0.07	4	0.18	2	7.93	2.98	1.11	4
	$\mathcal{F}_{5,\frac{\pi}{4},10}$	13.29	0.43	6.68	0.9	4.43	157.6	5.22	2.54	6
	$\mathcal{F}_{7,\frac{\pi}{4},10}$	24	0.9	13.3	1.44	9.35	2431.15	10.45	5.95	5
	$\mathcal{F}_{9,\frac{\pi}{4},10}$	36.05	2.77	30.18	1.79	21.23	3675.87	24.11	7.43	3
Grids	$\mathcal{G}_{2,1,10}$	5.26	0.04	1.32	0.18	0.69	1.95	1.32	0.55	3
	$\mathcal{G}_{2,2,10}$	10.61	0.18	3.33	0.28	1.39	14.93	1.44	0.66	4
	$\mathcal{G}_{2,3,10}$	15.97	0.64	6.01	1.98	2.41	62.33	3.41	6.96	6
	$\mathcal{G}_{2,4,10}$	25.17	2.77	11.23	5.87	3.61	317.8	8.14	13.21	3
	$\mathcal{G}_{2,5,10}$	37.3	4.5	16.06	13.59	5.48	1845.36	9.51	17.72	5
Random	$\mathcal{U}_{15}$	1.37	8.12	0.54	9.1	0.34	118.45	0.46	21.34	3
	$\mathcal{U}_{30}$	3.34	10.03	2.21	12.32	1.02	500.12	2.11	24.26	4
	$\mathcal{U}_{45}$	5.12	14.32	3.26	19.02	2.97	1002.87	3.07	32.6	6
	$\mathcal{U}_{60}$	8.45	17.01	6.32	23.35	5.98	1237.12	6.11	37.18	3

Table 5.5 gathers the main results of these simulations. Results exhibit that the choice of the discretization size is critical regarding the computational time. Indeed, going from a medium discretization to a narrow discretization divides on average the cost of the solution by 2, but the solution time is on average 18 times longer. Results for the SMILO procedure give evidence that it represents a good trade-off between finding an efficient solution while not taking too much time. Indeed, solutions found by the SMILO procedure are on average 41% more expensive than the medium discretization ones, but it takes 50% less time to find them. This result is especially useful for the random instances, where the original optimization model seemed less efficient.

Figure 5.9 depicts a visual summary of Table 5.5. Figure 5.9a highlights the influence of the discretization on the quality of the best solution found, and compares the solution found by the SMILO procedure to those obtained with the different discretizations. Results place the SMILO solution as an intermediate between the large and medium discretization solutions.

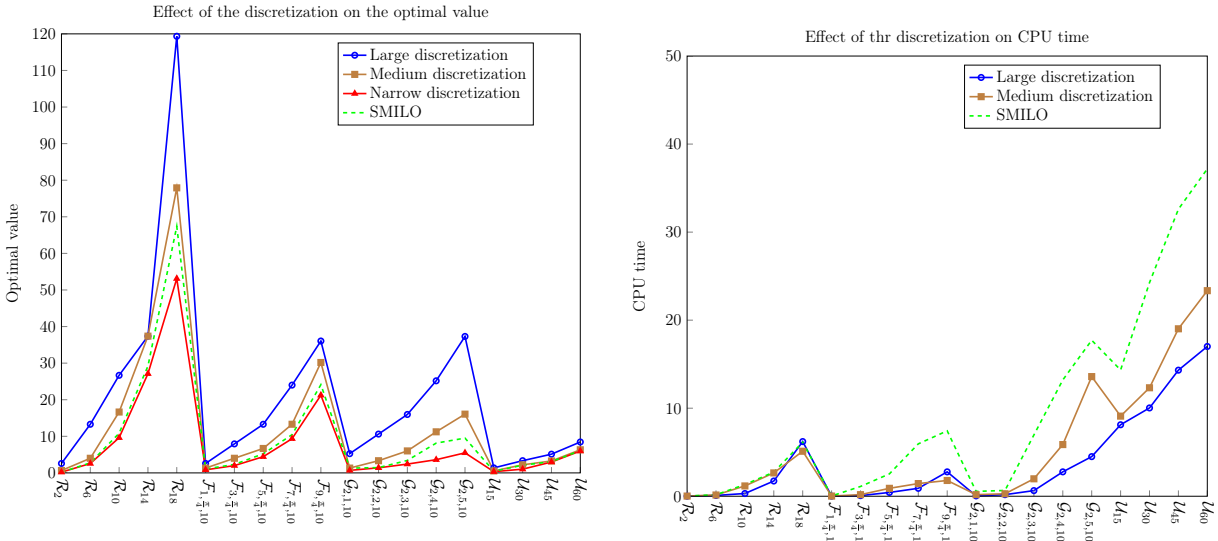

(a) Influence on objective value

(b) Influence on CPU time

Figure 5.9 – Influence of the discretization on the optimal value and the CPU time

Figure 5.9b compares the solution time of the SMILO procedure with that yielded by the small and medium discretizations. The solution times with the small discretization were not displayed on the chart, since most of these values are not of the same scale. Results show that the SMILO procedure needs less time than the model with the medium discretization in order to find the optimal value regarding the available set of maneuvers.

5.5.4 Evaluating the second decomposition method on the multi-level random benchmark

Table 5.6 gathers the computational results of the second decomposition method on the multi-level random benchmark.

In order to study the performances of the method, we compare it with the classical model. z_{ip} (respectively t_{ip}) correspond to the optimal value (respectively CPU time) of the second decomposition method using the first one as a subroutine. z^f_{best} (respectively t^f_{best}) denote the best value (respectively the CPU time) of the best solution found within a limit of one hour of computations. If the optimal solution is found within one hour, then the resolution stops. Otherwise, we give the value of the best solution found within one hour. Results exhibit very slow resolution times for the classical model. Indeed, only 6 instances out of 24 are solved to optimality within one hour. This observation is a consequence of the fact that the model does not exploit the geometry of the instance: instead of naturally dividing the instance into flight levels, it considers the instance as a whole, hence drastically increasing the complexity

Table 5.6 – Dimensions of the instances and computational results for the second decomposition method on the multi-level random benchmark

Case	Size		Resolution					
	$\|\mathcal{F}\|$	$\|\mathcal{L}\|$	z_{ip}	*nodes*	t_{ip}	CPLEX Calls	z^f_{best}	t^f_{best}
$\mathcal{M}_{100,10}$	100	10	6.27	0	3.01	20	5.16	2692.44
$\mathcal{M}_{100,12}$	100	12	4.96	0	1.49	24	4.96	2310.54
$\mathcal{M}_{100,14}$	100	14	4.93	0	0.54	28	4.93	2066.45
$\mathcal{M}_{100,16}$	100	16	3.92	0	0.95	32	3.92	1975.94
$\mathcal{M}_{100,18}$	100	18	3.33	0	0.61	36	3.33	1964.45
$\mathcal{M}_{100,20}$	100	20	2.98	0	0.39	40	2.98	1712.24
$\mathcal{M}_{150,10}$	150	10	18.15	0	2.85	20	23.05	3600
$\mathcal{M}_{150,12}$	150	12	12.45	0	2.47	24	19.05	3600
$\mathcal{M}_{150,14}$	150	14	9.67	0	1.16	28	17.03	3600
$\mathcal{M}_{150,16}$	150	16	9.03	0	1.71	32	16.15	3600
$\mathcal{M}_{150,18}$	150	18	7.05	0	0.9	36	12.48	3600
$\mathcal{M}_{150,20}$	150	20	2.68	32	0.62	40	6.12	3600
$\mathcal{M}_{200,10}$	200	10	13.4	35	5.63	20	45.2	3600
$\mathcal{M}_{200,12}$	200	12	12.71	0	4.03	24	31.02	3600
$\mathcal{M}_{200,14}$	200	14	11.97	25	4.42	28	29.45	3600
$\mathcal{M}_{200,16}$	200	16	12.04	0	3.5	32	22.08	3600
$\mathcal{M}_{200,18}$	200	18	8.15	0	1.85	36	18.45	3600
$\mathcal{M}_{200,20}$	200	20	5.36	0	3.3	40	12.45	3600
$\mathcal{M}_{250,10}$	250	10	30.24	234	8.12	20	101.35	3600
$\mathcal{M}_{250,12}$	250	12	24.15	42	8.1	24	80.15	3600
$\mathcal{M}_{250,14}$	250	14	21.45	0	5.12	28	78.11	3600
$\mathcal{M}_{250,16}$	250	16	18.04	0	4	32	64.15	3600
$\mathcal{M}_{250,18}$	250	18	16.41	0	4.26	36	24.48	3600
$\mathcal{M}_{250,20}$	250	20	11.05	0	3.81	40	21.35	3600

of the computations to perform. On the contrary, the decomposition method benefits from the geometry of the instances and the weak interdepedency between flight levels to perform a more efficient resolution. As a consequence, every instance is solved to optimality within 9 seconds.

5.6 Conclusions

In this article, we started by designing an optimization model for the air conflict resolution problem. To this end, we designed a graph whose vertices correspond to maneuvers and whose edges link conflict-free maneuvers of distinct aircraft. A solution to the problem corresponds

to a maximum clique of minimum cost in the graph. The cost structure used in the model is specific, since the cost of the vertices depends on the vertices belonging to the maximum clique. This specificity makes the model an original variant of the search for a maximum clique of minimum weight. The main advantage of our model is its flexibility, since the resolution process is fully separated from the modeling of the problem. As a consequence, the mathematical framework remains valid under a large variety of assumptions. This is an interesting feature for the community since in the future we will be able to compare this model to other existing models.

Since the clique search problem is $\mathcal{NP}$-hard, a sensitivity of the solution time regarding the number of maneuvers per aircraft could be expected. Besides, in practice the set of aircraft has weak geometric dependencies that could be taken advantage of. However, these dependencies do not appear explicitly in the model. To address these two observations, we designed two decomposition methods. The first one is a sequential mixed integer linear optimization procedure iteratively solving the problem while changing the discretization. With this method we achieve a trade-off between finding economically efficient solutions while not taking too much time. The second one uses this method as a subroutine of a meta-heuristic exploiting the geometry of the instances by solving local parts of the instances before solving them globally.

We performed tests for our model on structured instances known to be complex. Results exhibit small solution times (less than 15 seconds for instances involving up to 20 aircraft). For larger instances, solution times tend to slightly increase but remain almost real-time. Simulations highlight the sensitivity of the model regarding the number of maneuvers. In this setting, the first decomposition method corresponds to a good trade-off between solution time and cost efficiency. Moreover, it can be considered as an efficient way to solve the problem according to the user's preferences, whether they are more time or cost oriented. The second procedure solved instances with up to 250 aircraft divided between up to 20 flight levels in less than 5 seconds, whereas with the original model the optimal solution could not be found within an hour.

Further research will introduce uncertainties in our model. These uncertainties can be of different types: we can consider errors in the trajectory prediction, or introduce wind to have a more realistic footing for our study. Real-life instances would also be valuable to validate the performance of our model, and in particular instances with aircraft changing altitudes. For such instances, it would be of great interest to adapt the second procedure presented in this article.

CHAPITRE 6 ARTICLE 3 : SOLVING THE AIR CONFLICT RESOLUTION PROBLEM UNDER UNCERTAINTY AS AN ITERATIVE BI-OBJECTIVE MIXED INTEGER LINEAR PROGRAM

Auteurs : Thibault LEHOUILLIER, Moncef Ilies NASRI, Jérémy OMER, François SOUMIS, Guy DESAULNIERS.
Soumis à : Transportation Science.

Abstract

In this paper, we tackle the aircraft conflict resolution problem under uncertainties. We consider errors due to the wind effect, the imprecision on the aircraft speed prediction, and the delay in the execution of maneuvers. Using a geometrical approach, we derive an analytical expression for the minimum distance between aircraft, along with the corresponding probability of conflict. These expressions are incorporated into an existing deterministic model for conflict resolution. This model solves the problem as a maximum clique of minimum weight in a graph whose vertices represent possible maneuvers and where edges link conflict-free maneuvers of different aircraft. We then present a solution procedure focusing on two criteria, namely fuel efficiency and probability of using a recourse: we iteratively generate solutions of the Pareto front to provide the controller with a set of possible solutions where he/she can choose the one corresponding the most to his/her preferences. Intensive Monte-Carlo simulations validate the expressions derived for the minimum distance and the probability of conflict. Computational results highlight that up to 10 different solutions for instances involving up to 35 aircraft are generated within three minutes.

6.1 Introduction

6.1.1 Automating air traffic control

In the current air traffic management (ATM) organization, the air traffic control (ATC) is in charge of maintaining safety. To this end, controllers monitor the traffic to ensure the separation between all aircraft at all times. A projected loss of separation between two aircraft is called a *conflict* and must be solved by the controller. To this end, avoidance maneuvers are issued to the pilots of the involved aircraft to prevent the loss of separation. Maintaining safety in the airspace is a challenging task, especially in a context of increasing traffic. Indeed, the latest long-term forecast published by EUROCONTROL states that the traffic demand will increase by 20% to 80% between 2012 and 2035 (EUROCONTROL,

2013). Besides, a simulation-based study performed by Lehouillier *et al.* (2014) shows that for a 50% increase in traffic, the controllers in charge of busy sectors would have to solve 27 conflicts per hour on average. During the last decade a lot of research was conducted on the development of automated decision tools to help the controller. Such automated tools are recognized as key-components of future ATM systems like the Single European Sky ATM Research (see SESAR Joint Undertaking (2012)) project in Europe and the Next Gen (see Joint Planning and Development Office (2008) for details) program in the United States.

6.1.2 The air conflict resolution problem

One complex and central problem encountered in ATC is the air conflict resolution problem (CR). A conflict occurs when two aircraft are too close to each other regarding predefined horizontal and vertical separation distances of respectively 5NM and 1000ft. To solve a conflict, the controllers issue maneuvers that can consist of speed, heading or altitude changes. Given the current position, speed, acceleration and the predicted trajectory of a set of aircraft, the CR problem corresponds to identifying the conflict-free maneuvers that minimize a given cost function. The CR problem can be tackled following two different settings, namely deterministic and stochastic. The first one assumes that aircraft follow exact trajectory predictions, along with maneuvers applied without any errors. However, uncertainties are one of the reasons why ATC is a complicated task. The weather conditions, along with the incomplete knowledge of the physical characteristics of the aircraft and the imprecision during the communication and maneuver execution processes represent the main factors of uncertainty in ATC (Erzberger *et al.* (1997b)). In this context, the uncertainties cause a perturbation of the trajectory, inducing cross and along-track errors in the prediction of the trajectory. The along-track error (or longitudinal error) is the distance between the predicted aircraft position and the projection of the actual aircraft position on the predicted trajectory. The cross-track error (or lateral error) corresponds to the distance between the actual aircraft position and the predicted trajectory. Figure 6.1 illustrates these errors. They can jeopardize the conflict resolution process. To tackle this issue, stochastic resolution methods aim at solving the CR problem while taking into account these perturbations.

6.1.3 Literature review on the CR problem

The CR problem is one of the most widely studied problems in ATM. We provide a synthetic analysis of the studies that were most influential to our work, both in a deterministic and a stochastic setting.

A complete coverage of the existing literature on the deterministic CR problem may be found in the review performed in Martin-Campo (2010). Mixed integer linear and nonlinear

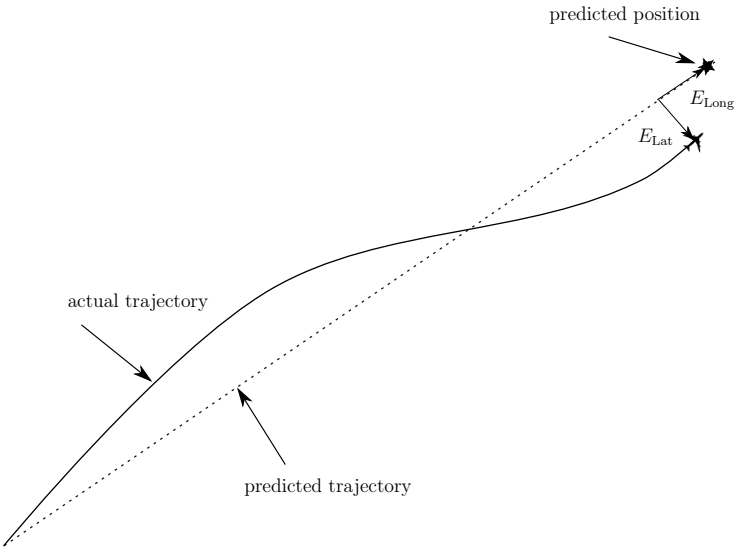

Figure 6.1 – Cross and along-track errors on an aircraft trajectory

programming are powerful theoretical frameworks for the study of CR. With the realistic restriction that the aircraft perform at most one maneuver at the initial time, Pallottino *et al.* (2002) exploit the geometry of the separation constraints to develop two mixed integer linear programs (MILPs) that allow either speed changes with constant headings or heading changes with constant speeds. Alonso-Ayuso *et al.* (2012) extend the model of Pallottino *et al.* (2002) by introducing continuous instead of instantaneous speed changes. More recently, Omer (2015b) develops a MILP with a space discretization using only the points of interest for the conflict resolution.

Uncertainties can be gathered and modeled as having a global impact on the trajectory prediction. Ballin et Erzberger (1996) quantify the along-track error by comparing prediction and actual data for the Dallas Fort Worth Airport. Results highlight that for a time horizon shorter than 20 minutes, the error follows a normal distribution. Irvine (2002) develops an expression of the minimum distance and the corresponding probability of conflict using a geometrical approach. The author models cumulative cross and along track errors that are affected to each aircraft at the beginning of the observation. After applying this initial perturbation, aircraft are assumed to evolve in a deterministic environment. Uncertainties can also be divided into different categories than can be modeled more specifically. For instance, Lygeros et Prandini (2002) model the effect of the wind and the resulting FMS correction. Cole *et al.* (1998) and Schwartz *et al.* (2000) conduct statistical studies comparing predictions to actual data in the Denver area to derive the correlation structure of the wind. Chaloulos et Lygeros (2007) study the perturbations due to imprecisions in the speed and air temperature measures. The authors model the error as a normal distribution.

When the uncertainties become too complex to derive exact probability expressions, Monte-Carlo simulations are often performed. Prandini *et al.* (2000) use Monte-Carlo simulations to develop a model where the wind correlates the cross and along track errors.

6.1.4 Critical analysis and contribution statement

The literature review highlights that numerous results have been established to solve the CR problem, both in the deterministic and the stochastic settings. Nevertheless, some features still need to be addressed. More specifically, we formulate three observations that we consider important when designing a resolution tool for the CR problem. The first one relies on the fact that robustness is critical in ATC. A large span of factors can have a dramatic impact on the conflict resolution. As a consequence, it is necessary to provide the controller with a tool as robust as possible. In other words, the controller needs to be ready to handle every possible situation. To this end, the mathematical framework in the developed decision tools needs to remain valid, whatever the hypotheses followed. Unfortunately, many models lack of consistency when it comes to the modification of hypotheses, like the introduction of uncertainties, or other modeling features concerning the aircraft dynamics. For instance, the constraints in Pallottino *et al.* (2002) are linear when aircraft perform either a heading change or a speed change, but become nonlinear when both are performed. The second observation is related to the multi-objective nature of the CR problem. Indeed, focusing on only one objective, like the fuel consumption, or the delays, does not necessarily reflect all the aspects of the problem, nor does it respect the users' preferences. Several multi-objective approaches of the CR problem have been performed (Menon *et al.* (1999); Tomlin *et al.* (1998b); Alonso-Ayuso *et al.* (2016)), and research needs to be conducted in this direction. The last observation we formulate is that in conflict resolution the notion of optimality is subjective. Indeed, depending on the objective to optimize, the optimal solution is not necessarily far better than other good solutions. As a consequence, providing the controller with only one solution can be restrictive, depending on the context and the controller's preferences. Few work has been done on methods generating a set of solutions instead of a single solution. For instance, satisficing game theory (see Stirling et Goodrich (1999) for a description of the theory) allows to generate a set of satisficing solutions regarding two criteria representing the preferences of the players in terms of efficiency or resource consumption. Applications to ATC have been considered (see, e.g., Archibald *et al.* (2008)), but the hypotheses are quite restrictive, and the model suffers from a lack of computational power.

Our main contributions in our effort to provide an answer to the aforementioned remarks are twofold. First, we provide an analytical expression of the minimum distance and the probability of conflict in a context allowing complex uncertainties: the error in wind predictions

is considered, along with the error on the aircraft speed prediction. We introduce the uncertainty on the delay in the execution of maneuvers, which to our knowledge has not been studied yet in the literature, although it is a reality in ATC. With this approach, we are able to cover a large span of uncertainties involved in ATC. Besides, these computations are fast compared to a simulation-based approach that can be more time consuming. Second, we model the CR problem as a bi-objective problem minimizing fuel consumption and the probability that the controller has to reissue maneuvers: we sequentially solve a mono-objective MILP. With this approach, we benefit from the powerful results yielded by MILPs, namely the guarantee of finding an optimal solution (if existing) in a short time, even for large and complex instances. Each iteration generates a solution that is immediately available to the user. The set of generated solutions is a tight approximation of the Pareto front of the solution. This method allows the user to choose which solution to apply within the generated set, depending on his/her preferences or other factors. The MILP used is taken from a preliminary study performed by Lehouillier *et al.* (2015b,a). It was chosen because it fully separates the modeling of the aircraft dynamics, maneuvers and cost function from the resolution process. As a consequence, the hypotheses considered do not jeopardize the validity of the proposed mathematical framework, and in particular the introduction of uncertainties. Besides, the fact that we are able to introduce uncertainties in the model from Lehouillier *et al.* (2015b) validates its robustness.

To evaluate the model, we first validate the computations derived for the probability of conflict by running Monte-Carlo simulations. We use several test beds generating 2000 random scenarios to verify the correctness of the developed theory. After the validation of the computations, we test our iterative resolution procedure by conducting intensive simulations on a benchmark of structured and random instances that are complex to solve. The aim of the experiments is to verify that our algorithm is able to provide the user with a set of solutions in a short period of time, while ensuring that separation is maintained in complex situations. The organization of the paper will be as follows. We formulate the problem in Section 6.2. We describe the mathematical model to be adapted in Section 6.3. We detail the iterative optimization procedure used to generate the set of solutions in Section 6.4. The method is then tested and analyzed through intensive experiments described in Section 6.5.

6.2 Problem Formulation

6.2.1 Aircraft dynamics

As in the majority of the literature, we use a three-dimensional point-mass model for aircraft dynamics. This model establishes relationships between the different physical parameters of

each aircraft.

$$\frac{dp_x}{dt} = V\cos\gamma\cos\chi \tag{6.1}$$
$$\frac{dp_y}{dt} = V\cos\gamma\sin\chi \tag{6.2}$$
$$\frac{dp_z}{dt} = V\sin\gamma \tag{6.3}$$
$$\frac{d\gamma}{dt} = \frac{g_0}{V}(n\cos\phi - \cos\gamma) \tag{6.4}$$
$$\frac{d\chi}{dt} = \frac{g_0}{V}\frac{n\sin\phi}{\cos\gamma} \tag{6.5}$$
$$\frac{dV}{dt} = \frac{F_T - F_D}{m} - g_0\sin\gamma \tag{6.6}$$

The position of the aircraft is given by the coordinates (p_x, p_y, p_z) of its center of gravity in a local coordinate system, (p_x,p_y) being its coordinates in a horizontal plane and p_z its altitude. The aircraft flies at speed V and the angles χ, ϕ and γ correspond respectively to its heading, roll and pitch. F_T and F_D denote the norm of the thrust and drag forces respectively, m is the aircraft mass, n is the load factor and g_0 corresponds to the gravitational acceleration. In this article, we make the assumption that aircraft are stabilized and follow a planar motion in a single flight level. Aircraft follow their trajectory with a stepwise constant acceleration. This assumption is realistic since it respects the time-continuity of speed, and it corresponds to a setting where maneuvers are performed smoothly.

6.2.2 Aircraft maneuvers

The maneuvers are horizontal maneuvers consisting in heading and speed changes. These maneuvers are performed dynamically in order to avoid a significant error in separation distance. Aircraft execute a speed or a heading change with a constant acceleration and turn angle, respectively, according to values extracted from Paielli (2003). Other types of maneuvers, i.e., flight level changes, could be considered without changing the validity of the mathematical resolution.

6.2.3 Aircraft trajectory recovery

We consider that aircraft follow a 4D contractual trajectory, which represents a compromise between the user's preferences and the capacity constraints of the network. The trajectories of the aircraft then have to meet time and space requirements over a sequence of 4D points. Noncompliance with this contract induces penalty fees to companies. As a consequence, it is important to make sure that, after resolving every conflict, every aircraft recovers its initial

4D trajectory. Ensuring a strict velocity control can be very costly and almost impossible in practice. Physicial recovery is required, whereas time recovery is optional, but it is favored by giving a penalty on the time shift between the 4D contract and the 4D trajectory after the maneuvers are performed.

6.2.4 Maneuver cost

The cost of a maneuver corresponds to the additional burnt to perform the maneuver, along with a time shift penalty. This measure serves as an indicator of the perturbation of the 4D trajectory induced by the executed maneuvers.
For a jet commercial aircraft f with constant altitude, the fuel consumption by time and distance unit is given by (6.7) and (6.8):

$$C_{t,f}\left(t, V_f(t)\right) = c_{1,f}\left(1 + \frac{V_f(t)}{c_{2,f}}\right) F_{T,f}(t) \tag{6.7}$$

$$C_{d,f}\left(t, V_f(t)\right) = \frac{C_{t,f}\left(t, V_f(t)\right)}{V_f(t)} \tag{6.8}$$

where $c_{1,f}$ and $c_{2,f}$ are numerical constants depending on the type of aircraft f that are extracted from the BADA performance tables EUROCONTROL (2011).
The time shift penalty is computed according to the method found in Omer (2013). The penalty corresponds to the extra fuel burnt to make up for the time shift.

6.2.5 Modeling the uncertainties

In this subsection, we detail the models used to describe the different uncertainties.

Error on wind prediction.

The aircraft are considered as flying within a wind field. Control commands are issued to reach the desired airspeed $\mathbf{v}_a$, while the control units monitoring the aircraft speed are ground-based. As a consequence, the groundspeed $\mathbf{v}_g$ can be linked to the airspeed. Let $\mathbf{w}(\mathbf{p}, t)$ denote the windspeed at position $\mathbf{p}$ at time t. We have that:

$$\mathbf{v}_g(t) = \mathbf{v}_a(t) + \mathbf{w}(\mathbf{p}(t), t) \tag{6.9}$$

The wind vector is decomposed in a *nominal* part corresponding to weather forecasts, and a *random* part describing the difference between the actual wind and its nominal part. The impact of the nominal wind of the aircraft dynamics is quite complex and was briefly studied in the literature. Most publications focus on the random part of the wind, and do not consider the nominal part. In this paper, we focus solely on the random wind.

The wind field is a set of random vectors $\mathbf{W}(\mathbf{p}, t)$ depending on the time and the point of space considered. Taking the wind into account complexifies the conflict resolution. Indeed, aircraft that are close from each other undergo highly correlated winds that will impact the conflict resolution. In this case, the error of prediction for the different aircraft become correlated. We follow the models presented in Lymperopoulos (2010). The authors simplify the computations performed in Cole *et al.* (1998) and Schwartz *et al.* (2000) in order to save execution time. The wind is stationary and isotropic, and each random vector $\mathbf{W}(\mathbf{p}, t)$ follows a zero-mean normal distribution such that the following conditions hold:

$$\mathbb{E}[\mathbf{W}(\mathbf{p}_1, t_1)] = 0, \forall t_1 \in \mathbb{R}_+, \forall \mathbf{p}_1 \in \mathbb{R}^2 \tag{6.10}$$

$$\mathbb{E}\left[\langle \mathbf{W}(\mathbf{p}_1, t_1) | \mathbf{W}(\mathbf{p}_2, t_2) \rangle\right] = 2f(t_1, \mathbf{p}_1, t_2, \mathbf{p}_2), \forall (t_1, t_2) \in \mathbb{R}_+^2, \forall (\mathbf{p}_1, \mathbf{p}_2) \in \mathbb{R}^4 \tag{6.11}$$

where f is the correlation function associated with the random wind developed in Cole *et al.* (1998).

We assume that the flight management system (FMS) compensates for the lateral errors, but does not correct the along-track errors. Indeed, the majority of commercial aircraft are equipped with 3D FMS which track only the cross-track errors.

Error on aircraft speed measures.

We consider the uncertainties due to the imprecision of speed and air temperature measures presented in Chaloulos et Lygeros (2007). These errors have an impact on the along-track speed of the aircraft which is modeled as a zero-mean normal variable independent from the other aircraft. Since these two uncertainties are highly time-correlated, the authors assumed they were constant over time.

Delays in the execution of maneuvers.

We model uncertainties induced by delays in the execution of maneuvers, which to our knowledge has not been studied yet.

In the literature, models always assume that the performance of the maneuvers is instantaneous. However, there are several actions required before the maneuver can actually be performed. First, the automated decision tool has to provide the controller with a feasible solution. Then, the controller has to process the solution and then communicate the corresponding instructions to the pilots, before they can execute the maneuvers.

More formally, let T_i denote the maneuver delay for aircraft i. T_i is decomposed as follows:

— the time required for the resolution tool to provide the controller with a feasible solution, denoted T^s;

— the time during which the controller analyses the solution and communicates it to the different aircraft, denoted T^c;
— the time required for the pilot of aircraft i to execute the communicated maneuver, denoted T_i^p.

In other words T_i is the sum of a term shared by all aircraft including the solution process and the controller's communication, and a term depending on the pilot of i. Figure 6.2 summarizes the whole process resulting in the delay.

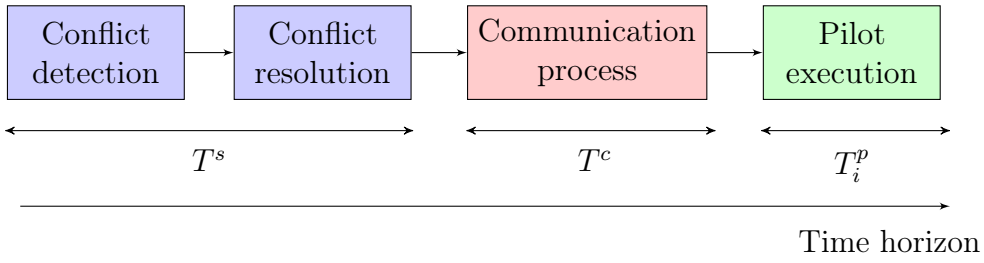

Figure 6.2 – Structure of the maneuver delay

6.2.6 Analytical expressions of the minimum distance and the probability of conflict

Expression of Irvine (2002).

In this paragraph, we detail the work presented by Irvine (2002) which serves as the foundation for the method we use to derive the expression of the probability of conflict. In his article, Irvine models the global impact of the uncertainties and the resulting cross and along-track errors, instead of modeling each source of error differently.

Let A_i and A_j be two aircraft flying at a stabilized altitude at speed $\mathbf{v}_i$ and $\mathbf{v}_j$, respectively. Their trajectories intersect in O with a crossing angle θ_{ij}. Let $x_i(t)$ and $x_j(t)$ denote the curvilinear abscissa at time t of A_i and A_j in a coordinate system centered on O. The distance between the two aircraft can be computed as follows:

$$d(t)^2 = x_i(t)^2 + x_j(t)^2 - 2x_i(t)x_j(t)\cos\theta_{ij} \tag{6.12}$$

If $d(t)$ is replaced by the separation distance required between A_i and A_j, denoted d^{sep}, Equation (6.12) defines an ellipse in the coordinate system (O, x_i, x_j). The aircraft follow straight-line trajectories at constant speed, hence the set of points $(x_i(t), x_j(t))_{t\geq 0}$ defines a straight line of slope

$$\frac{dx_j}{dx_i} = \frac{\frac{dx_j}{d_t}}{\frac{dx_i}{d_t}} = \frac{\mathbf{v}_j}{\mathbf{v}_i} = m \tag{6.13}$$

where m is the speed ratio between the two aircraft. If this line intersects the ellipse, then the aircraft are said to be in conflict. Figure 6.3 illustrates this condition.

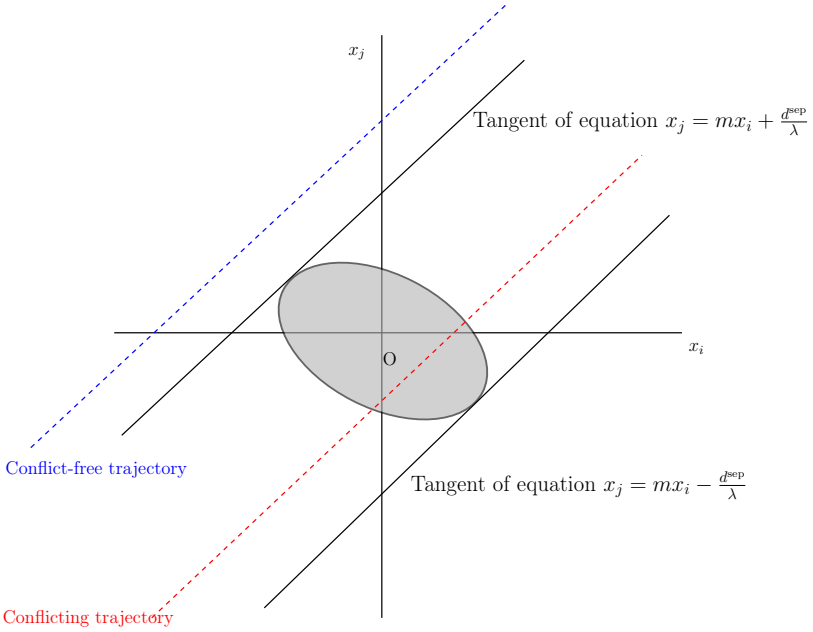

Figure 6.3 – Ellipse in the coordinate system (O, x_i, x_j)

To derive an analytical expression of this condition, the author uses the two tangents of the ellipse that are parallel to the parametric line $(x_i(t), x_j(t))_{t\geq 0}$. Their equations are given as follows:

$$x_j = mx_i \pm \frac{d^{\text{sep}}}{\lambda} \quad \text{where} \quad \lambda = \frac{\sin\theta_{ij}}{\sqrt{m^2 - 2m\cos\theta_{ij} + 1}}$$

The minimum distance between A_i and A_j in the deterministic case, denoted $d^{\min}$, can then be expressed as a function of the initial curvilinear abscissa of the two aircraft, x_i^0 and x_j^0.

$$d^{\min} = |\lambda(x_j^0 - mx_i^0)| \tag{6.14}$$

A_i and A_j are in conflict if and only if the minimum distance $d^{\min}$ is strictly less than the minimum separation distance allowed d^{sep}:

$$-d^{\text{sep}} < \lambda(x_j^0 - mx_i^0) < d^{\text{sep}}$$

Irvine then considers along-track errors and makes the assumption that within the range of along-track distances for which conflict is possible, the along-track error is approximately

constant and that the aircraft flies with its predicted speed. This assumption is used to quantify the cumulative along-track error between $t = 0$ and the instant where the two aircraft are the closest from each other in the deterministic case, denoted $t = \tau_{ij}$, given by

$$\tau_{ij} = \frac{(x_j^0 + mx_i^0)\cos\theta_{ij} - (x_i^0 + mx_j^0)}{||\mathbf{v}_i||(1 - 2m\cos\theta_{ij} + m^2)} \tag{6.15}$$

This value is chosen for τ_{ij} because the computation of the instant where the two aircraft are the closest from each other in the stochastic case is hard in practice. Consequently, deriving a handy formula of the probability of conflict would not be possible. Besides, considering τ_{ij} is a realistic assumption, since for the time intervals considered, the difference due to the approximation would be negligible.
The cumulative along-track error, denoted $\Delta L(\tau_{ij})$, follows a normal distribution $\mathcal{N}(0, \alpha_\sigma \tau_{ij})$, where α_σ is a constant. This error is applied to the initial position of the aircraft which then evolves in an entirely deterministic environment. This yields a new expression of the minimum distance in an uncertain setting, denoted $D^{\min}$.

$$D^{\min} = |\lambda(x_j^0 + \Delta L_j(\tau_{ij}) - mx_i^0 - m\Delta L_i(\tau_{ij}))| \tag{6.16}$$

$D^{\min}$ is the sum of a deterministic term with the sum of independent random variables. The sum of independent, normally distributed random variables is also normally distributed, with a mean equal to the sum of the means of the individual distributions, and variance equal to the sum of the variances of the individual distributions. As a consequence, we have that $D^{\min}$ follows a normal distribution of mean μ_d and variance σ_d^2 where

$$\mu_d = \lambda(x_j^0 - mx_i^0) \tag{6.17}$$

$$\sigma_d^2 = (\alpha_\sigma \tau)^2(1 + m)^2 \tag{6.18}$$

Irvine applies a similar reasoning for the impact of cross-track errors, but since we assume that the FMS compensates for these errors, in our article, we do not give any details about it. The probability of conflict $\mathbb{P}_c$ is given by

$$\mathbb{P}_c = \mathbb{P}\big(|\lambda(x_j^0 + \Delta L_j(\tau) - mx_i^0 - m\Delta L_i(\tau))| < d^{\text{sep}}\big) \tag{6.19}$$

$$= \frac{1}{\sigma_d\sqrt{2\pi}} \int_{-d^{\text{sep}}-\mu_d}^{d^{\text{sep}}-\mu_d} \exp\Big(-\frac{u^2}{2\sigma_d^2}\Big)\,\mathrm{d}u \tag{6.20}$$

$$= \Phi\Big(\frac{d^{\text{sep}} - \mu_d}{\sigma_d}\Big) - \Phi\Big(\frac{-d^{\text{sep}} - \mu_d}{\sigma_d}\Big) \tag{6.21}$$

where Φ is the cumulative distribution function of the standard normal distribution.

Enriching the formula.

In this subsection, we modify the formula derived by Irvine by introducing the errors on the wind prediction, the speed measures, and the delay in the execution of maneuvers. These errors are independent.
We note these cumulative errors $\Delta X_i(\tau_{ij})$ and $\Delta X_j(\tau_{ij})$, respectively. They can be decomposed as follows:

$$\Delta X_i(\tau_{ij}) = \Delta W_i(\tau_{ij}) + \Delta S_i(\tau_{ij}) + \Delta D_i(\tau_{ij}) \tag{6.22}$$
$$\Delta X_j(\tau_{ij}) = \Delta W_j(\tau_{ij}) + \Delta S_j(\tau_{ij}) + \Delta D_j(\tau_{ij}) \tag{6.23}$$

where $\Delta W_.$, $\Delta S_.$ and $\Delta D_.$ denote the cumulative error due to the wind, the speed prediction and the maneuver delay, respectively. Subsection 6.2.5 yields the following expressions for $\Delta W_.$ and $\Delta S_.$:

$$\Delta W_i(\tau_{ij}) = \frac{\langle \mathbf{W}|\mathbf{v}_i\rangle}{||\mathbf{v}_i||}\tau_{ij} \qquad \Delta S_i(\tau_{ij}) = \Upsilon_i \tau_{ij} \tag{6.24}$$
$$\Delta W_j(\tau_{ij}) = \frac{\langle \mathbf{W}|\mathbf{v}_j\rangle}{||\mathbf{v}_j||}\tau_{ij} \qquad \Delta S_j(\tau_{ij}) = \Upsilon_j \tau_{ij} \tag{6.25}$$

where Υ_i and Υ_j denote the error due to speed measures for A_i and A_j, respectively.
The cumulative along-track error due to the maneuver delay is slightly more complex to determine. For the sake of clarity, we give an illustrative example in Figure 6.4 where two aircraft A_i and A_j flying with a speed $\mathbf{v}_i^0$ and $\mathbf{v}_j^0$ have to perform a heading change of value θ_i and θ_j, respectively. They perform these maneuvers with a delay corresponding to random variables denoted T_i and T_j, respectively.
Figure 6.4 highlights that the crossing point of the aircraft trajectories was changed due to the delay in the execution of the maneuvers. As a consequence, there is a difference between the new initial curvilinear abscissas $\tilde{x}_i^0$ and $\tilde{x}_j^0$ and the ones in the deterministic setting x_i^0 and x_j^0. This difference, denoted ΔD_i^0 and ΔD_j^0, is computed as follows:

$$\Delta D_i^0 = T_i||\mathbf{v}_i^0|| - T_i||\mathbf{v}_i^0||\cos\theta_i - \frac{T_j||\mathbf{v}_j^0||\sin\theta_j}{\sin\theta_{ij}} - \frac{T_i||\mathbf{v}_i^0||\sin\theta_i\cos\theta_{ij}}{\sin\theta_{ij}} \tag{6.26}$$

$$\Delta D_j^0 = T_j||\mathbf{v}_j^0|| - T_j||\mathbf{v}_j^0||\cos\theta_j - \frac{T_i||\mathbf{v}_i^0||\sin\theta_i}{\sin\theta_{ij}} - \frac{T_j||\mathbf{v}_j^0||\sin\theta_j\sin\theta_{ij}}{\sin\theta_{ij}} \tag{6.27}$$

If $t < T_i$ then A_i has not started its maneuver yet and flies at speed $\mathbf{v}_i^0$. If $t \geq T_i$ then A_i has flown during T_i at speed $\mathbf{v}_i^0$ before changing its speed to $\mathbf{v}_i$. Since after T_i, aircraft A_i flies at

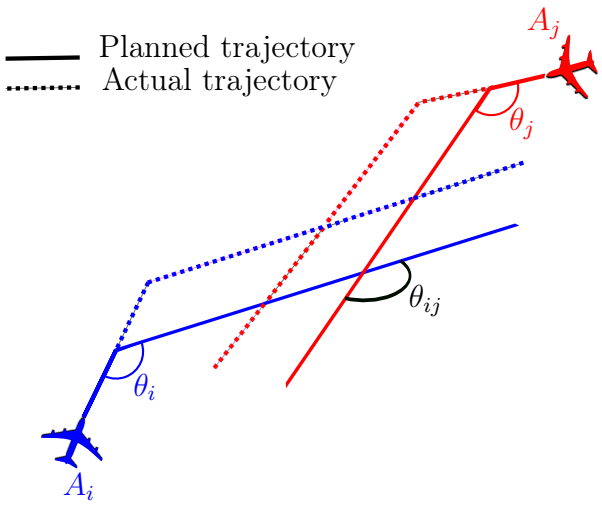

Figure 6.4 – Illustration of a maneuver delay for two aircraft performing heading changes

speed v_i like it is supposed to, the cumulative along-track error due to the delay T_i until τ_{ij} is in fact cumulated on the interval $]0, T_i]$. The value of this error is derived by

$$\Delta D_i(T_i) = T_i(||\mathbf{v}_i^0|| - \mathbf{v}_i) \tag{6.28}$$

Variables $\Delta D_i(\tau_{ij})$ and $\Delta D_j(\tau_{ij})$ are derived with

$$\Delta D_i(\tau_{ij}) = \Delta D_i(T_i) + \Delta D_i^0 \tag{6.29}$$

$$\Delta D_j(\tau_{ij}) = \Delta D_j(T_j) + \Delta D_j^0 \tag{6.30}$$

yielding the following expressions:

$$\Delta D_i(\tau_{ij}) = 2T_i||\mathbf{v}_i^0|| - T_i\mathbf{v}_i - T_i||\mathbf{v}_i^0||\cos\theta_i - \frac{T_j||\mathbf{v}_j^0||\sin\theta_j}{\sin\theta_{ij}} - \frac{T_i||\mathbf{v}_i^0||\sin\theta_i\cos\theta_{ij}}{\sin\theta_{ij}} \tag{6.31}$$

$$\Delta D_j(\tau_{ij}) = 2T_j||\mathbf{v}_j^0|| - T_j\mathbf{v}_j - T_j||\mathbf{v}_j^0||\cos\theta_j - \frac{T_i||\mathbf{v}_i^0||\sin\theta_i}{\sin\theta_{ij}} - \frac{T_j||\mathbf{v}_j^0||\sin\theta_j\cos\theta_{ij}}{\sin\theta_{ij}} \tag{6.32}$$

To derive the new expression of the minimum distance between aircraft A_i and A_j, we aggregate the errors $\Delta X_i(\tau_{ij})$ and $\Delta X_j(\tau_{ij})$ into

$$D^{\min} = \left| \lambda\Big(x_j^0 + \Delta X_j(\tau_{ij})\Big) - m\Big(x_i^0 + \Delta X_i(\tau_{ij}\Big) \right| \tag{6.33}$$

$$\begin{aligned} = \Bigg| & \lambda\Big(\big(x_j^0 + \Delta W_j(\tau_{ij}) + \Delta S_j(\tau_{ij}) + \Delta D_j(\tau_{ij})\big) \\ & - m\big(x_i^0 + \Delta W_i(\tau_{ij}) + \Delta S_i(\tau_{ij}) + \Delta D_i(\tau_{ij})\big)\Big) \Bigg| \end{aligned} \tag{6.34}$$

We simplify Equation (6.34) in order to determine an approximation of the distribution of variable $D^{\min}$.

In order to derive an analytical expression of the probability, we perform the computation with the hypothesis of a constant wind, which modifies the along-track speed of an aircraft flying at speed $\mathbf{v}$ by a factor $\dfrac{\langle \mathbf{w}|\mathbf{v}\rangle}{||\mathbf{v}||}$. This assumption seems reasonable since the considered intervals of detection and resolution are quite small and the wind is highly time-correlated. The terms related to the wind then correspond to

$$\begin{aligned} \Delta W_j(\tau_{ij}) - m\Delta W_i(\tau_{ij}) = & T_j \frac{\langle \mathbf{W}|\mathbf{v}_j^0\rangle}{||\mathbf{v}_j^0||} + (\tau_{ij} - T_j)\frac{\langle \mathbf{W}|\mathbf{v}_j\rangle}{\mathbf{v}_j} \\ & - m\ \left(T_i \frac{\langle \mathbf{W}|\mathbf{v}_i^0\rangle}{||\mathbf{v}_i^0||} + (\tau_{ij} - T_i)\frac{\langle \mathbf{W}|\mathbf{v}_i\rangle}{||\mathbf{v}_i||} \right) \end{aligned} \tag{6.35}$$

We approximate T_i and T_j by the mean of their distribution μ_{T_i} and μ_{T_j} in the quadratic terms, in order to find the analytical expression of the probability of conflict. This approximation is acceptable, since in Section 6.5 we use a distribution of T_i where the standard deviation is small compared to the mean. Equation (6.35) can be rewritten:

$$\begin{aligned} \Delta W_j(\tau_{ij}) - m\Delta W_i(\tau_{ij}) = & \left\langle \mathbf{W} \middle| \mu_{T_j} \frac{\mathbf{v}_j^0}{||\mathbf{v}_j^0||} + (\tau_{ij} - \mu_{T_j})\frac{\mathbf{v}_j}{||\mathbf{v}_j||} \right. \\ & \left. - m\mu_{T_i}\frac{\mathbf{v}_i^0}{||\mathbf{v}_i^0||} - m(\tau_{ij} - \mu_{T_i})\frac{\mathbf{v}_i}{||\mathbf{v}_i||} \right\rangle \end{aligned} \tag{6.36}$$

$$= \langle \mathbf{W}|\mathbf{u}\rangle \tag{6.37}$$

The terms involving the error on speed prediction can be simplified into

$$\Delta S_j(\tau_{ij}) - m\Delta S_i(\tau_{ij}) = \Upsilon_j \tau_{ij} - m\Upsilon_i \tau_{ij} \tag{6.38}$$

$$= \tau_{ij}(\Upsilon_j - m\Upsilon_i) \tag{6.39}$$

The terms related to the maneuver delay correspond to

$$\Delta D_j(\tau_{ij}) - m\Delta D_i(\tau_{ij}) = r_j T_j - m r_i T_i \tag{6.40}$$

where

$$r_j = ||\mathbf{v}_j|| - ||\mathbf{v}_j^0|| \cos\theta_j + \frac{||\mathbf{v}_j^0|| \sin\theta_j}{\tan\theta_{ij}} + \frac{m||\mathbf{v}_j^0|| \sin\theta_j}{\sin\theta_{ij}}$$
$$r_i = ||\mathbf{v}_i|| - ||\mathbf{v}_i^0|| \cos\theta_i + \frac{||\mathbf{v}_i^0|| \sin\theta_i}{\tan\theta_{ij}} + \frac{||\mathbf{v}_i^0|| \sin\theta_i}{m \sin\theta_{ij}}$$

Equations (6.35), (6.39) and (6.40) yield a simplified expression for $D^{\min}$:

$$D^{\min} = \left|\lambda(x_j^0 - mx_i^0) + \lambda\big((\Upsilon_j - m\Upsilon_i)\tau_{ij} + r_j T_j - m r_i T_i + \langle \mathbf{W}|\mathbf{u}\rangle\big)\right| \tag{6.41}$$

Equation (6.41) expresses $D^{\min}$ as a deterministic term $\lambda\big(x_j^0 - mx_i^0\big)$, added with the sum of the following independent random variables

— $(\Upsilon_j - m\Upsilon_i)\tau_{ij} \sim \mathcal{N}\,(0, (1+m)\sigma_\Upsilon \tau_{ij})$;
— $r_j T_j \sim \mathcal{N}(r_j \mu_{T_j}, r_j \sigma_{T_j})$;
— $-m r_i T_i \sim \mathcal{N}(-m r_i \mu_{T_i}, m r_i \sigma_{T_i})$;
— $\langle \mathbf{W}|\mathbf{u}\rangle \sim \mathcal{N}(0, \sigma_{\mathbf{W}}||\mathbf{u}||)$.

$D_{\min}$ follows a normal distribution of mean μ_D and variance σ_D^2 given by

$$\mu_D = \lambda\big((x_j^0 + r_j\mu_{T_j}) - m(x_i^0 + m r_i \mu_{T_i})\big) \tag{6.42}$$
$$\sigma_D^2 = \lambda^2\big(\sigma_\Upsilon^2(1+m)^2\tau_{ij}^2 + (m r_i \sigma_{T_i})^2 + (r_j\sigma_{T_j})^2 + (\sigma_{\mathbf{W}}||\mathbf{u}||)^2\big) \tag{6.43}$$

The probability of A_i and A_j being in conflict corresponds to the probability of the event $|D^{\min}| < d^{\text{sep}}$:

$$\begin{aligned}\mathbb{P}(|D^{\min}| < d^{\text{sep}}) &= P(-d^{\text{sep}} < D^{\min} < d^{\text{sep}}) \\ &= \Phi\Big(\frac{d^{\text{sep}} - \mu_D}{\sigma_D}\Big) - \Phi\Big(\frac{-d^{\text{sep}} - \mu_D}{\sigma_D}\Big)\end{aligned}$$

6.3 Deterministic Model

In this section, we describe the resolution method developed by Lehouillier *et al.* (2015b,a) that will serve as a foundation for the optimization procedure presented in Section 6.4. The main idea is to model the CR problem as a maximum clique of minimum weight problem. To this end, we build a graph whose vertices represent maneuvers for the different aircraft, and where edges link conflict-free maneuvers of different aircraft. A maximum clique of minimum weight yields a conflict-free situation of minimal cost.

The advantage of this process is that it fully separates the modeling of aircraft dynamics, the separation verification and the costs computations from the resolution: whatever the hypotheses considered, and in particular taking into account uncertainties, the proposed

mathematical framework will remain valid. The remainder of this section highlights the key elements of modeling and resolution of the model.

6.3.1 Graph construction

In this subsection, we introduce the *conflict graph* $\mathcal{G} = (\mathcal{V}, \mathcal{E})$ used to model the CR problem. The set of vertices is defined as $\mathcal{V} = [\![1; |\mathcal{M}|]\!]$, where $\mathcal{M}$ denotes the set of possible maneuvers for all aircraft. We denote $\mathcal{V}_f$ the set of vertices corresponding to aircraft f.
Let $(i, j) \in \mathcal{V} \times \mathcal{V}$ be a pair of vertices representing maneuvers $(m_i, m_j) \in \mathcal{M} \times \mathcal{M}$ of aircraft $(f_i, f_j) \in \mathcal{F} \times \mathcal{F}$. For $i \neq j$, we write $m_i \square m_j$ when no conflict occurs if aircraft f_i follows maneuver m_i while aircraft f_j performs maneuver m_j. The set of edges $\mathcal{E}$ corresponds to the pairs of maneuvers performed by two different aircraft without creating conflicts:

$$\mathcal{E} = \{(i, j) \in \mathcal{V} \times \mathcal{V}, i \neq j : m_i \square m_j\} \tag{6.44}$$

Proposition 6.3.1(Lehouillier *et al.* (2015b)) links the cliques in $\mathcal{G}$ to the CR problem:

Proposition 6.3.1. *Let $\mathcal{C}$ be a clique in graph $\mathcal{G}$. Then $\mathcal{C}$ represents a set of conflict-free maneuvers for a subset of $\mathcal{F}$ of cardinality $|\mathcal{C}|$.*

For a more synthetic presentation, we consider in this subsection that maneuvers and vertices are equivalent without loss of generality. As explained in the previous subsection, the cost of a maneuver depends on its execution, which itself varies with the maneuvers of the other aircraft. As a consequence, we need to define the cost of the edges before the cost of the vertices.
Again, for ease of presentation, an edge $e = (i, j)$ is considered as a pair of maneuvers. We compute the cost of an edge $e = (i, j)$ as a pair constituted of the cost of maneuvers i and j, denoted $C_i^{(i,j)}$ and $C_j^{(i,j)}$.
Let us consider a maneuver i. The cost of each edge linking i to another maneuver j corresponds to an execution time t_i^j which is the minimum time during which i and j have to be executed before a safe return can be performed by at least one of the corresponding aircraft.
To determine the cost of i, denoted c_i, we need to compute the time t_i during which it is actually applied. If i is not in the optimal solution, then $t_i = 0$. Otherwise, t_i is given by

$$t_i = \max_{j \in \mathcal{V} \cap \mathcal{C}} t_i^j \tag{6.45}$$

Equation (6.45) states that maneuver i has to be applied long enough in order to be conflict-free

with every other chosen maneuver. As a consequence, we can determine c_i:

$$c_i = \begin{cases} \max\limits_{j \in \mathcal{V} \cap \mathcal{C}} C_i^{(i,j)} & \text{if } i \in \mathcal{C} \\ 0 & \text{otherwise} \end{cases}$$

6.3.2 MILP formulation

In our model the costs of the vertices are not determined a priori, since they depend on which vertices are in the clique. As a consequence, the dedicated algorithms of existing graph theory libraries cannot be used in this study. To address this issue, we formulate our problem as a MILP that can be solved with any generic MILP solver.

The decision variables of the model all relate to the vertices of the graph. They correspond to the choice of the vertices in the clique and the cost of each vertex:

— $x_i = \begin{cases} 1 & \text{if vertex } i \text{ is part of the maximum clique} \\ 0 & \text{otherwise} \end{cases}$

— $c_i \in \mathbb{R}_+$ is the cost of vertex i.

The clique search can then be modeled as the following MILP, denoted MIP:

$$\text{minimize} \sum_{i \in \mathcal{V}} c_i \tag{6.46}$$

$$\text{subject to } x_i + x_j \leq 1, \forall (i,j) \in \mathcal{V} \times \mathcal{V} \setminus \mathcal{E} \tag{6.47}$$

$$\sum_{i \in \mathcal{V}} x_i = |\mathcal{F}| \tag{6.48}$$

$$c_i \geq C_i^{(i,j)}(x_i + x_j - 1), \forall (i,j) \in \mathcal{E} \tag{6.49}$$

$$x_i \in \{0;1\}, \forall i \in \mathcal{V} \tag{6.50}$$

$$c_i \geq 0, \forall i \in \mathcal{V} \tag{6.51}$$

The objective function (6.46) minimizes the cost of the maneuvers. Constraints (6.47) are clique constraints stating that two nonadjacent vertices must not be part of the clique. In terms of conflict resolution, it means that two maneuvers in conflict must not be part of the solution. Constraint (6.48) defines the cardinality of the maximum clique. Constraints (6.49) are used to compute the cost of the vertices: if a vertex is in the maximum clique, then its cost must be greater than the cost on every edge connecting it to other vertices in the clique. Otherwise, no particular constraint is imposed on the vertex cost. Constraints (6.50)–(6.51) are binarity and nonnegativity constraints, respectively.

6.3.3 Inserting uncertainties into the deterministic model

In this subsection, we explain how the expression of the probability of conflict between two aircraft derived in Subsection 6.2.6 is used to modify the deterministic model presented in this section.
An edge exists between two maneuvers if they are conflict-free. In other words, if the probability of conflict associated with these maneuvers is 0. If they are in conflict (i.e if the probability of conflict was 1), then no edge is drawn between the corresponding vertices. To take into account the uncertainties, we change the necessary condition to build an edge.
The set of edges $\mathcal{E}$ is defined by

$$\mathcal{E} = \{(i,j) \in \mathcal{V} \times \mathcal{V}, i \neq j : \mathbb{P}_c(i,j) < \ \delta_s\} \tag{6.52}$$

where δ_s is a security threshold restricting the set of possible maneuvers. δ_s represents an upper bound on the probability that a conflict remains after the maneuvers are issued. We remind here that a remaining conflict will always be solved: the controller will issue another set of maneuvers. In other words, δ_s can be regarded as an upper bound on the probability that the controller uses a recourse to solve the problem once again.
This adaptation of the deterministic setting makes a good pairing with the expression computed in Subsection 6.2.6. Indeed, when the set of possible maneuvers becomes very large, the number of probabilities to compute would require a huge computational effort if they were determined through simulation, whereas with our approach, we determine these values instantaneously.

6.4 Bi-Objective Optimization Procedure

In this section, we detail the bi-objective approach designed to solve the problem. This method optimizes the CR problem according to two criteria depicting the efficiency and the probability of having recourse related to a solution. It iteratively solves the model MIP according to the first criterion, while imposing a certain improvement on the second criterion between two consecutive resolutions. Each resolution results in a solution approximating the Pareto front of the problem. In the end, the method provides the air traffic controller with a set of solutions corresponding to different trade-offs between efficiency and probability of using a recourse.

6.4.1 Optimization Criteria

The first criterion of optimization corresponds to the objective function of the mathematical program MIP presented in Section 6.3:

$$z_e = \sum_{i \in \mathcal{V}} c_i \tag{6.53}$$

This objective is the total amount of additional fuel burnt induced by the chosen maneuvers, and represents the aspect of a solution related to its economical efficiency. Indeed, it is an indicator on the perturbation of the planned trajectories and gives an insight into the effort required to catch up with the initial flight plan after the maneuver is performed. In addition to the perturbation of the set of aircraft itself, this criterion also illustrates the perturbation on surrounding traffic.
The second criterion is given by

$$z_s = \sum_{i \in \mathcal{V}} \sum_{\substack{j \in \mathcal{V} \\ j \neq i}} P_{ij} x_i x_j \tag{6.54}$$

where P_{ij} is the probability of conflict of maneuvers i and j, and x_i and x_j are the decision variables corresponding to whether or not maneuvers i and j are chosen. Value z_s corresponds to the expected number of conflicts potentially remaining after the solution is applied. This is a relevant measure for the controller as it gives an idea of the potential additional effort required to solve the problem once again in the close future. The higher z_s is, the higher the probability of re-issuing avoidance maneuvers will be. Variable z_s represents an indicator of the additional workload and cognitive charge that will potentially be required in order to definitely solve the problem.
To keep the expression of z_s linear in the decision variables, we apply Fortet's linearization (Fortet (1960)). We introduce a new set of binary variables y_{ij} respecting the following constraints:

$$y_{ij} \leq x_i, \forall i \in \mathcal{V}, \forall j \in \mathcal{V} \tag{6.55}$$

$$y_{ij} \leq x_j, \forall i \in \mathcal{V}, \forall j \in \mathcal{V} \tag{6.56}$$

$$y_{ij} \geq x_i + x_j - 1, \forall i \in \mathcal{V}, \forall j \in \mathcal{V} \tag{6.57}$$

$$\tag{6.58}$$

yielding a new expression of z_s.

$$z_s = \sum_{i \in \mathcal{V}} \sum_{j \in \mathcal{V}} P_{ij} y_{ij} \tag{6.59}$$

Algorithm 6.1 describes the mechanics of the iterative procedure. The user-defined parameters are the security threshold δ_s used to build the conflict graph, and an improvement thresholds δ_i for the second criterion, respectively. The algorithm starts by solving the program MIP: it finds the optimal solution for the first criterion of value z_e. We compute z_s the value of this solution for the second criterion. The point (z_e, z_s) is a Pareto-optimal point, since it is globally optimal for the first criterion. The value of p is then used to add the constraint (6.60) to MIP:

$$\sum_{i \in \mathcal{V}} \sum_{j \in \mathcal{V}} P_{ij} y_{ij} \leq p - \delta_i \tag{6.60}$$

Constraint (6.60) simply reflects the minimum improvement required on the second criterion. The value of the parameter δ_i can be considered as a factor of granularity of the Pareto front. MIP is then solved once again, and the values of the two criteria are updated. The algorithm continues until the value of the second criteria becomes smaller than the threshold p_f.

Algorithm 6.1. Iterative bi-objective optimization procedure (IBIOP)

1: **procedure** IBIOP(δ_s, p_f, δ_i)
2: Input: Set of aircraft $\mathcal{F}$, set of maneuvers $\mathcal{M}$
3: Parameters: security thresholds δ_s, p_f , improvement threshold δ_i
4: Build the conflict graph according to $\mathcal{F}$, $\mathcal{M}$ and δ_s
5: $z_e \leftarrow +\infty$, $z_s \leftarrow +\infty$
6: Solve MIP
7: $z_e \leftarrow$ optimal value of MIP
8: $z_s \leftarrow$ value of second criterion for optimal solution of MIP
9: **while** $z_s \geq p_f$ **do**
10: Add constraint $\sum_{i \in \mathcal{V}} \sum_{j \in \mathcal{V}} P_{ij} y_{ij} \leq p - \delta_i$ to MIP
11: Solve MIP
12: $z_e \leftarrow$ optimal value of MIP
13: $z_s \leftarrow$ value of second criterion for optimal solution of MIP

6.5 Results

This section is organized as follows. Subsection 6.5.1 describes the values assigned to the different parameters for the experiments. Subsection 6.5.2 tests the validity of the assumptions made in the computations in Subsection 6.2.6. Computational results are detailed in Subsection 6.5.3. Subsection 6.5.4 provides a quantitative analysis of a Pareto

front for a particular example.

6.5.1 Parameter values and simulations of the uncertainties distributions

In this subsection, we define the values assigned to the different parameters of the random variables distributions, and we describe the methods used to generate the random samples used for the Monte-Carlo simulations.

Parameter values of the uncertainties distributions.

We give the values assigned to the parameters of the distributions of the uncertainties.

Probability distribution of the wind: The simulated wind follows a zero-mean normal distribution of standard deviation $\sigma_{\mathbf{W}} = 5.4$kt, according to the model described in Chaloulos et Lygeros (2007).

Probability distribution of the error on speed prediction: We follow the model presented in Chaloulos et Lygeros (2007), where the error on speed prediction is a zero-mean normal variable of standard deviation $\sigma_{\Upsilon} = 7.9$kt.

Probability distribution of the maneuver delays: As no data on these delays exist to our knowledge, we interviewed an experienced air traffic controller to obtain an insight into what those values could be. As a result, we decided to use these following values:

— $T^c + T^s \sim \mathcal{N}(\mu_{T^{c,s}}, \sigma_{T^{c,s}})$ where $\mu_{T^{c,s}} = 30$ seconds and $\sigma_{T^{c,s}} = 10$ seconds;

— $\forall i \in \mathcal{F}, T_i^p \sim \mathcal{N}(\mu_{T_i^p}, \sigma_{T_i^p})$ where $\mu_{T_i^p}$ is a random variable uniformly distributed between 20 and 40 seconds, and $\sigma_{T_i^p} = 10$ seconds.

Monte-Carlo simulations.

For the simulation of aircraft trajectories, we generate random values for the wind according to the method developed by Lymperopoulos (2010). The author performs a time and space discretization of the wind field, and iteratively computes at each time step the wind values at point of the grid according to the wind values computed at the previous time step, using correlation functions. The values of the normal distribution for the error on speed prediction and on the maneuver delay are generated according to the Box-Muller method described in Rubinstein et Kroese (2011), which simulates centered normal random variables using uniformly distributed random variables.

6.5.2 Validating the calculus through simulations

In this subsection, we validate the assumptions made in Subsection 6.2.6, by checking the validity of the approximation of the probability of conflict derived in Subsection 6.2.6 by comparing it to the probability obtained through simulations.

To this end, we study a test case representing a conflict situation with two aircraft i and j crossing each other with an angle θ (the set of values for theta is $\{60°; 90°; 120°\}$). To avoid the conflict, they start their maneuver at 100NM from the crossing point of their trajectories. We designed different scenarios corresponding to a couple of maneuvers (M_i, M_j) consisting in either speed or heading changes. The speed maneuvers range from -6% to 6% with a 1% step and the heading changes range from $-10°$ to $10°$ with a $1°$ step. In total, we have 545 scenarios. For each scenario, 2000 independent random samples are generated.
To validate the approximation of the probability of conflict derived in Subsection 6.2.6, for each scenario we computed the value of the approximated probability of conflict, and we simulated 2000 random scenario samples to estimate the probability of conflict. The same process was performed for the minimum distance between the two aircraft.

Table 6.1 – Comparison of the simulation results and the calculus for the minimum distance and the probability of conflict

Configuration		Difference of separation distance		Difference of probabilities	
Maneuvers	Crossing angle (°)	Absolute Mean (NM)	Variance (NM)	Mean (%)	Variance
H/H	60	0.09	0.01	0.68	0.02
H/H	90	0.10	0.02	0.70	0.01
H/H	120	0.13	0.01	0.61	0.04
S/H	60	0.16	0.01	0.80	0.03
S/H	90	0.12	0.01	0.72	0.12
S/H	120	0.11	0.01	0.50	0.14
S/S	60	0.05	0.01	0.62	0.02
S/S	90	0.16	0.03	0.66	0.04
S/S	120	0.14	0.01	0.66	0.11

Table 6.1 highlights that the average simulated minimum distance is close to the computed one. Depending on the type of maneuver and the crossing angle, it ranges from 0.05 NM to 0.16 NM. The variance is really small, meaning that the difference between the two distances is usually close to the mean. Probabilities of conflict computed and simulated are almost identical, with a difference always under 1% for the considered instances, meaning that the expression derived in Subsection 6.2.6 is a really good approximation of the simulated probability.
Figure 6.5 highlights the results of Table 6.1 graphically, and focuses on two aircraft crossing with an angle of 50° and performing heading changes to avoid the conflict. Figure 6.5a

compares the average of the computed distribution of the minimum distance with the average minimum distance simulated. Figure 6.5b compares the computed and simulated probability of conflict. Scenarios are sorted on the horizontal axis following decreasing values of the compared quantities. The plotted functions are stepwise, because the difference in maneuver magnitudes from one scenario to the other are discrete, which has a significant impact on the minimum distance and the resulting probability of conflict.

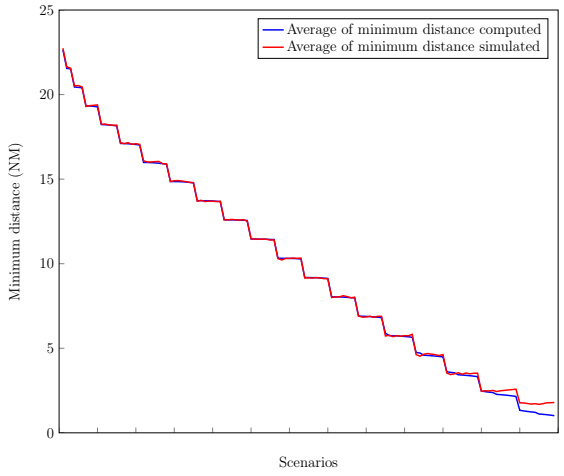

(a) Comparison of the average minimum distance simulated and the mean of the computed distribution of the minimum distance

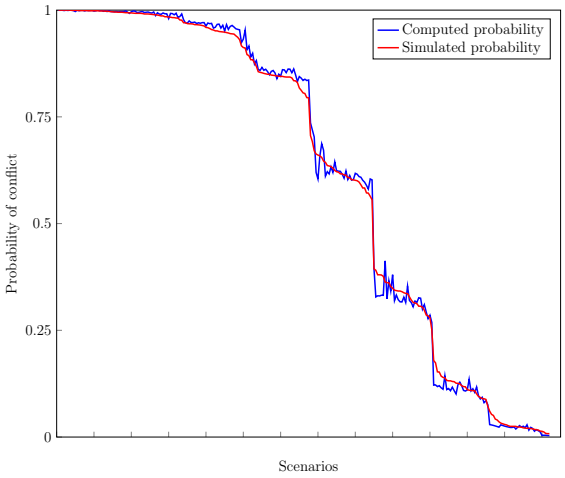

(b) Comparison of the computed and simulated probability of conflict

Figure 6.5 – Comparison of calculus and simulations for two aircraft performing heading changes to avoid at the intersection of their planned trajectories making a 50° angle

6.5.3 Computational results

Benchmark description

Structured benchmark. This benchmark gathers three types of instances. The first set is roundabout instances $\mathcal{R}_n$, where n aircraft are distributed on the circumference of a 100NM-radius circle and fly towards the center at the same speed and altitude. The second set is crossing flow instances $\mathcal{F}_{n,\theta,d}$, where two trails of n aircraft separated by d nautical miles intersect each other with an angle θ. The last type of instance is a grid $\mathcal{G}_{n,d}$ constituted of two crossing flow instances $\mathcal{F}_{n,\frac{\pi}{2},d}$ with a 90° angle, one instance being translated 15NM North-East from the other. Aircraft considered for the conducted experiments are Airbus A-320 flying at 450 kt on flight level FL330. An example of these instances is given on Figure 6.6.

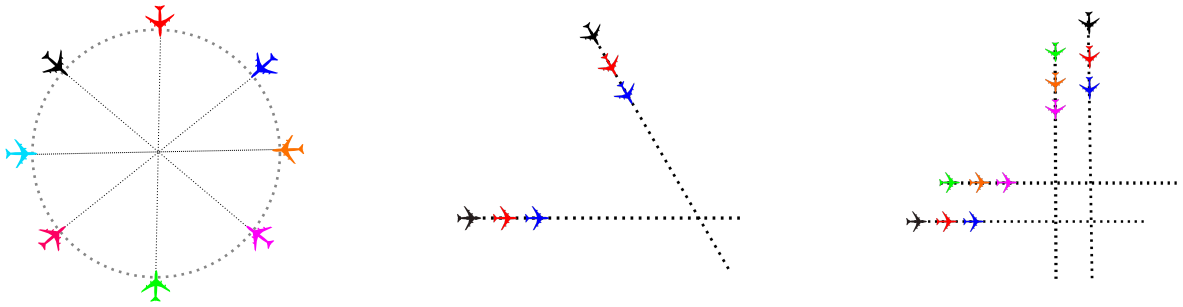

(a) Roundabout $\mathcal{R}_8$ (b) Crossing Flow $\mathcal{F}_{3,\frac{\pi}{4},10}$ (c) Grid $\mathcal{G}_{3,10}$

Figure 6.6 – Examples of instances of the benchmark

Random benchmark. This benchmark consists of random instances, where aircraft are uniformly distributed within a square sector with side length 50NM. To avoid generating infeasible instances, we perform a preprocessing before solving the problem: for each pair of aircraft that will loose separation within the first 30 seconds of observation, we randomly delete one of the aircraft. For a desired number of aircraft, we generate 15% more aircraft to anticipate the effect of the preprocessing. If more aircraft than desired remain after the preprocessing, extra aircraft are then randomly removed until the number is reached.

Computational results.

All tests were performed on a computer equipped with the following hardware: Intel Core i7-3770 processor, 3.4 GHz, 8-GB RAM. The algorithms were implemented in C++ and relies on CPLEX 12.5.1.0 CPL (2014) with default options to solve every instance. For instances with up to 10 aircraft, heading changes range from $-10°$ to $10°$ with a $2°$ step. For instances with more than 10 aircraft, the possible heading changes are $\pm 5°$, $\pm 10°$, $\pm 15°$ and $\pm 20°$. In addition, aircraft can also perform speed changes of $\pm 3\%$ and $\pm 6\%$. The parameters of the IBIOP procedure were assigned the following values:

— security threshold for a maneuver $\delta_s = 5\%$;
— improvement threshold for safety $\delta_i = 1\%$;
— the stopping criterion $p_f \leq 1\%$.

Table 6.2 gathers information about the instance dimensions, the generated solutions and computational results. The headings are given as follows:

— $|\mathcal{F}|$: number of aircraft;
— $|\mathcal{V}|$: number of vertices;
— $|\mathcal{E}|$: number of edges;
— 1^{sol} : first generated solution of the Pareto front, expressed as the pair (c_1, c_2) of the

values of the two criteria, where c_1 is expressed in kilograms of fuel and c_2 is the expected number of conflicts;

— L^{sol} : last generated solution of the Pareto front, expressed as the pair (c_1, c_2) of the values of the two criteria, where c_1 is expressed in kilograms of fuel and c_2 is the expected number of conflicts;

— T^r : resolution time (in seconds);

— Nb^p : number of generated solutions of the Pareto front.

Table 6.2 – Computational results

	Instance size			Solutions explored		Resolution	
	$\|\mathcal{F}\|$	$\|\mathcal{V}\|$	$\|\mathcal{E}\|$	1^{sol}	D^{sol}	T^r	Nb^p
$\mathcal{R}_4$	4	60	571	(12.26 ; 0.053)	(15.19 ; 0.005)	0.67	2
$\mathcal{R}_6$	6	90	1296	(32.12 ; 0.107)	(44.46 ; 0.009)	6.69	7
$\mathcal{R}_8$	8	120	2256	(77.04 ; 0.0917)	(100.7 ; 0.008)	8.58	8
$\mathcal{R}_{10}$	10	110	2647	(151.9 ; 0.072)	(252.3 ; 0.008)	11.69	5
$\mathcal{R}_{12}$	12	156	6215	(337.6 ; 0.184)	(370.3 ; 0.007)	24.17	4
$\mathcal{R}_{16}$	16	208	10924	(562.2 ; 0.137)	(914.8 ; 0.008)	139.7	11
$\mathcal{F}_{1,60,10}$	2	30	83	(5.85 ; 0.035)	(9.13 ; 0.001)	0.09	2
$\mathcal{F}_{2,60,10}$	4	60	717	(20.73 ; 0.037)	(21.79 ; 0.002)	1.26	2
$\mathcal{F}_{4,60,10}$	8	120	3543	(55.90 ; 0.045)	(59.48 ; 0.009)	7.46	2
$\mathcal{F}_{6,60,10}$	12	156	6027	(134.7 ; 0.023)	(137.6 ; 0.008)	42.92	2
$\mathcal{G}_{2,10}$	8	120	3690	(73.15 ; 0.078)	(90.20 ; 0.008)	30.9	5
$\mathcal{G}_{3,10}$	12	156	11034	(382.8 ; 0.020)	(480.1 ; 0.007)	82.89	4
$\mathcal{U}_{15}$	15	195	6940	(14.42 ; 0.0512)	(22.15 ; 0.002)	45.12	4
$\mathcal{U}_{25}$	25	325	12313	(65.07 ; 0.014)	(89.24 ; 0.004)	7.46	2
$\mathcal{U}_{35}$	35	455	33127	(89.15 ; 0.021)	(120.05 ; 0.009)	130.02	2

First, we observe that all the instances met the stopping criteria, yielding solutions with less than 0.01 expected conflicts. Results highlight that for instances with less than 10 aircraft, the solution time stays shorter than 30 seconds while on average 5 different solutions are generated. This achievement is meaningful for the air traffic controller, since he/she is able to access a small set of different solutions within a short period of time. For instances with more than 10 aircraft, solution times tend to slightly increase to reach up to two and a half minutes to generate 9 solutions (instance $\mathcal{R}_{16}$). Even though it seems far from real-time, the advantage of our procedure is that it generates solutions on the fly, meaning that the controllers has at least one or two possible solutions within the first seconds of the resolution if he/she needs to act quickly. Those solutions have a higher probability of using a recourse, but by concept it gives to the controller a certificate that at least each pair of aircraft has less than 5% chances of needing another avoidance maneuver in the future. An observation

worth mentioning is that the total solution time is closely linked to the value of the security threshold δ_s and the stopping criterion. Indeed, their values will mostly influence the number of generated Pareto-front solutions. Moreover, for the experiments we choose to have a large set of possible maneuvers for each aircraft, which also has an impact on the solution time. A smaller set of maneuvers would result in a shorter execution time, especially if we delete the largest maneuvers, which represent the vertices with higher degrees. Indeed, those nodes have an impact on the number of cliques and on the search of a maximal clique of minimum weight.

6.5.4 Quantitative analysis of a solution set

We now focus on the solutions generated by our procedure applied to the instance depicted on Figure 6.7. One aircraft intersects a train of two aircraft separated by 20 NM. The algorithm parameters were identical to the ones for the other tests.

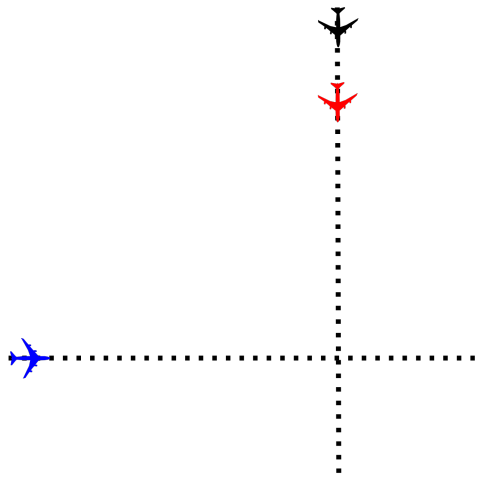

Figure 6.7 – Example for the analysis of the generated solutions

In order to get an insight into the effect of considering uncertainties on the chosen maneuvers, we remind that the deterministic solution is worth 5.54 kilograms of fuel. The generated solutions during the resolution are displayed on Figure 6.8. The first solution $(6.66; 0.35)$, was computed in 0.29 seconds. Every half second, a new solution is generated until the eighth and last one $(47.47; 0.009)$ which was computed in 6.22 seconds.
We can divide the generated solutions into two clusters, depending on their geometrical characteristics. The first cluster includes the first five generated solutions, where the blue aircraft flies between the two others, as evidenced on Figure 6.9a. Figure 6.9b describes the second cluster including the last three generated solutions. The blue aircraft performing a heading change, while the two others slow down.

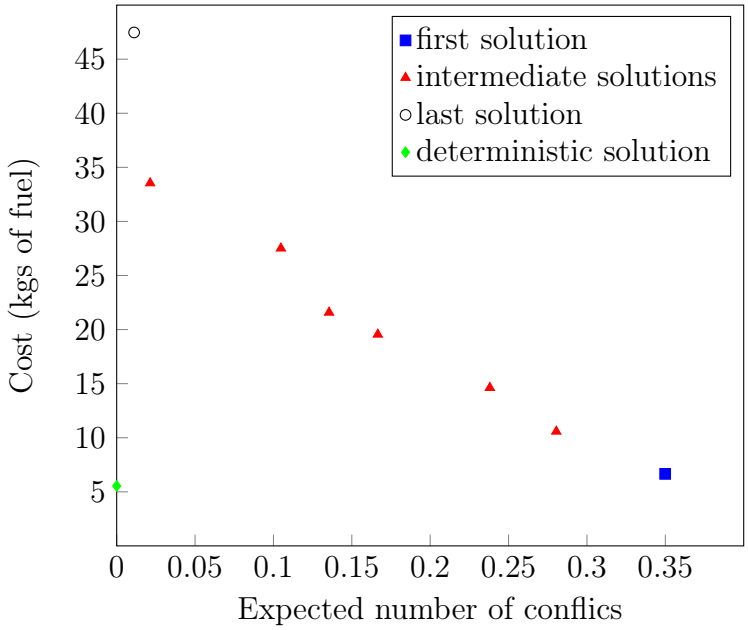

Figure 6.8 – Generated Pareto solutions for instance $\mathcal{R}_8$

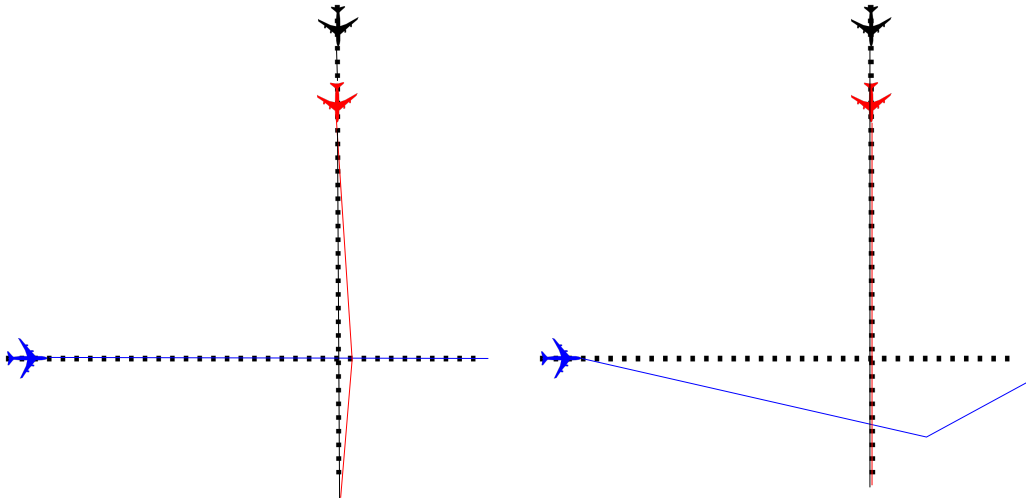

(a) First cluster (b) Second cluster

Figure 6.9 – Two different geometrical solutions for the example

The interpretations of these results are two-fold. First, it shows that there is a discontinuity in the geometry of the generated solutions, instead of having the same pattern repeated with a different magnitude. Second, it provides the controller with a visual outlook of the solutions, and he/she can easily identify which ones will be easier to communicate, or which ones will be the more robust.

Depending on the preferences of the controller, the quality of the solution will differ regarding one criterion or the other. For instance, if the controller aims at efficiency, he/she will apply the solution costing 6.66 kilograms of fuel, but where in 35% of the scenarios he/she will need to issue new maneuvers in order to ensure separation. If he/she aims at saving potential workload, he/she will choose a solution with less than 1% chances of having to re-issue maneuvers, but costing 47.47 kilograms of fuel. If his/her preferences are more mixed, he/she still has six other possible solutions that he can choose.

6.6 Conclusions

In this article, we tackled the air conflict resolution problem under uncertainty. With our work, we provide the controller with a decision analysis tool generating a set of solutions representing different trade-offs between several criteria. The model is robust, since we consider a large span of uncertainties, including errors due to the wind, the imprecision of speed prediction. We also presented a new type of uncertainty: the delay in the execution of maneuvers. As a consequence, we cover a large part of the possible uncertainties that can arise during a conflict resolution. We computed the conflict probabilities and integrated them within an optimization model which is flexible, since it fully separates the modeling from the resolution process. Hence, the underlying mathematical framework remains valid, whatever the hypotheses considered. We focused on two objective that are relevant for conflict resolution, namely the extra fuel consumption, which serves as a performance index, and the expected number of conflicts, which serves as an indicator of potential additional workload required to re-issue avoidance maneuvers. We solve the problem by iteratively solving the aforementioned model, hence taking advantage of its power. Each resolution generates a solution of the Pareto front of the problem. At the end of the simulation run, the controller has a set of solutions where he can choose the one to apply, depending on the context and its preferences.

Monte-Carlo simulations validated the theory, and intensive simulations highlighted interesting results. Complex instances with up to 20 aircraft are solved within seconds, and an average of 5 different solutions are generated within two minutes.

Further research will focus on the extension of the method to aircraft with changing altitudes, in order to consider a larger variety of problems. A rolling-horizon procedure will also be the center of new research, allowing us to run continuous simulations of real-life data sets.

CHAPITRE 7 DISCUSSION GÉNÉRALE

Dans cette thèse, nous avons présenté une étude de coûts et de complexité du trafic futur, afin de quantifier des objectifs de recherche en optimisation du trafic aérien. Nous avons également formulé un modèle mathématique pour la détection et la résolution déterministe de conflits entre aéronefs. Ce modèle a ensuite été étendu au cas non déterministe, où nous avons intégré diverses incertitudes, et où nous avons présenté une méthode itérative bi-objectif permettant d'approcher le front de Pareto du problème.

7.1 Synthèse des travaux

L'objectif premier de cette thèse était le développement de modèles mathématiques pour la détection et la résolution de conflits entre aéronefs.
Dans le chapitre 4, nous avons présenté une étude de coûts et de complexité basée sur du futur trafic français. Cette étude est novatrice et importante pour notre domaine, dans le sens où elle permet à la fois de donner une légitimité aux modèles de résolution de conflits existant, tout en quantifiant des valeurs cibles en termes d'objectifs de recherche pour le futur.
Dans le chapitre 5, nous avons présenté un modèle déterministe de détection et de résolution de conflits entre aéronefs. La force du modèle vient de sa flexibilité : en effet, le formalisme mathématique présenté reste valide, et ce quelles que soient les hypothèses faites sur la dynamique des avions, leur trajectoire, les manœuvres et la fonction de coût. Au-delà de la robustesse, notre algorithme pourrait être utile pour comparer différents travaux de la communauté, dans la mesure où nous pourrions ajuster les hypothèses faites sur les avions pour retomber sur des modèles existants. De plus, la formulation mathématique présentée est une nouvelle variante du problème de recherche de clique maximale de poids minimum dans un graphe. En effet, afin de garder un graphe compact, les coûts des sommets ne sont plus connus *a priori* car ils dépendent des sommets de la clique. Enfin, nous présentons deux méthodes de décomposition permettant de traiter de grosses instances de façon efficace : la solution de coût minimum pour un ensemble de 250 avions répartis sur 20 niveaux est trouvée en moins de 10 secondes.
Dans le chapitre 6, nous avons étendu le problème en introduisant des incertitudes : les erreurs sur les prévisions météorologiques, les erreurs de mesure de la vitesse des aéronefs, ainsi que le délai aléatoire dans l'exécution des manœuvres par les pilotes. À notre connaissance, ce type d'incertitudes est une première dans le domaine. Ces erreurs nous permettent de trouver une formule analytique de la probabilité de conflits entre chaque paire d'aéronefs. Nous utilisons cette formule pour adapter le modèle présenté au chapitre 5. Nous présentons

ensuite une méthode bi-objectif permettant de générer itérativement un ensemble de solutions approchant le front de Pareto du problème. Ces solutions représentent différents choix pour le contrôleur en termes d'équilibre entre l'efficacité des solutions et leur sécurité. Cette méthode est innovante car elle permet de générer un ensemble de solutions plutôt qu'une seule solution. Ceci est intéressant pour le domaine de la résolution de conflits car la notion d'optimalité n'est pas forcément pertinente. En effet, il existe de nombreuses "bonnes solutions" proches de la solution optimale, et il peut être intéressant pour les contrôleurs de les avoir à leur disposition.

7.2 Limitations de la solution proposée et améliorations futures

L'étude faite au chapitre 4 et les méthodes mathématiques présentées dans les chapitres 5 et 6 apportent certes des éléments nouveaux, mais restent néanmoins perfectibles.
L'étude faite au chapitre 4 permet d'obtenir une intuition sur les besoins futurs en optimisation, et permet d'identifier les potentiels goulots d'étranglement dans le système de gestion du trafic. Néanmoins, certains des composants de l'étude auraient besoin d'être améliorés afin d'avoir des résultats encore plus pertinents. Par exemple, la procédure d'augmentation du trafic pourrait permettre de différencier plusieurs modes de croissance suivant la zone concernée. Également, l'augmentation de trafic devrait pouvoir respecter les limites de capacité des aéroports, ce qui pourrait changer les flots survolant les secteurs. Nous pourrions développer de nouvelles métriques de coûts ou de complexité reflétant plus les tendances à décrire. Plus particulièrement, plutôt que de décrire le total des coûts de retards et des coûts en carburant, nous pourrions par exemple donner les coûts moyens par vol.
Le modèle présenté au chapitre 5 pourrait gagner en pertinence opérationnelle en prenant en compte plusieurs aspects techniques. Plus particulièrement, nous pourrions baser notre calcul de séparation et de protocoles d'évitement suivant des normes comme ICAO (2001), qui considère différentes distances de sécurité en fonction du type d'aéronef considéré. Nous pourrions définir un ensemble de manœuvres correspondant plus à ce qui se fait dans la pratique. En effet, les manœuvres de changement de niveaux de vol sont de plus en plus courantes pour des vols en évolution (en train de changer d'altitude), et elles permettent de réduire le nombre de conflits potentiels à gérer par le contrôle aérien. De plus, les vols en évolution représentent une partie non négligeable du trafic (50% du trafic français par exemple), et devraient être considérés dans des recherches futures. L'étude devrait être étendue au cadre à plusieurs secteurs, car le scénario à un seul secteur a ses limites. En effet, l'impact de la résolution de conflits sur les flots amont, aval et sur les secteurs adjacents n'est pas étudié. Notre modèle le prend partiellement en compte, en imposant de rattraper le contrat 4D après avoir effectué les manœuvres. Néanmoins, la coordination du flot avec les secteurs

adjacents reste difficile à quantifier. Finalement, des instances de test représentant du trafic réel seraient utiles car nous pourrions étudier les performances de notre modèle dans un cadre plus concret.

Des améliorations techniques du modèle décrit au chapitre 5 sont à prévoir. Par exemple, les fonctions permettant de calculer le coût des manœuvres pourraient être affinées. Également, il faudrait étendre la seconde méthode de décomposition afin de pouvoir l'appliquer à n'importe quel type d'instances. En d'autres termes, il faudrait développer une procédure générique permettant de décomposer une instance en sous-parties suivant leur géométrie, ainsi que les procédures définissant la proximité entre sous-parties, ainsi que la procédure de sélection. Ce point de recherche est crucial, car les résultats montrent la puissance de la méthode, et il serait dommage de ne pas pousser la recherche dans cette direction.

Le modèle présenté au chapitre 6 nécessite des améliorations. La première consistera à trouver si possible plus de données relatives au délai d'exécution des manœuvres. Ces données nous permettraient de modéliser de façon plus pertinente l'aléa en découlant. Il faudrait aussi étendre la formule analytique de probabilité de conflit entre aéronefs au cas tridimensionnel, afin de couvrir plus de possibilités lors de la résolution de conflits. Il serait également intéressant de faire une étude de sensibilité de la méthode itérative à ses différents paramètres d'entrée. Plus particulièrement, nous voudrions étudier comment la valeur de ces paramètres impacte le nombre de solutions générées, leurs similarités, et voir si cela reste pertinent d'un point de vue besoin du contrôleur. Une modification de la méthode devrait être envisagée, afin d'éviter de générer occasionnellement des solutions faiblement dominées. Il serait également nécessaire de développer une procédure de résolution par horizon glissant, qui permettrait de disposer d'un outil informatique plus proche d'un processus complet de résolution de conflits. La valeur ajoutée de cette méthode serait de pouvoir déterminer le meilleur instant pour déclencher les manœuvres. En effet, dans un cadre incertain, il peut être parfois judicieux d'attendre, afin d'observer les réalisations des incertitudes avant de prendre une décision.

CHAPITRE 8 CONCLUSION

En conclusion, nous avons fourni dans cette thèse une étude économique visant à quantifier les objectifs de recherche en contrôle aérien. Nous avons ensuite développé un modèle mathématique pour la détection et la résolution de conflits entre aéronefs. La force de ce modèle vient de sa flexibilité, qui nous permet de couvrir un large spectre d'hypothèses sans changer le processus de résolution. Enfin, nous avons étendu ce modèle au contexte incertain. Plus particulièrement, nous avons suivi une étude bi-objectif du problème nous permettant de fournir au contrôleur un ensemble de solutions représentant différents compromis entre efficacité et sécurité. Avec ces travaux, nous espérons avoir fait un pas dans la bonne direction, en ayant développé des outils mathématiques performants répondant à un besoin opérationnel futur qu'il sera impératif de satisfaire.

Cette thèse est le fruit de quatre années de travail : des hauts, des bas, et beaucoup d'entre-deux. Dans tous les cas, je suis fier d'avoir pu mener ce travail jusqu'ici. Pour conclure, je vous laisse sur la citation suivante, qui décrit bien des moments de ma thèse :

"Research is what I'm doing when I don't know what I'm doing."
—Wernher von Braun

RÉFÉRENCES

(2014). CPLEX v12.5. User's manual for CPLEX. Rapport technique 11/03/08-08, IBM ILOG.

ADMINISTRATION, F. A. (2011). Introduction to TCAS II - version 7.1. Rapport technique, Federal Aviation Administration.

ALAM, S., SHAFI, K., ABBASS, H. et BARLOW, M. (2009). An ensemble approach for conflict detection in free flight by data mining. *Transportation Research Part C*, 17, 298–317.

ALLIOT, J.-M., BOSC, J.-F., DURAND, N. et MAUGIS, L. (1997). CATS : A complete air traffic simulator. *16th Digital Avionics System Conference*.

ALLIOT, J.-M. et DURAND, N. (2011). A mathematical analysis of the influence of wind uncertainty on MTCD efficiency. *The controller, Meteorology and ATC*, 1, 17–19.

ALONSO-AYUSO, A., ESCUDERO, L. F. et MARTIN-CAMPO, F. J. (2010). Collision avoidance in the air traffic management : A mixed integer linear optimization approach. *IEEE Transactions on Intelligent Transportation Systems*, 11, 826–837.

ALONSO-AYUSO, A., ESCUDERO, L. F. et MARTIN-CAMPO, F. J. (2011). Collision avoidance in air traffic management : A mixed-integer linear optimization approach. *IEEE Transactions on Intelligent Transportation Systems*, 12, 47–57.

ALONSO-AYUSO, A., ESCUDERO, L. F. et MARTIN-CAMPO, F. J. (2012). A mixed 01 nonlinear optimization model and algorithmic approach for the collision avoidance in ATM : Velocity changes through a time horizon. *IEEE Transactions on Intelligent Transportation Systems*, 39, 3136–3146.

ALONSO-AYUSO, A., ESCUDERO, L. F. et MARTIN-CAMPO, F. J. (2016). Multiobjective optimization for aircraft conflict resolution. a metaheuristic approach. *European Journal of Operational Research*, 248, 691–702.

ALONSO-AYUSO, A., ESCUDERO, L. F., MARTIN-CAMPO, F. J. et MLADENOVIĆ, N. (2014). A VNS metaheuristic for solving the aircraft conflict detection and resolution problem by performing turn changes. *Journal of Global Optimization*, 63, 583–596.

ARCHIBALD, J. K., HILL, J. C., JEPSEN, N., STIRLING, W. C., FROST, R. L. *ET AL.* (2008). A satisficing approach to aircraft conflict resolution. *IEEE Transactions on Systems, Man, and Cybernetics, Part C : Applications and Reviews*, 38, 510–521.

BALLIN, M. G. et ERZBERGER, H. (1996). *An analysis of landing rates and separations at the Dallas/Fort Worth International Airport*, vol. 110397. Ames Research Center, National Aeronautics and Space Administration.

BARNIER, N. et ALLIGNOL, C. (2009). 4D trajectory deconfliction through departure time adjustment. *8th USA-Europe air traffic management research and developpment seminar, Napa,CA,USA*. 1–24.

BARNIER, N. et BRISSET, P. (2004). Graph coloring for air traffic flow management. *Annals of Operations Research*, 130, 163–178.

BASHLLARI, A., KACIROTI, N., NACE, D. et FUNDO, A. (2007). Conflict probability estimations based on geometrical and Bayesian approaches. *IEEE Transactions on Intelligent Transportation Systems*. IEEE, 479–484.

BAYEN, A., GRIEDER, P., MEYER, G. et TOMLIN, C. (2005). Lagrangian delay predictive model for sector-based air traffic flow. *Journal of Guidance, Control and Dynamics*, 28, 1015–1026.

BEATTY, R., HSU, R., BERRY, L. et ROME, J. (1999). Preliminary evaluation of flight delay propagation through an airline schedule. *Air Traffic Control Quarterly*, 7, 259–270.

BERTSIMAS, D. et PATTERSON, S. S. (1998). The air traffic flow management problem with enroute capacities. *Operations Research*, 46, 406–422.

BERTSIMAS, D. et PATTERSON, S. S. (2000). The traffic flow management rerouting problem in air traffic control : A dynamic network flow approach. *Transportation Science*, 34, 239–255.

BICCHI, A. et PALLOTTINO, L. (2000). On optimal cooperative conflict resolution for air traffic management systems. *IEEE Transactions on Intelligent Transportation Systems*, 1, 221–231.

BOARD, E. (1995). *Special report on free flight*. Aviation Week and Space Technology.

BOMZE, I. M., BUDINICH, M., PARDALOS, P. M. et PELILLO, M. (1999). The maximum clique problem. D.-Z. Du et P. M. Pardalos, éditeurs, *Handbook of Combinatorial Optimization*, Springer. 1–74.

BROCHARD, M. (2009). Erasmus final report v1.1. technical report d4.6. Rapport technique, EUROCONTROL, Eurocontrol Experimental Centre, Bretigny, France.

CARPENTER, B. et KUCHAR, J. (1997). Probability-based collision alerting logic for closely-spaced parallel approach. *35th AIAA Aerospace Sciences Meeting Exhibit, Reno, NV, USA*.

CETEK, C. (1999). Realistic speed change maneuvers for air traffic conflict avoidance and their impact on aircraft economics. *International Journal of Civil Aviation*, 1, 62–73.

CHALOULOS, G. et LYGEROS, J. (2007). Effect of wind correlation on aircraft conflict probability. *Journal of Guidance, Control, and Dynamics*, 30, 1742–1752.

CHIANG, Y., KLOSOWSKI, J. T., LEE, C. et MITCHELL, J. S. B. (1997). Geometric algorithms for conflict detection and resolution in air traffic management. *36th IEEE Conference on Decision and Control, San Diego, CA, USA*, 10–12.

CHRISTODOULOU, M. et COSTOULAKIS, C. (2004). Nonlinear mixed integer programming for aircraft collision avoidance in free flight. *IEEE Melecon 2004, Dubrovnik, Croatia.* vol. 1, 327–330.

CHRISTODOULOU, M. et KODAXAKIS, S. (2006). Automatic commercial aircraft-collision avoidance in free flight :The three-dimensional problem. *IEEE Transactions on Intelligent Transportation Systems.* vol. 7, 242–249.

CHRISTODOULOU, M. A. et KONTOGEORGOU, C. (2008). Collision avoidance in commercial aircraft free flight via neural networks and non-linear programming. *International Journal of Neural Systems*, 18, 371–387.

CLARKE, J.-P., SOLAK, S., REN, L. et VELA, A. (2013). Determining stochastic airspace capacity for air traffic flow management. *Transportation Science*, 47, 542–559.

COLE, R., RICHARD, C., KIM, S. et BAILEY, D. (1998). Assessment of the Rapid Update Cycle (RUC) with near real-time aircraft reports. Rapport technique, MIT - Lincoln Laboratory.

COOK, A. et TANNER, G. (2009). The challenge of managing airline delay costs. *Conference on Air Traffic Management (ATM) Economics.* vol. 1.

COOK, A. et TANNER, G. (2011a). Modelling the airline costs of delay propagation. *AGIFORS Airline Operations Conference, London, UK.*

COOK, A. J. et TANNER, G. (2011b). European airline delay cost reference values.

COOK, A. J., TANNER, G. et ANDERSON, S. (2004). Evaluating the true cost to airlines of one minute of airborne or ground delay : Final report.

DOWEK, G., GESER, A. et MUNOZ, C. (2001). Tactical conflict resolution and resolution in 3D airspace. *4th USA-Europe Air Traffic Management Research and Development Seminar, Santa Fe, NM, USA*, 1–10.

DUONG, V. et HOFFMAN, E. (1997). Conflict resolution advisory service in autonomous aircraft operations. *16th Digital Avionics Systems Conference, Irvine, CA, USA*, 9, 10–17.

DURAND, N. et ALLIOT, J. (2009). Ant-colony optimization for air traffic conflict resolution. *8th USAEurope Air Traffic Management Research and Development Seminar, Napa, CA, USA*, 1–6.

DURAND, N., ALLIOT, J. et MEDIONI, F. (2000). Neural nets trained by genetic algorithms for collision avoidance. *Applied Artificial Intelligence.*

DURAND, N., ALLIOT, J. et NOAILLES, J. (1996). Automatic aircraft conflict resolution using genetic algorithms. *Proceedings of the Symposium on Applied Computing, Philadelphia*.

ERZBERGER, H. et PAIELLI, R. (1997). Conflict probability estimation for free flight. *AIAA Journal of Guidance, Control and Dynamics*, 20, 588–596.

ERZBERGER, H., PAIELLI, R., ISAACSON, D. et ESHOW, M. (1997a). Conflict detection and resolution in the presence of prediction error. *1st USA-Europe Air Traffic Management Research and Development Seminar, Saclay, France*, 1–19.

ERZBERGER, H., PAIELLI, R. A., ISAACSON, D. R. et ESHOW, M. M. (1997b). Conflict detection and resolution in the presence of prediction error. *1st USA/Europe Air Traffic Management R&D Seminar, Saclay, France*. Citeseer, 17–20.

EUROCONTROL (1998). Aircraft performance summary tables for the Base of Aircraft Data (BADA) revision 3.0. Rapport technique, EUROCONTROL.

EUROCONTROL (2010). Eurocontrol seven year forecast : Flight movements and service unit 2013–2019. Rapport technique, Eurocontrol - STATFOR.

EUROCONTROL (2011). Basic CFMU handbook, General & CFMU systems.

EUROCONTROL (2011). User manual for the Base of Aircraft Data (BADA). Rapport technique 11/03/08-08, Eurocontrol.

EUROCONTROL (2012). Performance review report for 2012. Rapport technique, EUROCONTROL.

EUROCONTROL (2013). Eurocontrol long-term forecast : IFR flight movements 2013–2035. Rapport technique, EUROCONTROL - STATFOR.

FARLEY, T. et ERZBERGER, H. (2007). Fast-time simulation evaluation of a conflict resolution algorithm under high air traffic demand. *Proceedings of the 7th USA/Europe Air Traffic Management R&D Seminar, Barcelona, Spain*.

FORTET, R. (1960). Applications de l'algebre de Boole en recherche opérationelle. *Revue Française de Recherche Opérationelle*, 4, 17–26.

FRAZZOLI, E., MAO, Z.-H., OH, J.-H. et FERON, E. (1999). Resolution of conflicts involving many aircraft via semidefinite programming. *AIAA Journal of Guidance, Control and Dynamics*, 24, 79–86.

GALDINO, A., MUNOZ, C. et AYALA-RINCON, M. (2007). Formal verification of an optimal air traffic conflict resolution and recovery algorithm. *14th Workshop on Logic, Language, Information and Computation, Rio de Janeiro, Brésil*. 177–188.

GAO, Y., ZHANG, X. et GUAN, X. (2012). Cooperative multi-aircraft conflict resolution based on co-evolution. *Instrumentation & Measurement, Sensor Network and Automation (IMSNA), 2012 International Symposium on*. IEEE, vol. 1, 310–313.

GLOVER, W. et LYGEROS, J. (2004). Simplified multi-aircraft models for conflict detection and resolution algorithms. *HYBRIDGE D1*, 4.

GOLDBERG, D. (1989). *Genetic Algorithms*. Addison Wesley.

HOEKSTRA, J., GENT, R. V. et RUIGROK, R. (1998). Conceptual design of free flight with airborne separation assurance. *AIAA Guidance, Navigation, Control Conference, Boston, MA, USA*, 4239, 807–817.

HU, J., PRANDINI, M. et SASTRY, S. (2002). Optimal coordinated maneuvers for three dimensional aircraft conflict resolution. *AIAA Journal of Guidance, Control and Dynamics*, 25, 888–900.

HU, J., PRANDINI, M. et SASTRY, S. (2003). Optimal coordinated motions of multiple agents moving on a plane. *SIAM J. Control and Optimization*, 42, 637–668.

ICAO (2001). 4444* procedures for air navigation services. *Air Traffic Management http ://www. paris. icao. int/or www. icao. int*.

IRVINE, R. (2002). A geometrical approach to conflict probability estimation. *Air Traffic Control Quarterly*, 10, 85–113.

IRVINE, R. (2003). Target miss distance to achieve a required probability of conflict. *5th ATM Seminar, Budapest, Hungary*.

JARDIN, M. R. (2003). *Toward Real-Time en Route Air Traffic Control Optimization*. Thèse de doctorat, Stanford University.

JOINT PLANNING AND DEVELOPMENT OFFICE (2008). Next gen air transportation system integrated work plan, technical report. Rapport technique.

KARP, R. M. (1972). Reducibility among combinatorial problems. R. E. Miller, J. W. Thatcher et J. D. Bohlinger, éditeurs, *Complexity of Computer Computations*, Springer US. 85–103.

KOPARDEKAR, P., PREVOT, T. et JASTRZEBSKI, M. (2008). Traffic complexity measurement under higher levels of automation and higher traffic densities. *Proceedings of the Guidance, Navigation, and Control Conference and Exhibit*.

KROZEL, J. (1997). Strategic conflict detection and resolution for free flight. *36th IEEE Conference on Decision and Control, San Diego, CA, USA*, 1822–1828.

KUCHAR, J. K. et YANG, L. C. (2000). A review of conflict detection and resolution modeling methods. *IEEE Transactions on Intelligent Transportation Systems*, 1, 179–189.

LEHOUILLIER, T., OMER, J., SOUMIS, F. et ALLIGNOL, C. (2014). Interactions between operations and planning in air traffic control. *Proceedings of the 2nd International Conference of Research in Air Transportation, Istanbul*.

LEHOUILLIER, T., OMER, J., SOUMIS, F. et DESAULNIERS, G. (2015a). A flexible framework for solving the air conflict detection and resolution problem using maximum cliques in a graph. *11th USA/Europe Air Traffic Management R&D Seminar, June 23-27, Lisbon, Portugal*.

LEHOUILLIER, T., OMER, J., SOUMIS, F. et DESAULNIERS, G. (2015b). A new variant of the minimum-weight maximum-cardinality clique problem to solve conflicts between aircraft. H. A. Le Thi, T. Pham Dinh et N. T. Nguyen, éditeurs, *Modelling, Computation and Optimization in Information Systems and Management Sciences*, Springer International Publishing, vol. 359 de *Advances in Intelligent Systems and Computing*. 3–14.

LULLI, G. et ODONI, A. (2007). The European air traffic flow management problem. *Transportation Science*, 41, 431–443.

LYGEROS, J. et PRANDINI, M. (2002). Aircraft and weather models for probabilistic collision avoidance in air traffic control. *IEEE Conference on Decision and Control*. IEEE ; 1998, vol. 3, 2427–2432.

LYMPEROPOULOS, I. (2010). *Sequential Monte Carlo methods in air traffic management*. Thèse de doctorat, Diss., Eidgenössische Technische Hochschule ETH Zürich, Nr. 19004, 2010.

LYMPEROPOULOS, I. et LYGEROS, J. (2010). Sequential monte carlo methods for multi-aircraft trajectory prediction in air traffic management. *International Journal of Adaptive Control and Signal Processing*, 24, 830–849.

MAJUMDAR, A., OCHIENG, W. et POLAK, J. (2002). Estimation of European airspace capacity from a model of controller workload. *Journal of Navigation*, 55, 381–403.

MAO, Z.-H., FERON, E., DUGAIL, D. et BILIMORIA, K. (2005). Stability of intersecting aircraft flows under decentralized conflict avoidance rules. *IEEE Transactions on Intelligent Transportation Systems*. vol. 6, 357–369.

MARTIN-CAMPO, F. J. (2010). *The collision avoidance problem : Methods and algorithms*. Thèse de doctorat.

MENON, P., SWERIDUK, G. et SRIDHAR, B. (1999). Optimal strategies for free-flight air traffic conflict resolution. *Journal of Guidance, Control, and Dynamics*, 22, 202–211.

MUKHERJEE, A. et HANSEN, M. (2007). A dynamic stochastic model for the single airport ground holding problem. *Transportation Science*, 41, 444–456.

OMER, J. (2013). *Modèles déterministes et stochastiques pour la résolution de conflits aériens*. Thèse de doctorat, ISAE, Toulouse, France.

OMER, J. (2015a). Comparison of mixed-integer linear models for fuel-optimal air conflict resolution with recovery. *IEEE Transactions on Intelligent Transportation Systems*, PP, 1–12.

OMER, J. (2015b). A space-discretized mixed-integer linear model for air-conflict resolution with speed and heading maneuvers. *Computers & Operations Research*, 58, 75–86.

PAIELLI, R. A. (2003). Modeling maneuver dynamics in air traffic conflict resolution. *Journal of guidance, control, and dynamics*, 26, 407–415.

PALLOTTINO, L., FERON, E. et BICCHI, A. (2002). Conflict resolution problems for air traffic management systems solved with mixed integer programming. *IEEE Transportation and Intelligent Transportation Systems*, 3, 3–11.

PANNEQUIN, J., BAYEN, A., MITCHELL, I., CHUNG, H. et SASTRY, S. (2007). Multiple aircraft deconflicted path planning with weather avoidance constraints. *AIAA Guidance, Navigation and Control Conference, Hilton Beach, SC, USA*. 1–12.

PENG, L. et LIN, Y. (2010). Study on the model for horizontal escape maneuvers in TCAS. *IEEE Transactions on Intelligent Transportation Systems*, 11, 392–398.

PRANDINI, M. et HU, J. (2008). Application of reachability analysis for stochastic hybrid systems to aircraft conflict prediction. *IEEE Transactions on Automatic Control, Notre Dame, IN, USA*. 4036–4041.

PRANDINI, M., HU, J., LYGEROS, J. et SASTRY, S. (2000). A probabilistic approach to aircraft conflict detection. *IEEE Transactions on Intelligent Transportation Systems*, 1, 199–220.

QI, FEI, M. (2012). Flight conflict resolution for civil aviation based on ant colony optimization. *Computational Intelligence and Design (ISCID), 2012 Fifth International Symposium on*. IEEE, vol. 1, 239–241.

RAGHUNATHAN, A. U., GOPAL, V., SUBRAMANIAN, D., BIEGLER, L. T. et SAMAD, T. (2004). Dynamic optimization strategies for three-dimensional conflict resolution of multiple aircraft. *Journal of Guidance, Control, and Dynamics*, 27, 586–594.

RESMERITA, S., HEYMANN, M. et MEYER, G. (2003). A framework for conflict resolution in air traffic management. *42nd IEEE Conference on Decision and Control*. IEEE, vol. 2, 2035–2040.

RTCA (1983). Minimum performance specifications for TCAS airborne equipment. Rapport technique, Radio Technical Commitee on Aeronautics. Document No. RTCA/DO185.

RTCA (1995). *Final Report of RTCA Task Force 3 Free Flight Implementation*. RTCA Incorporated.

RUBINSTEIN, R. Y. et KROESE, D. P. (2011). *Simulation and the Monte Carlo method*, vol. 707. John Wiley & Sons.

SCHOUWENAARS, T. (2006). *Safe trajectory planning of autonomous vehicles*. Thèse de doctorat, Massachusetts Institute of Technology.

SCHWARTZ, B. E., BENJAMIN, S. G., GREEN, S. M. et JARDIN, M. R. (2000). Accuracy of ruc-1 and ruc-2 wind and aircraft trajectory forecasts by comparison with acars observations. *Weather and Forecasting*, 15, 313–326.

SESAR JOINT UNDERTAKING (2012). European ATM master plan, edition 2. Rapport technique.

SHERALI, H. D., COLE SMITH, J. et TRANI, A. A. (2002). An airspace planning model for selecting flight-plans under workload, safety, and equity considerations. *Transportation Science*, 36, 378–397.

SHERALI, H. D., SMITH, J. C., TRANI, A. A. et SALE, S. (2000). National airspace sector occupancy and conflict analysis models for evaluating scenarios under the free-flight paradigm. *Transportation Science*, 34, 321–336.

SHERALI, H. D., STAATS, R. W. et TRANI, A. A. (2003). An airspace planning and collaborative decision - making model : Part I - Probabilistic conflicts, workload, and equity considerations. *Transportation Science*, 37, 434–456.

SHERALI, H. D., STAATS, R. W. et TRANI, A. A. (2006). An airspace-planning and collaborative decision-making model : Part II - Cost model, data considerations, and computations. *Transportation Science*, 40, 147–164.

SHEWCHUN, J., JAE-HYUK, O. et FERON, E. (1997). Linear matrix inequalities for free flight problems. *36th IEEE Conference on Decision and Control, San Diego, CA, USA*. vol. 3, 2417–2422.

STEINER, M. et KROZEL, J. (2009). Translation of ensemble-based weather forecasts into probabilistic air traffic capacity impact. *Proceedings of the 28th Digital Avionics Systems Conference, October 25–29, Orlando, FL*.

STIRLING, W. C. et GOODRICH, M. A. (1999). Satisficing games. *Information Sciences*, 114, 255–280.

TAILLARD, É. D. et VOSS, S. (2002). Popmusic — partial optimization metaheuristic under special intensification conditions. *Operations Research/Computer Science Interfaces Series*, Springer Science + Business Media. 613–629.

TOMLIN, C., PAPPAS, G. et SASTRY, S. (1998a). Conflict resolution for air traffic management : A study in multiagent hybrid systems. *IEEE Transactions on Automatic Control*, 43, 509–521.

TOMLIN, C., PAPPAS, G. J. et SASTRY, S. (1998b). Conflict resolution for air traffic management : A study in multiagent hybrid systems. *IEEE Transactions on Automatic Control*, 43, 509–521.

VELA, A., SOLAK, S., CLARKE, J.-P., SINGHOSE, W. E., BARNES, E. R. et JOHNSON, E. L. (2011). Near real-time fuel-optimal en route conflict resolution. *IEEE Transactions on Intelligent Transportation Systems*, 12, 47–57.

VELA, A., SOLAK, S., FERON, E., FEIGH, K., SINGHOSE, W. et CLARKE, J.-P. (2009a). A fuel optimal and reduced controller workload optimization model for conflict resolution. *Digital Avionics Systems Conference, 2009. DASC '09. IEEE/AIAA 28th*. 3.C.3–1 –3.C.3–16.

VELA, A., SOLAK, S., SINGHOSE, W. E. et CLARKE, J.-P. (2009b). A mixed integer program for flight-level assignment and speed control for conflict resolution. *Proceedings of the 48th IEEE Conference on Decision and Control*. Shanghai, China, 5219–5226.

VELA, A. E. (2011). *Understanding conflict-resolution taskload : implementing advisory conflict-detection and resolution algorithms in an airspace*. Thèse de doctorat, Georgia Institute of Technology.

VELA, A. E., SALAUN, E., SOLAK, S., FERON, E., SINGHOSE, W. et CLARKE, J.-P. (2009c). A two-stage stochastic optimization model for air traffic conflict resolution under wind uncertainty. *Digital Avionics Systems Conference, 2009. DASC'09. IEEE/AIAA 28th*. IEEE, 2–E.

VISINTINI, A. L., GLOVER, W., LYGEROS, J. et MACIEJOWSKI, J. (2006). Monte Carlo optimization for conflict resolution in air traffic control. *Intelligent Transportation Systems, IEEE Transactions on*, 7, 470–482.

VIVONA, R., KARR, D. et ROSCOE, D. (2006). Pattern-based genetic algorithm for airborne conflict resolution. *AIAA Guidance, Navigation and Control Conference and Exhibit, Keystone, Colorado*.

VRANAS, P. B., BERTSIMAS, D. et ODONI, A. R. (1994a). Dynamic ground-holding policies for a network of airports. *Transportation Science*, 28, 275–291.

VRANAS, P. B., BERTSIMAS, D. J. et ODONI, A. R. (1994b). The multi-airport ground-holding problem in air traffic control. *Operations Research*, 42, 249–261.

WU, Q. et HAO, J.-K. (2015). A review on algorithms for maximum clique problems. *European Journal of Operational Research*, 242, 693–709.

ZEGHAL, K. et HOFFMAN, E. (1999). Design of cockpit displays for limited delegation of separation assurance. *18th Digital Avionics Systems Conference, Sharp, DC, USA*.

ZHOU, K., DOYLE, J. C., GLOVER, K. *ET AL.* (1996). *Robust and optimal control*, vol. 40. Prentice Hall New Jersey.